UNIVERSITÄT WÜRZBURG
Lehrstuhl für Mathematik VI - Angewandte Analysis

Masterarbeit zur Erlangung des akademischen Grades eines Master of Science (Mathematische Physik)

Multispecies Traffic Models Based on the Lighthill-Whitham and the Aw-Rascle Model

Eingereicht bei:
Prof. Dr. Christian Klingenberg

Erstellt von:
Marie-Christine Meltzer
Unterer Beerer 17a, 97236 Randersacker

26. Februar 2016

Contents

List of Figures

1 Introduction

In today's life we are used to a great mobility related to traveling and also for trading goods. This mobility depends a lot on road traffic. Getting from one place to another and receiving desired goods should be as fast as possible. Hence, it is of interest to make this process more and more effective. Because of that the road traffic has been studied by mathematicians for a long time. There exist scientific observations of traffic going back to 1934 like in Greenshields [1934]. From that starting point there are many different ways of describing and modeling traffic situations. The aim of all these models is to understand traffic from a mathematical point of view and optimize different properties.

In this thesis we consider a macroscopic traffic observation which means that we assume a huge number of cars on the road and model the variables describing the lot of cars and not each single car as a microscopic consideration would do. Due to that, we deal with partial differential equations.

A famous and well studied model describing the traffic density and its flow, is the model of Lighthill-Whitham and Richards (LWR). It is deduced from the trivial assumption of conservation of cars. First, we discuss the derivation, solutions and special features of this model.

The wish to discriminate different types of vehicles like for example cars and trucks leads to the consideration of a multi species extension of this model that has already been proposed in literature. This extension leads to difficulties in proving well-posedness at the stage of two species already since it provides an umbilic point where the system is not hyperbolic and hence we are not able to use the theory available for hyperbolic systems. Due to that, the solution for the Riemann problem is studied properly around the critical point in this thesis to see whether the lack of hyperbolicity affects the solution or not.

In addition, we try to get rid of the umbilic point by varying the model through the flow or the velocity function. The result of this approach is the existence of even more umbilic points. We also consider a three species model and compute its umbilic points afterward. Due to the complexity of the corresponding expressions, we are not able to prove and compute everything algebraically and we use the help of Mathematica.

Secondly, we introduce another macroscopic traffic model which Aw-Rascle and Zhang (ARZ) discovered. It is derived from the LWR model through a second partial differential equation modeling the velocity of the cars. For this model, we derive the Chapman Enskog expansion to understand its relaxation behavior towards an equilibrium velocity. This expansion also shows the connection between the LWR and the ARZ model because the LWR can be understood as the limit of the ARZ model. The other way around we

can interpret the ARZ as an extension of the LWR model because the Chapman Enskog expansion provides a viscous right hand side for the LWR model.

For consistency, we develop a multi species extension of the ARZ model similar to the LWR one. The multi species model has not been studied, yet, and we do not prove well-posedness, either. Instead, we focus on the Chapman Enskog expansion again and see if we observe the same connection and relaxation behavior as for the one species model. Different from the one species model, we are not able to prove parabolicity from the characteristic traffic features. Instead, one obtains inequalities for the corresponding functions that lead to a viscous right hand side.

We also study a variation of the traffic functions to consider special traffic situations. There, we examine the parabolicity of the conservation law with right hand side by the consideration of two different examples.

2 Lighthill-Whitham-Richards (LWR) Model

In this chapter, we introduce the fundamental variables to describe traffic from a macroscopic point of view. Then, we derive the LWR model from conservation of cars and the fundamental diagram of traffic flow which was first studied by Lighthill and Whitham [1955] and Richards [1956].

2.1 The fundamental traffic variables

We start with the discussion of the fundamental traffic variables. We assume a huge number of cars and hence model the traffic as a whole. Due to that we look for variables describing the traffic properties and not the single cars. For this macroscopic observation there are three of them. Moreover, we consider a one-lane road where all traffic participants are of one species and overtaking is forbidden. Then, we model the velocity, the density and the traffic flow as functions of space $x \in \mathbb{R}$ and time $t \in \mathbb{R}^+$. Since the cars move in one direction it is sufficient to consider one space dimension. Hence, x is a scalar variable. We are able to observe this variables in experiments and so it is possible to compare our results with reality.

Since we consider a huge number of cars the velocity $u(x,t)$ does not describe the speed of each single car but the average of all cars. We obtain a velocity field that gives one value of velocity for every point on the road for all time t. Each car drives with the speed given by the field. We can observe this quantity by measuring the velocities of cars at a point of the road and then taking the mean value.

The traffic density $\rho(x,t)$ measures the number of cars on a certain segment of the road. For example, we get the number of cars per kilometer. For this quantity one gets experimental data by counting the number of cars on a piece of road at a fixed time.

Finally, the traffic flow $f(x,t)$ is the third macroscopic variable. It is defined as the number of cars passing a point of the road in a certain amount of time, for example the number of cars passing per hour. For this variable we can create experimental data by counting the cars passing the observer in a given time interval.

Now, the three traffic variables are connected by the following relation. If we measure

the number of cars passing a fixed point of the road in a small time interval δt, we obtain $u(x,t)\rho(x,t)\delta t$. Then, the traffic flow is given by the number of cars per time. This yields

$$f(x,t) = u(x,t)\rho(x,t)$$

and we can summarize the results in the next proposition.

Theorem 2.1.1. *For a macroscopic approach, the fundamental traffic variables are the velocity $u(x,t)$, the density $\rho(x,t)$ and the flow $f(x,t)$. All three variables depend on space $x \in \mathbb{R}$ and time $t \in \mathbb{R}^+$. They are connected through the relation*

$$f(x,t) = u(x,t)\rho(x,t). \tag{2.1}$$

As a next step, we deduce a partial differential equation (PDE) modeling these three variables.

2.2 Conservation of cars and fundamental diagram of traffic flow

After the derivation of the fundamental variables $u(x,t), \rho(x,t)$ and $f(x,t)$ in the last section, we now introduce the conservation law found by Lighthill and Whitham [1955] and Richards [1956] modeling these variables .

Let $u(x,t), \rho(x,t)$ and $f(x,t)$ be continuous in x and t. We regard the route section between $x = a$ and $x = b$. The number of cars N there is given by

$$N = \int_a^b \rho(x,t)dx. \tag{2.2}$$

Then, in case that there are no entries or exits on this section the number of cars is conserved. It only changes by flow through a or b. Hence, the number of cars inside this segment equals the flow through the boundaries like in Haberman [1998]

$$\frac{dN}{dt} = f(a,t) - f(b,t).$$

Together with (2.2) we obtain

$$\frac{d}{dt}\int_a^b \rho(x,t)dx = f(a,t) - f(b,t).$$

The fundamental theorem of differentiation and integration yields

$$f(a,t) - f(b,t) = -\int_a^b \frac{\partial}{\partial x} f(x,t)dx$$

and so we get

$$\int_a^b \left(\frac{\partial}{\partial t}\rho(x,t) + \frac{\partial}{\partial x} f(x,t) \right) dx = 0.$$

Since the interval $[a, b]$ was chosen arbitrarily, equation (2.2) is fulfilled, if

$$\partial_t \rho(x,t) + \partial_x f(x,t) = 0.$$

We derived a nonlinear PDE from the conservation of cars which is also called a scalar conservation law. With (2.1) one can write

$$\partial_t \rho(x,t) + \partial_x (\rho(x,t)u(x,t)) = 0.$$

Still, there are two variables modeled by the PDE, the density and the velocity. We need another condition to solve the PDE. Therefore, we introduce the fundamental diagram of traffic flow. From experimental observation, like in Haberman [1998], one can assume that the velocity only changes with the density.

$$u(x,t) = u(\rho(x,t)).$$

This relation yields

$$f(x,t) = u(\rho(x,t))\rho(x,t) = f(\rho(x,t))$$

for the traffic flow and we thus get a PDE modeling just the density

$$\partial_t \rho(x,t) + \partial_x f(\rho(x,t)) = 0. \tag{2.3}$$

There are different possibilities to describe the flow function f. As a first step we rewrite the velocity

$$u(\rho) = V\psi(\rho)$$

with a maximal velocity $V > 0$ and the monotone $\mathcal{C}^1-$function $\psi(\rho)$ for which we claim $\psi(0) = 0$ and $\psi' < 0$.

From now on, we omit writing the variables x and t. The different expressions of the function $\psi(\rho)$ are presented in Rosini [2013]. The Greenberg velocity function is one example

$$\psi(\rho) = \lambda \ \ ln\left(\frac{\rho_{max}}{\rho}\right)$$

with $\lambda \in \mathbb{R}^+$ and with the maximal density $\rho_{max} > 0$. The most common one is the Greenshields function found by Greenshields [1934]

$$\psi(\rho) = 1 - \frac{\rho}{\rho_{max}} \tag{2.4}$$

which is also the one we will use for the further analysis of the PDE (2.3). An example of Greenshields velocity function is plotted in figure 2.1 together with the flow function. Figure (b) is also called the fundamental diagram of traffic flow. If we insert the Greenshields function into (2.3), we finally obtain the LWR model which was found independently by Lighthill and Whitham [1955] and Richards [1956].

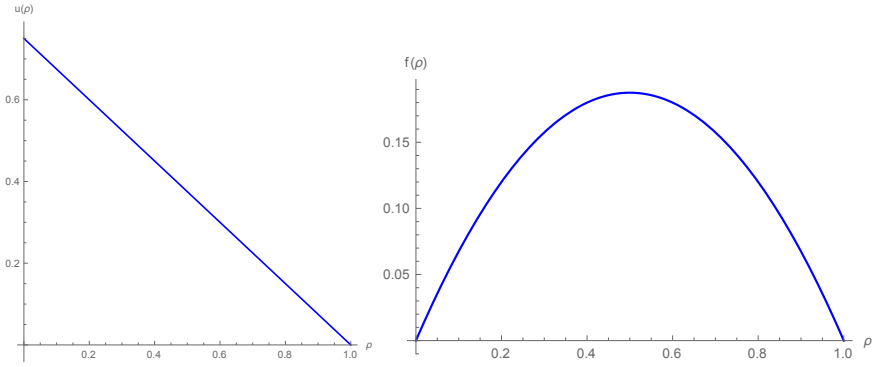

(a) Greenshields velocity function.

(b) The corresponding flow function.

Figure 2.1: Fundamental diagram of traffic flow with $V = 0.75$ and $\rho_{max} = 1$.

Theorem 2.2.1. *The LWR model is given by the nonlinear partial differential equation*

$$\partial_t \rho(x,t) + \partial_x f(\rho(x,t)) = 0 \tag{2.5}$$

with the flow function $f(\rho) = (V\rho(1-\rho))$ *where* $V > 0$ *describes the maximal velocity and the maximal density* ρ_{max} *is normalized. It models the traffic density* $0 \leq \rho(x,t) \leq 1$ *under the assumption that the velocity is a function of the density, only. Due to this, the LWR model is called an equilibrium traffic model.*

In the next section we consider the Riemann Problem for the LWR model and construct the solution to this initial value problem.

2.3 The Riemann Problem

Since the fundamental variables are known and the LWR model is introduced in (2.3), we now define the corresponding Riemann Problem (RP) and discuss its solution. Note, that with solution we mean a solution in the weak sense as is defined in Rosini [2013] since it may be discontinuous. Because the PDE (2.3) models ρ we have to give values for the density as initial datum. The RP is given by

$$\begin{aligned} &\partial_t \rho + \partial_x f(\rho) = 0 \\ &\rho(x,0) = \begin{cases} \rho^L & \text{for} \quad x < 0 \\ \rho^R & \text{for} \quad x > 0 \end{cases} \end{aligned} \tag{2.6}$$

with $f(\rho) = V\rho(1-\rho)$ where $V > 0$ and $0 \leq \rho \leq 1$ and ρ^L, $\rho^R \in \mathbb{R}$. We now want to discuss the different types of the solution to the RP like it is done in Shearer and Levy [2015] and Lax [1957]. The flow function $f(\rho)$ is strictly concave. Then, by Dafermos [2010], for $\rho^L < \rho^R$ the solution to the RP consists of a single shock wave with speed σ which has to fulfill the Rankine Hugoniot condition.

Lemma 2.3.1. *A shock connecting a state $\rho^L \in \mathbb{R}$ to a state $\rho^R \in \mathbb{R}$ with speed $\sigma \in \mathbb{R}$ has to fulfill the Rankine Hugoniot condition*

$$\sigma(\rho^L - \rho^R) = f(\rho^L) - f(\rho^R). \tag{2.7}$$

With Greenshields velocity function one gets for the traffic flow

$$\begin{aligned}\sigma(\rho^L - \rho^R) &= f(\rho^L) - f(\rho^R) \\ &= \rho^L V(1-\rho^L) - \rho^R V(1-\rho^R) \\ &= V(\rho^L - \rho^R)(1-\rho^L-\rho^R),\end{aligned}$$

and thus the shock speed is given by

$$\sigma = V(1-\rho^L-\rho^R) \tag{2.8}$$

for $\rho^L \neq \rho^R$. Then from Rosini [2013], the solution of the RP (2.6) has the form

$$\rho(x,t) = \begin{cases} \rho^L & \text{for} \quad x < \sigma t \\ \rho^R & \text{for} \quad x > \sigma t \end{cases}. \tag{2.9}$$

Moreover, the shock wave satisfies the Lax entropy condition stated in (3.24). This is proven in the next theorem. In figure 2.2 the blue line shows a shock curve connecting the left and right state of an exemplary RP.

Corollary 2.3.2. *Given the Riemann problem (2.6) with $\rho^L < \rho^R$ the solution consists of a shock wave with speed (2.8).*

$$\rho(x,t) = \begin{cases} \rho^L & \textit{for} \quad x < \sigma t \\ \rho^R & \textit{for} \quad x > \sigma t \end{cases}. \tag{2.10}$$

The shock connecting ρ^L to ρ^R fulfills the Lax admissibility criterion (3.24) for a single PDE because the following inequality holds for the flow f

$$f'(\rho^L) \geq \sigma \geq f'(\rho^R). \tag{2.11}$$

Proof. Since, the flow is given by $f(\rho) = V\rho(1-\rho)$ with the Greenshields velocity function we can compute the derivative

$$f'(\rho) = V(1-2\rho)$$

and insert the left and right state for $\rho^L < \rho^R$. Then, we obtain

$$\begin{aligned}f'(\rho^L) =& V(1-2\rho^L) \\ >& V(1-\rho^L-\rho^R) \\ =& \sigma\end{aligned}$$

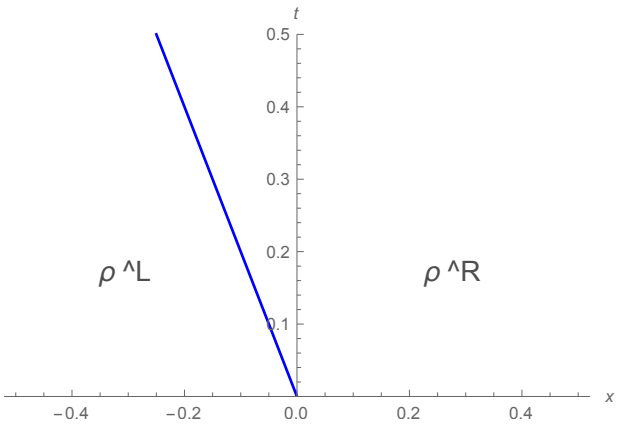

Figure 2.2: A sample of a shock curve connecting the left ($\rho^L = 0.5$) to the right ($\rho^R = 1.0$) state with speed σ as solution to the corresponding RP.

for the right state and

$$\begin{aligned} f'(\rho^R) =& V(1 - 2\rho^R) \\ <& V(1 - \rho^L - \rho^R) \\ =& \sigma \end{aligned}$$

for the left one. Hence, the Lax inequality holds. □

The shock solution is a discontinuous solution to the RP. The solution holds the values of the initial datum and as time develops the location of the discontinuity travels with speed σ. An example of a fitting traffic situation can be observed, if there is a traffic jam on the road. Due to that, the cars have to brake when they notice the congestion. This happens instantaneous and is described by a shock. We discuss this situation again in the next section where we consider traffic examples.

Now, we deal with the case that $\rho^L > \rho^R$. Therefore, the solution consists of a rarefaction wave connecting the left and right state smoothly. The solution is determined in Rosini [2013]

$$\rho(x,t) = \begin{cases} \rho^L & \text{for} \quad \dfrac{x}{t} < f'(\rho^L) \\ G\left(\dfrac{x}{t}\right) & \text{for} \quad f'(\rho^L) < \dfrac{x}{t} < f'(\rho^R) \\ \rho^R & \text{for} \quad \dfrac{x}{t} > f'(\rho^R) \end{cases} \tag{2.12}$$

with $G\left(\frac{x}{t}\right) = (f')^{-1}$. Since the flow f is a strictly concave, smooth function of ρ the derivative f' is a linear and smooth function and we can define $(f')^{-1}$.

Corollary 2.3.3. *For a Riemann problem with $\rho^L > \rho^R$ the solution is given by a rarefac-*

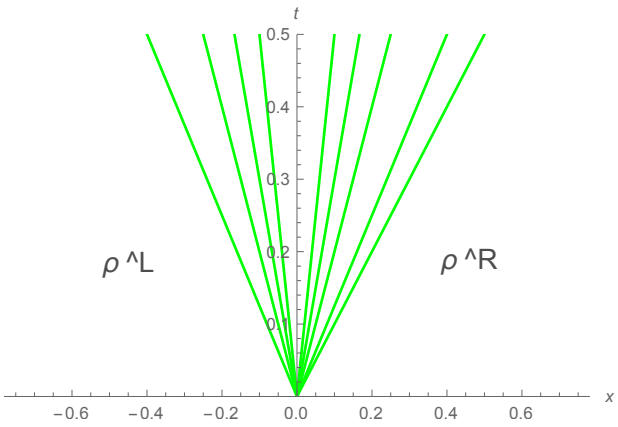

Figure 2.3: Example of a rarefaction wave (green fan) with $V = 1$ and the RP $\rho^L = 0.9,\ \rho^R = 0.01$.

tion wave

$$\rho(x,t) = \begin{cases} \rho^L & for \quad \frac{x}{t} < V(1-2\rho^L) \\ \frac{1}{2}\left(1 - \frac{x}{Vt}\right) & for \quad V(1-2\rho^L) < \frac{x}{t} < V(1-2\rho^R). \\ \rho^R & for \quad \frac{x}{t} > V(1-2\rho^R) \end{cases} \tag{2.13}$$

Proof. The derivative of the flow function $f(\rho)$ is given by

$$f'(\rho) = V(1-2\rho)$$

and solving for ρ yields

$$\rho = \frac{1}{2}\left(1 - \frac{f'(\rho)}{V}\right).$$

With this we get the function $G(x/t)$ as

$$G\left(\frac{x}{t}\right) = \frac{1}{2}\left(1 - \frac{x}{Vt}\right)$$

and equation (2.13) from (2.12). □

In 2.3 we see an example of a rarefaction wave smoothly connecting the left and right state in the x-t-plane. Note that in contrast to the shock wave a rarefaction wave is a continuous solution to the RP. The initial values are smoothed out by the rarefaction as time develops. A possible traffic example is the acceleration of cars due to lighter traffic ahead. We present this situation in the next part. Altogether we have proven the well-posedness of the RP for the LWR model. Additionally, Lax [1957] has shown that the solutions are unique.

Theorem 2.3.4. *The RP of the LWR model with the Greenshields velocity function (2.6) is well-posed. For $\rho^L < \rho^R$ the solution consists of a single shock (2.9) with speed σ (2.8) and for $\rho^L > \rho^R$ it provides a rarefaction wave as in (2.12).*

The technique of wave front tracking presents us information about the well-posedness of the more general Cauchy problem as is considered in Rosini [2013]. For this, it is essential that the Riemann problem is well-posed. Due to that, we skip the observation of other initial value problems than the RP and go on with the already mentioned examples. Moreover, we study the so called particle paths of the vehicles.

2.4 Car paths

We have already introduced the LWR model and discussed the solution to the RP. As a next step, we construct the solution for two traffic examples and compute the function that describes the movement of the cars, i.e. the car path.

First, we introduce the car paths. The path of a car $p(t)$ can be described with the help of the velocity function

$$\frac{dp(t)}{dt} = u(t, p(t)) = u(\rho(t, p(t))), \tag{2.14}$$

where the second equality holds due to the assumption that the velocity only depends on the density. This is an ordinary differential equation (ODE). As initial datum we take the car's location x_0 at time $t = 0$

$$p(0) = x_0.$$

We choose the Greenshields velocity function which is continuous and decreasing. But for well-posedness of (2.14) we need to check the density as a function of t and $p(t)$. Since we consider a RP as initial datum we are not provided with a continuous density function and so we are not able to use standard theorems of well-posedness for ODE with continuous right hand sides. In Colombo and Marson [2003] the well-posedness of (2.14) with initial data $p(0) = x_0$ is discussed. It turns out that since

$$\frac{u(0) - u(\rho)}{u(0) - f'(\rho)} = \frac{1}{2} \in [0, 1 - \alpha)$$

for all α in the interval $(1/2, 0)$ the conditions in the well-posedness theorem of Colombo and Marson [2003] hold. This guarantees us the existence of an unique, so called Filippov solution. Now, we discuss the solutions to (2.14) with $p(0) = x_0$. We again differ between the cases $\rho^L < \rho^R$ and $\rho^L > \rho^R$.

First consider $\rho^L < \rho^R$. From the last section, we know that the solution consists of a shock with speed σ. It can be positive or negative depending on ρ^L and ρ^R

$$\sigma = \begin{cases} < 0 & \text{for} \quad 1 < \rho^L + \rho^R < 2 \\ \geq 0 & \text{for} \quad 0 < \rho^L + \rho^R \leq 1 \end{cases}.$$

We compute the velocity of cars with $x_0 < 0$ at time $t = 0$

$$\begin{aligned} u(x,t) &= u(\rho(x,t)) \\ &= V(1-\rho^L) \end{aligned}$$

and for cars with $x_0 > 0$

$$\begin{aligned} u(x,t) &= u(\rho(x,t)) \\ &= V(1-\rho^R). \end{aligned}$$

Only the paths of cars starting left of the shock intersect with it. This happens at time

$$t = \frac{x_0}{\sigma - V(1-\rho^L)}.$$

Thus, one can integrate the ODE for $t < x_0/\sigma - V(1\rho^L)$ and for $t > x_0/\sigma - V(1-\rho^L)$ and we obtain

$$\begin{aligned} p(t) =& Vt(1-\rho^L) + c_1 \\ p(t) =& Vt(1-\rho^R) + c_2 \end{aligned}$$

with constants $c_1, c_2 > 0$ which are given by the starting point of the cars x_0. Altogether, we find a function $p_{x_0}(t)$ describing the path of a car for $\rho^L < \rho^R$ starting at $x = x_0$

$$p_{x_0}(t) = \begin{cases} Vt(1-\rho^L) + x_0 & \text{for} \quad t < \dfrac{x_0}{\sigma - V(1-\rho^L)} \\ Vt(1-\rho^R) + x_0 & \text{for} \quad t > \dfrac{x_0}{\sigma - V(1-\rho^L)} \end{cases}. \tag{2.15}$$

The following example describes a situation fitting to this case.

Example 2.4.1. *Congestion ahead.*
Consider a situation of a traffic jam with end at $x = 0$. Assume that the maximal velocity is set to $V = 1$. Hence, for ρ^R we have maximal density $\rho^R = 1$. For ρ^L we choose $\rho^L = 0.5$. The solution is given by a shock with speed $\sigma = -0.5$ from (2.9)

$$\rho(x,t) = \begin{cases} 0.5 & \textit{for} \quad x < -0.5t \\ 1 & \textit{for} \quad x > -0.5t \end{cases}. \tag{2.16}$$

The characteristics can be seen in figure 2.4. We observe that this solution is discontinuous. The characteristics end in the shock. Then, from (2.15) we obtain the car path

$$p_{x_0}(t) = \begin{cases} 0.5t + x_0 & \textit{for} \quad t < -x_0 \\ x_0 & \textit{for} \quad t > -x_0 \end{cases}. \tag{2.17}$$

Figure 2.5 (a) shows the car paths for this example in the x-t-plane. The shock is marked by the red line while the blue arrows plot the car paths for different starting points x_0. We see that on the left side of the shock the cars move with constant velocity until they close up

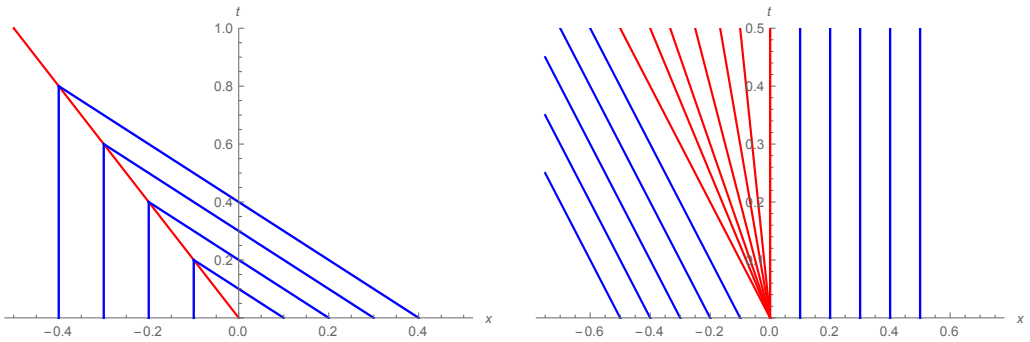

(a) For $\rho^L < \rho^R$ the solution to the corresponding RP consists of a shock.

(b) For $\rho^L > \rho^R$ the solution consists of a rarefaction wave.

Figure 2.4: Sample of characteristics for a shock and a rarefaction wave. The red lines stand for the shock or boundaries of the rarefaction. The blue lines describe the characteristics.

to the congestion. This is when the information of the denser traffic reaches them. Then, they have to stop due to the traffic situation in front of them. The cars on the right side of the shock do not move. As more cars arrive at the jam the end of it wanders to the left. This can be observed because the shock has negative speed and hence as time develops more and more cars are forced to stop.

The particle paths look different for the case $\rho^L > \rho^R$ where the solution to the RP consists of a rarefaction wave (2.13). The path of cars is again described by (2.14). We have to solve the ODE left, right and inside of the rarefaction fan. The fan like region is restricted by the characteristic speed for ρ^L and ρ^R.

$$\begin{aligned} f'(\rho^L) &= V(1 - 2\rho^L) \\ f'(\rho^R) &= V(1 - 2\rho^R). \end{aligned}$$

Just as for the shock, on the left and right hand side of the fan the velocity of cars for $t = 0$ is constant and given by the velocity function. We again compute it for a car with $x_0 < 0$

$$\begin{aligned} u(x,t) &= u(\rho(x,t)) \\ &= V(1 - \rho^L) \end{aligned}$$

and for a car with $x_0 > 0$

$$\begin{aligned} u(x,t) &= u(\rho(x,t)) \\ &= V(1 - \rho^R). \end{aligned}$$

As time passes, the paths of cars with starting point left of the rarefaction, i.e. with $x_0 < 0$, intersect with the boundary of the fan for

$$t = \frac{|x_0|}{f'(\rho^L)}.$$

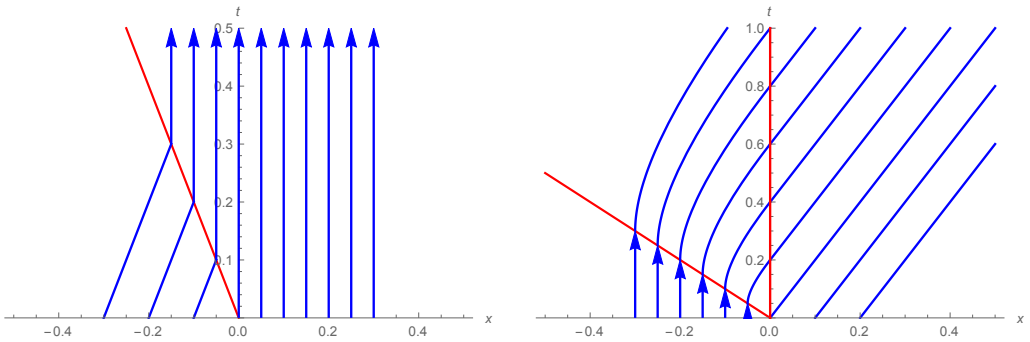

(a) Congestion ahead. The PDE is solved by a shock and the cars have to brake instantly when the information of the jam ahead reaches them.

(b) A traffic light turns green. Here, the cars accelerate until they cross the light and then drive on with constant velocity.

Figure 2.5: Car paths for two special traffic situations located at $x = 0$ with $V = 1$. The red lines describe the shock or the boundaries of the rarefaction and the blue lines describe the car paths for different initial data x_0.

Then, for $t < |x_0| / f'(\rho^L)$, i.e. left of the rarefaction, the path for a car with $x_0 < 0$ is described by

$$p(t) = Vt(1 - \rho^L) + x_0$$

and for a car starting on the right side of the rarefaction, i.e. $x_0 > 0$, the path is described by

$$p(t) = Vt(1 - \rho^R) + x_0.$$

Inside the fan like region of the rarefaction the speed of the characteristics equals

$$\frac{x}{t} = \frac{df}{d\rho} = V(1 - 2\rho).$$

Solving for ρ

$$\rho = \frac{1}{2}\left(1 - \frac{x}{Vt}\right),$$

and inserting this in (2.14) yields a linear non homogeneous ODE

$$\frac{dp(t)}{dt} = \frac{V}{2} + \frac{p(t)}{2t}. \tag{2.18}$$

The homogeneous equation has the solution

$$p(t) = Bt^{\frac{1}{2}} \tag{2.19}$$

with the constant $B > 0$. The general solution is given by

$$p(t) = Vt + Bt^{\frac{1}{2}} \tag{2.20}$$

where the initial condition determines B. After passing the right boundary of the fan the cars have the same constant velocity as the ones with $x_0 > 0$. So, the paths of cars are straight lines left and right of the fan but curves inside. The next example deals with a situation where we have this case.

Example 2.4.2. *Traffic light turns green.*
Consider a road with a traffic light at $x = 0$ and assume that the light was red for a certain period. Behind the stoplight there are no vehicles that passed the light but we consider that cars entered from a different road and we set $\rho^R = 0.5$. This example describes a traffic light controlling a junction. Since, behind the light a lot of cars arrived during the red period, we have $\rho^L = 1$. If the traffic light turns green the cars behind the light accelerate until they reach a velocity fitting to the traffic situation ahead. The solution to this RP consists of a rarefaction wave. We again set $V = 1$. Figure 2.4 confirms that this solution is continuous. The rarefaction fan smooths out the different speed of characteristics on the left and right side. With (2.12) the solution is given by

$$\rho(x,t) = \begin{cases} 1 & \text{for} \quad \frac{x}{t} < -1 \\ 0.5\left(1 - \frac{x}{t}\right) & \text{for} \quad -1 < \frac{x}{t} < 0. \\ 0.5 & \text{for} \quad \frac{x}{t} > 0 \end{cases} \tag{2.21}$$

Then, the boundaries of the fan can be computed

$$\begin{aligned} f'(\rho^L) =& V(1 - 2\rho^L) \\ =& -V \\ =& -1, \\ f'(\rho^R) =& V(1 - 2\rho^R) \\ =& 0 \end{aligned}$$

and for a car starting left of the fan we get $p_{x_0}(t) = x_0$ because it does not move there. The path intersects the fan at time

$$t = \frac{|x_0|}{V} = |x_0|\,.$$

Inside of the fan, i.e. for $|x_0|/V < t < 0$ we get the ODE (2.18) with solution

$$p(t) = Vt + Bt^{\frac{1}{2}} = t + Bt^{\frac{1}{2}}$$

where we have to determine B. For this purpose, we demand that

$$p_{x_0}(0) = x_0$$

and get $B = -2(|x_0|)^{\frac{1}{2}}$. Altogether, the car path inside the fan is given by

$$p(t) = Vt - 2(|x_0|\,Vt)^{\frac{1}{2}}$$

where we set the absolute value of x_0. *After accelerating and passing the light at* $x = 0$ *the cars drive on for* $t = 4\,|x_0|\,/V$ *with the constant velocity given by*

$$u(\rho^R) = 0.5V = 0.5.$$

There, the solution to the ODE is given by

$$p(t) = 0.5Vt + c$$

and we determine c *by claiming that the path of a car is continuous and obtain* $c = 2x_0$. *All in all, the car path for* $x_0 < 0$ *is described by*

$$p_{x_0}(t) = \begin{cases} x_0 & \textit{for} \quad t < |x_0| \\ t - 2(|x_0|\,t)^{\frac{1}{2}} & \textit{for} \quad |x_0| < t < 4\,|x_0| \\ 0.5t + 2x_0 & \textit{for} \quad t > 4\,|x_0| \end{cases}.$$

and for $x_0 > 0$ we obtain

$$p_{x_0}(t) = 0.5t + x_0. \tag{2.22}$$

The corresponding x-t-plot can be seen in figure 2.5 (b). The boundaries of the rarefaction fan are marked by the red lines. The blue lines describe the car paths. We see that left of the fan the cars do not move and start to accelerate when the information of the green light in front reaches them. After passing the light they adapt their velocity to the situation behind the light. Note that inside of the rarefaction fan the paths are given by a curve instead of a line caused by the acceleration of the cars.

The presented examples are generic because for different values of ρ^L and ρ^R the general manner of the car paths does not change.

With these two examples we close the section for the standard LWR model and start the discussion of an extension of this model allowing two or three different kinds of vehicles on the road. For consistency we compare the extensions with the standard LWR model.

3 LWR Model for two species

Since there is a significant variation in the participants of traffic, it is of interest to distinguish the traffic members in groups of fast and slow moving vehicles. For this purpose, we extend the LWR model introduced in the last chapter to a two species model with different species of vehicles like it was done by Benzoni-Gavage and Colombo [2003]. For two species the LWR model is given by two PDEs. The first one describes the fast moving species 1 with density $\rho_1 \geq 0$ and velocity $V_1 > 0$ and the other PDE models the second species 2 with $\rho_2 \geq 0$ and $V_2 > 0$. The maximal density is set to 1, thus one gets $\rho_1 + \rho_2 \leq 1$. The equations are coupled through the velocity function $\mathbf{U}(\rho_1, \rho_2) = (U_1(\rho_1, \rho_2), U_2(\rho_1, \rho_2))^\intercal$. Since species 1 describes the faster vehicles, we require $V_1 > V_2$. Altogether, the system to describe two species of cars can be defined.

Definition 3.0.3. *The LWR model for two species is given by the system of partial differential equations*

$$\begin{aligned} \partial_t \rho_1 + \partial_x f_1(\rho_1, \rho_2) &= 0 \\ \partial_t \rho_2 + \partial_x f_2(\rho_1, \rho_2) &= 0 \end{aligned} \tag{3.1}$$

with $\mathbf{f}(\rho_1, \rho_2) = (f_1, f_2)^\intercal = (\rho_1 U_1(\rho_1, \rho_2), \rho_2 U_2(\rho_1, \rho_2))^\intercal$. *It is defined on the simplex*

$$\mathcal{S} = \{(\rho_1, \rho_2) \in \mathbb{R}^2 | \rho_1, \rho_2 \geq 0; \rho_1 + \rho_2 \leq 1\}. \tag{3.2}$$

We now study this system and see whether it is well-posed or not. This provides some difficulties, since (3.1) is not strictly hyperbolic in $\mathcal{S}$. In the following section, we show that the existence of an umbilic point, where the eigenvalues coalesce and hence the system is not hyperbolic, cannot be avoided. Then, we consider the RP with the extended Greenshields function for the second species absent, i.e the initial data equals zero for the second species, to check the extension's convenience with the LWR model. After the study of solutions to this RP we examine continuous dependence and introduce the general RP and also a variation of the velocity function.

3.1 General velocity function

First of all, one can examine the hyperbolicity of system (3.1) for a general velocity function $\mathbf{U}(\rho_1, \rho_2) = (V_1 \psi(\rho_1, \rho_2), V_2 \psi(\rho_1, \rho_2))^T$. We request that ψ is a monotone decreasing $\mathcal{C}^1$-function, i.e. $\psi' < 0$, $\psi(0) = 1$ and $\psi(1) = 0$. Moreover, ψ should only depend on the sum of the densities $r = \rho_1 + \rho_2$. Thus, we get $\psi(\rho_1, \rho_2) = \psi(r)$ and system (3.1) becomes

$$\begin{aligned} \partial_t \rho_1 + \partial_x(\rho_1 V_1 \psi(r)) &= 0 \\ \partial_t \rho_2 + \partial_x(\rho_2 V_2 \psi(r)) &= 0. \end{aligned}$$

Writing the two equations as one vector-valued equation

$$\partial_t \boldsymbol{\rho} + \partial_x \mathbf{f}(\boldsymbol{\rho}) = \mathbf{0}$$

with $\boldsymbol{\rho} = (\rho_1, \rho_2)^\intercal$ and $\mathbf{f}(\boldsymbol{\rho}) = (\rho_1 V_1 \psi(r), \rho_2 V_2 \psi(r))^\intercal$ yields the Jacobian $J(\boldsymbol{\rho})$ of the system

$$\partial_t \boldsymbol{\rho} + J(\boldsymbol{\rho}) \partial_x \boldsymbol{\rho} = \mathbf{0}.$$

It is given by

$$J(\boldsymbol{\rho}) = \begin{pmatrix} V_1(\psi(r) + \psi'(r)\rho_1) & V_1\psi'(r)\rho_1 \\ V_2\psi'(r)\rho_2 & V_2(\psi(r) + \psi'(r)\rho_2) \end{pmatrix}.$$

To compute the eigenvalues of $J(\boldsymbol{\rho})$ we look at the characteristical polynomial

$$\pi(\boldsymbol{\rho}) = (\beta_1 - \lambda)(\beta_2 - \lambda) - \alpha_1\alpha_2$$

where

$$\begin{aligned} \beta_i &= V_i(\psi(r) + \rho_i\psi'(r)) \\ \alpha_i &= V_i\rho_i\psi'(r). \end{aligned}$$

Then, the eigenvalues are found as the roots of $\pi(\boldsymbol{\rho})$

$$\lambda_{1/2} = \frac{1}{2}\left[(\beta_1 + \beta_2) \pm \sqrt{(\beta_1 - \beta_2)^2 + 4\alpha_1\alpha_2}\right].$$

Since $\rho_1, \rho_2 \geq 0$ and $V_1, V_2 > 0$, the discriminant δ of the eigenvalues

$$\begin{aligned} \delta &= (\beta_1 - \beta_2)^2 + 4\alpha_1\alpha_2 \\ &= (V_1(\psi + \rho_1\psi') - V_2(\psi + \rho_2\psi'))^2 + 4V_1V_2\rho_1\rho_2(\psi')^2 \end{aligned}$$

is always greater or equal than zero. Hence, system (3.1) is hyperbolic. The eigenvalues coalesce if $\delta = 0$. The equation

$$(V_1(\psi + \rho_1\psi') - V_2(\psi + \rho_2\psi'))^2 + 4V_1V_2\rho_1\rho_2(\psi')^2 = 0 \tag{3.3}$$

has a real solution only for $\rho_1 = 0$ or $\rho_2 = 0$. Moreover, since we claimed $V_1 > V_2$ and $\psi' < 0$ the particular possibility to find a solution to (3.3) is

$$\rho_2 = 0 \quad \text{and} \quad (V_2 - V_1)\psi(\rho_1) = V_1\rho_1\psi'(\rho_1).$$

By recalling the properties of the function ψ we see that the function

$$\rho_1 \mapsto (V_2 - V_1)\psi(\rho_1) - V_1\rho_1\psi'(\rho_1)$$

changes its sign between $\rho_1 = 0$ and $\rho_1 = 1$, if ψ is a $\mathcal{C}^1$-function. Thus, for $\rho_2 = 0$ there is always one value of ρ_1 where the discriminant vanishes and therefore the eigenvalues coalesce.

Proposition 3.1.1. *System (3.1) is strictly hyperbolic in $\mathcal{S}$ except for one value on the ρ_1-axis, where its two eigenvalues coalesce. This happens for every $\mathcal{C}^1$-velocity function $\mathbf{U}(r) = (V_1\psi(r), V_2\psi(r))^T$ with $\psi(0) = 1$ and $\psi(1) = 0$.*

The assumptions we make about the function ψ are inspired by the characteristical behavior of traffic, thus they are reasonable. But then, we see that there is no way in finding a velocity function for which the eigenvalues of system (3.1) are distinct on the whole set (3.2). The LWR model for two species provides one umbilical point where the eigenvalues are the same and hence at this point the system is not strictly hyperbolic. We have to ask for the consequences of the existence of this point on the well-posedness of (3.1). Another system, where hyperbolicity is not strictly given, is studied by Keyfitz and Kranzer [1979/80] and Liu et al. [2016]. Yet, the model discussed here differs from the Keyfitz-Kranzer model because there the umbilic point lies in the interior of the set of definition. In our case the umbilic point lies on the boundary of the simplex $\mathcal{S}$.

Since the model delivers one umbilic point for every choice of a $\mathcal{C}^1$-function ψ we consider a special velocity function from now on.

3.2 Greenshields velocity function

The last subsection showed that there always exists one point in the set $\mathcal{S}$ from (3.2), where system (3.1) is not strictly hyperbolic. Yet, we study the LWR model for the Greenshields velocity function which is the most common velocity function for the one species LWR model. We investigate the well-posedness of this model for the Riemann problem. Proposition 3.1.1 implies that for initial data with small variation around any state different from the umbilic point the Riemann problem is well-posed for all times as is discussed in Bressan [2000]. But we do not know what happens near the umbilic point and for initial data that does not fulfill small variation. These features are important for the here discussed model and so we have to address the well-posedness by discussing the Riemann problem. We are not allowed techniques like vanishing viscosity or entropy solution due to the lack of global hyperbolicity.

For two species we could extend the Greenshields function (2.4) to $\mathbf{U}(\rho_1, \rho_2) = (V_1(1 - \rho_1 - \rho_2), V_2(1 - \rho_1 - \rho_2))^\intercal$. Then, the flux function is

$$\mathbf{f}(\rho_1, \rho_2) = (\rho_1 V_1(1 - \rho_1 - \rho_2), \rho_2 V_2(1 - \rho_1 - \rho_2))^\intercal \tag{3.4}$$

and we get the system

$$\begin{aligned} \partial_t \rho_1 + \partial_x(\rho_1 V_1(1 - \rho_1 - \rho_2)) = 0, \\ \partial_t \rho_2 + \partial_x(\rho_2 V_2(1 - \rho_1 - \rho_2)) = 0, \end{aligned} \tag{3.5}$$

with maximal speeds $V_1 > V_2 > 0$ and $\rho_1, \rho_2 \in \mathcal{S}$, where

$$\mathcal{S} = \{(\rho_1, \rho_2) | \rho_1, \rho_2 \geq 0; \rho_1 + \rho_2 \leq 1\}.$$

The following statement holds.

Theorem 3.2.1. *System (3.5) is strictly hyperbolic in $\mathcal{S}\backslash\{\boldsymbol{\rho}^u\}$. At $\boldsymbol{\rho}^u$*

$$\boldsymbol{\rho}^u = (\rho_1^u, 0) \quad \textit{with} \quad \rho_1^u = \frac{V_1 - V_2}{2V_1 - V_2},$$

the eigenvalues λ_1 and λ_2 coalesce.

Proof. Using the results from the last subsection, the Jacobian matrix of the system is given by

$$J(\rho_1, \rho_2) = \quad (1 - \rho_1 - \rho_2) \begin{pmatrix} V_1 & 0 \\ 0 & V_2 \end{pmatrix} - \begin{pmatrix} V_1\rho_1 & V_1\rho_1 \\ V_2\rho_2 & V_2\rho_2 \end{pmatrix}. \tag{3.6}$$

The eigenvalues

$$\begin{aligned}
\lambda_1 =& \frac{1}{2}\Big[V_1(1 - 2\rho_1 - \rho_2) + V_2(1 - \rho_1 - 2\rho_2) \\
& - \sqrt{(V_1(1 - 2\rho_1 - \rho_2) - V_2(1 - \rho_1 - 2\rho_2))^2 + 4V_1V_2\rho_1\rho_2}\Big] \\
\lambda_2 =& \frac{1}{2}\Big[V_1(1 - 2\rho_1 - \rho_2) + V_2(1 - \rho_1 - 2\rho_2) \\
& + \sqrt{(V_1(1 - 2\rho_1 - \rho_2) - V_2(1 - \rho_1 - 2\rho_2))^2 + 4V_1V_2\rho_1\rho_2}\Big]
\end{aligned}$$

coincide at $\boldsymbol{\rho}^u$ and since the function ψ is $\mathcal{C}^1$ and monotone, there is no other value in $\mathcal{S}$ where this happens. Moreover, the eigenvalues are real for $V_1, V_2 > 0$ and $\rho_1, \rho_2 \geq 0$. Thus, system (3.5) is strictly hyperbolic in $\mathcal{S}\backslash\{\rho_u\}$. □

Indeed, by plotting the points where the eigenvalues merge for some special values of V_1, V_2 we see in (3.1) that there is only one point in the set $\mathcal{S}$ where this happens. One can mention that the eigenvalues, i.e. the characteristic speeds, are always less or equal than the car velocities. This is an important feature of the model because traffic participants are only influenced by the incidents in front of them. It implies that the speed of the solution to the RP must be slower or equal the maximal velocities of cars. As has already been stated in Benzoni-Gavage and Colombo [2003] the LWR model for two species fulfills this property. With the abbreviations from the last section (3.1)

$$\begin{aligned}
\beta_i &= V_i(\psi + \psi'\rho_i) \\
\alpha_i &= -V_i\psi'\rho_i \\
\delta &= (\beta_1 - \beta_2)^2 + 4\alpha_1\alpha_2
\end{aligned} \tag{3.7}$$

one could write the eigenvalues as

$$\begin{aligned}
\lambda_1 &= \frac{1}{2}(\beta_1 + \beta_2 - \sqrt{\delta}) \\
\lambda_2 &= \frac{1}{2}(\beta_1 + \beta_2 + \sqrt{\delta}).
\end{aligned}$$

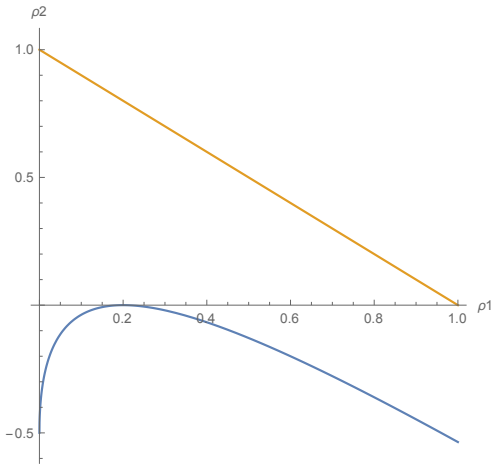

Figure 3.1: Values of ρ_1, ρ_2 where the eigenvalues coalesce for $V_1 = 1$ and $V_2 = 0.75$ together with the simplex $\mathcal{S}$.

Then, they are ordered as follows

$$\lambda_1 \leq \lambda_2.$$

Mention that for $\rho_2 = 0$ the eigenvalues are linear functions in ρ_1 and intersect at ρ_1^u. For the eigenvalues we get

$$\begin{aligned} \lambda_1(\rho_1, 0) &= \begin{cases} V_2(1-\rho_1) & \text{for} \quad \rho_1 < \rho_1^u \\ V_1(1-2\rho_1) & \text{for} \quad \rho_1 > \rho_1^u \end{cases}, \\ \lambda_2(\rho_1, 0) &= \begin{cases} V_1(1-2\rho_1) & \text{for} \quad \rho_1 < \rho_1^u \\ V_2(1-\rho_1) & \text{for} \quad \rho_1 > \rho_1^u \end{cases}. \end{aligned} \tag{3.8}$$

This feature will be important later on.

With the above abbreviations (3.7), a choice of corresponding eigenvectors is given by

$$\mathbf{v}_1 = \begin{pmatrix} \lambda_1 - \beta_2 - \alpha_1 \\ \lambda_1 - \beta_1 - \alpha_2 \end{pmatrix}, \mathbf{v}_2 = \begin{pmatrix} -\lambda_2 + \beta_2 - \alpha_1 \\ \lambda_2 - \beta_1 + \alpha_2 \end{pmatrix}. \tag{3.9}$$

Lemma 3.2.2. *In the umbilic point $\boldsymbol{\rho}^u = (\rho_1^u, 0)$ the Jacobian matrix is not diagonizable and, in addition to its eigenvalues, its eigenvectors coalesce, too. Hence, for this value there exists no basis of eigenvectors for system (3.5).*

Proof. If we insert the umbilic point into the Jacobian (3.6) we get the matrix

$$J(\rho_1^u, 0) = \begin{pmatrix} V_1(1-2\rho_1^u) & -V_1\rho_1^u \\ 0 & V_2(1-\rho_1^u) \end{pmatrix}$$

which is not diagonizable. By inserting $\boldsymbol{\rho}^u$ into (3.9) we see that

$$\mathbf{v}_1(\rho_1^u, 0) = \mathbf{v}_2(\rho_1^u, 0) = \begin{pmatrix} -V_1\rho_1^u \\ 0 \end{pmatrix}$$

indeed the eigenvalues are the same and hence there exists no basis of eigenvectors in the umbilic point. □

We discuss this feature more properly when dealing with rarefaction waves for the Riemann problem.

The next proposition describes the characteristic fields like in Serre [1999].

Proposition 3.2.3. *In $\mathcal{S}\backslash\{\boldsymbol{\rho}^u\}$ the first characteristic field is genuinely nonlinear. The second characteristic field is linearly degenerate for $\rho_1 + \rho_2 = 1$ and genuinely nonlinear elsewhere.*

For the proof of this statement we refer to Benzoni-Gavage and Colombo [2003] because the standard technique by computing $d\lambda_i \cdot \mathbf{v}_i$ does not work, here. We also state arguments about the invariance of the set $\mathcal{S}$. By Hoff [1985] the following statement holds

Proposition 3.2.4. *A set is locally invariant under a strictly hyperbolic and genuinely nonlinear system of conservation laws if the domain is convex and the normal to the boundary is a left eigenvector of the system.*

We already know that (3.39) is not strictly hyperbolic and that for $\rho_1 + \rho_2 = 1$ it is linearly degenerate. But nevertheless, from

$$\begin{aligned} (1,1)J &= -(\rho_1 V_1 + \rho_2 V_2)(1,1) \\ (1,0)J &= V_1(1-\rho_2)(1,0) \\ (0,1)J &= V_2(1-\rho_1)(0,1) \end{aligned} \tag{3.10}$$

we see that the normals to the convex set $\mathcal{S}$ are indeed left eigenvectors of the Jacobian J of (3.5). Thus, we suppose that $\mathcal{S}$ is invariant what implies that for initial data inside $\mathcal{S}$ the solution will lie inside, too.

With the above discussion one can now study the Riemann Problem.

3.2.1 The Riemann Problem on the ρ_1-axis

After the examination of general features of the LWR model for two species for the Greenshields velocity function, we investigate its well-posedness. As we have already seen, the existence of the umbilic point hinders us from using existence and uniqueness theorems of hyperbolic conservation laws. Hence, we start with the discussion of existence for a special RP. The general Riemann Problem (RP) is given by system (3.5) with initial data

$$\boldsymbol{\rho}(x,0) = \begin{cases} \boldsymbol{\rho}^L = (\rho_1^L, \rho_2^L) & \text{for} \quad x < 0 \\ \boldsymbol{\rho}^R = (\rho_1^R, \rho_2^R) & \text{for} \quad x > 0 \end{cases}.$$

Because we have seen that (3.5) is not strictly hyperbolic, the question is whether the existence of the umbilical point influences the solution of the RP or not. Note, that if we define system (3.5) on $\mathcal{S}\backslash\{\boldsymbol{\rho}^u\}$, then it will indeed be strictly hyperbolic and thus

the solution to the RP can be found by following the standard Lax-theory (Lax [1957]). Moreover, (3.5) is well-posed on all initial data with small variation for all times (Bressan [2000]). But if we take the point $\boldsymbol{\rho}^u$ into account, it will not be clear whether the solution to the RP problem is well-defined. Nevertheless, we can use the Lax-theory to discover the Lax curves and construct the solution to the RP while taking care of what happens near the umbilic point. The algebraic terms are hard to handle and there exists no direct proof of the well-posedness. But one can examine how the umbilical point affects the solution of the RP for a special case. Hence, consider the situation where the slower species is absent at the beginning, i.e. $\rho_2^L, \rho_2^R = 0$. This yields the RP on the ρ_1-axis, which is (3.5) together with the

$$\boldsymbol{\rho}(x,0) = \begin{cases} \boldsymbol{\rho}^L = (\rho_1^L, 0) & \text{for} \quad x < 0 \\ \boldsymbol{\rho}^R = (\rho_1^R, 0) & \text{for} \quad x > 0 \end{cases}. \tag{3.11}$$

Then, we have to include $\boldsymbol{\rho}^u$ into the discussion since the initial data lies on the same axis as the umbilic point. Given any point $\boldsymbol{\rho}$ in $\mathcal{S}$, the Lax curves $\mathcal{L}^i(\boldsymbol{\rho})$ are determined by the integral rarefaction curve of the i-th eigenvector along increasing λ_i together with the Hugoniot shock curves. We state a general feature of the curves first and then describe the Hugoniot curves.

Lemma 3.2.5. *By examining the eigenvectors and dealing with ρ_2 as a function of ρ_1, one sees that the integral curves are monotone and concave, while the Hugoniot curves are concave but may have a maximum in the interior of $\mathcal{S}$.*

Proof. For the above eigenvectors (3.6) the following inequalities hold

$$\begin{aligned} v_{11} \leq 0; \quad v_{12} \leq 0 \\ v_{21} \leq 0; \quad v_{22} \geq 0 \end{aligned}$$

where $\mathbf{v}_i = (v_{i1}, v_{i2})^\intercal$ for $i = 1, 2$. Moreover, the equivalences

$$\begin{aligned} v_{11} = 0 \Longleftrightarrow \rho_1 = 0 \text{ and } min\{\beta_1, \beta_2\} = \beta_2 \\ v_{12} = 0 \Longleftrightarrow \rho_2 = 0 \text{ and } min\{\beta_1, \beta_2\} = \beta_1 \end{aligned}$$

cannot both be fulfilled in $\mathcal{S}$ since $\beta_1 = \beta_2$ does not hold for $V_1 \neq V_2$ as we have seen in (3.7). The same counts for the second eigenvector, since

$$\begin{aligned} v_{21} = 0 \Longleftrightarrow \rho_1 = 0 \text{ and } min\{\beta_1, \beta_2\} = \beta_2 \\ v_{22} = 0 \Longleftrightarrow \rho_2 = 0 \text{ and } min\{\beta_1, \beta_2\} = \beta_1. \end{aligned}$$

Hence, the integral curves are monotone. For the curvature see Benzoni-Gavage and Colombo [2003]. □

As a next step we compute the solutions to the RP (3.11). Since the flux function (3.4) is concave in each entry, the solution to the RP for one species consists of shocks if $\rho_1^L < \rho_1^R$ and of rarefaction waves if $\rho_1^L > \rho_1^R$. First, we turn to the discontinuities. The shock curves

are described with the help of the Rankine Hugoniot (RH) condition. For a given point $\boldsymbol{\rho}^L = (\rho_1^L, 0)$ a shock of the first family through this point, tangent respectively to $\mathbf{v}_1$, is denoted by $\mathcal{S}_1(\boldsymbol{\rho}^L)$. Similarly, a shock of the second family is given by $\mathcal{S}_2(\boldsymbol{\rho}^L)$, tangent respectively to $\mathbf{v}_2$.

Proposition 3.2.6. *A shock exiting $\boldsymbol{\rho}^L \in \mathcal{S}$ and a shock entering $\boldsymbol{\rho}^R \in \mathcal{S}$ need to fulfill the Rankine Hugoniot condition*

$$\begin{aligned} \sigma(\boldsymbol{\rho}^L - \boldsymbol{\rho}) &= \mathbf{f}(\boldsymbol{\rho}^L) - \mathbf{f}(\boldsymbol{\rho}), \\ \gamma(\boldsymbol{\rho} - \boldsymbol{\rho}^R) &= \mathbf{f}(\boldsymbol{\rho}) - \mathbf{f}(\boldsymbol{\rho}^R) \end{aligned} \tag{3.12}$$

with shock speeds $\sigma \in \mathbb{R}$ and $\gamma \in \mathbb{R}$ and $\boldsymbol{\rho} \in \mathcal{S}$.

If $\boldsymbol{\rho}$ belongs to the ρ_1-axis, i.e. $\boldsymbol{\rho} = (\rho_1, 0)$ we are able to describe the Hugoniot curves completely. Therefore, look at the Hugoniot set through the point $\boldsymbol{\rho}^0 \in \mathcal{S}$

$$\mathcal{H}(\boldsymbol{\rho}^0) = \{(\rho_1, \rho_2) \in \mathbb{R}^2, \sigma \in \mathbb{R} |\ (3.13) \text{ holds}\}$$

with

$$\left\{ \begin{aligned} \rho_1((1-\rho_1-\rho_2)V_1 - \sigma) &= \rho_1^0((1-\rho_1^0-\rho_2^0)V_1 - \sigma) \\ \rho_2((1-\rho_1-\rho_2)V_2 - \sigma) &= \rho_2^0((1-\rho_1^0-\rho_2^0)V_2 - \sigma) \end{aligned} \right\}. \tag{3.13}$$

On the ρ_1-axis we have $\rho_2^0 = 0$ and thus

$$\left\{ \begin{aligned} \rho_1((1-\rho_1-\rho_2)V_1 - \sigma) &= \rho_1^0((1-\rho_1^0)V_1 - \sigma) \\ \rho_2((1-\rho_1-\rho_2)V_2 - \sigma) &= 0 \end{aligned} \right\}.$$

Proposition 3.2.7. *For $\boldsymbol{\rho}^0 = (\rho_1^0, 0)$ the Hugoniot curves can be described depending on where ρ_1^0 lies on the ρ_1-axis.*

1. *If $\rho_1^0 = 0$, then $\mathcal{H}^2(\boldsymbol{\rho}^0) = \{\rho_2 = 0\}$ and $\mathcal{H}^1(\boldsymbol{\rho}^0) = \{\rho_1 = 0\}$.*
2. *If $\rho_1^0 < \rho_1^u$, then $\mathcal{H}^2(\boldsymbol{\rho}^0) = \{\rho_2 = 0\}$ and $\mathcal{H}^1(\boldsymbol{\rho}^0)$ is monotone in ρ_1 and exits $\mathcal{S}$ at a point with $\rho_2 = 0$ and $\rho_1 > \rho_1^u$.*
3. *If $\rho_1^* > \rho_1^0 > \rho_1^u$, then $\mathcal{H}^1(\boldsymbol{\rho}^0) = \{\rho_2 = 0\}$ and $\mathcal{H}^2(\boldsymbol{\rho}^0)$ is monotone in ρ_1 and exits $\mathcal{S}$ at a point with $\rho_2 = 0$ and $0 < \rho_1 < \rho_1^u$.*
4. *If $\rho_1^0 > \rho_1^*$, then $\mathcal{H}^1(\boldsymbol{\rho}^0) = \{\rho_2 = 0\}$ and $\mathcal{H}^2(\boldsymbol{\rho}^0)$ is monotone in ρ_1 and exits $\mathcal{S}$ at a point with $\rho_1 = 0$ and $0 < \rho_2 < 1$.*
5. *If $\rho_1^0 = 1$, then $\mathcal{H}^1(\boldsymbol{\rho}^0) = \{\rho_2 = 0\}$ and $\mathcal{H}^2(\boldsymbol{\rho}^0) = \{\rho_1 + \rho_2 = 1\}$.*

where $\rho_1^* = 1 - V_2/V_1$.

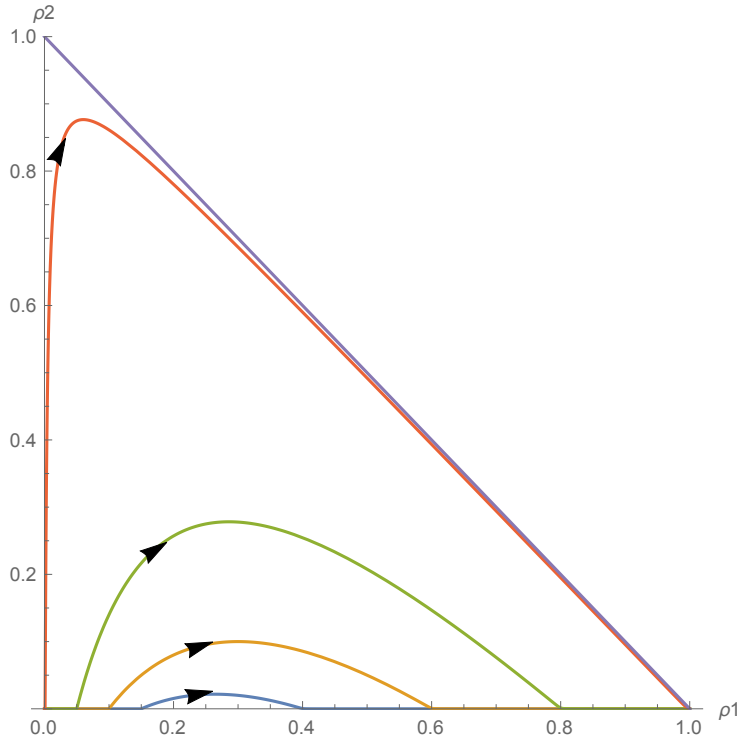

Figure 3.2: A sample of $\mathcal{H}^1$-curves for $\rho_1^0 < \rho_1^u$ and $\rho_2^0 = 0$ with $V_1 = 1$ and $V_2 = 0.75$. (The umbilic point is $\boldsymbol{\rho}^u = (0.2, 0)$.)

Proof. Study the Hugoniot set (3.13). The hyperbolae are given by

$$\rho_2(\rho_1) = \frac{(\rho_1 - \rho_1^0)((V_1 - V_2)(1 - \rho_1) - \rho_1^0 V_1)}{(V_1 - V_2)\rho_1 + \rho_1^0 V_2}.$$

□

In figure (3.2) and (3.3) one sees a sample of the Hugoniot curves for $V_1 = 1$ and $V_2 = 0.75$.
The next proposition confirms that the Hugoniot curves are tangent to the congestion axis, except at the boundaries.

Proposition 3.2.8. *The Hugoniot curves intersect the* $\{\rho_1 + \rho_2 = 1\}$*-axis only for* $\rho_1^0 = 0$ *or* $\rho_1^0 = 1$.

Proof. Set the expression for the Hugoniot curve equal to the function $\rho_2(\rho_1) = 1 - \rho_1$. □

As a next step, we want to find solutions to the RH condition and see whether there is

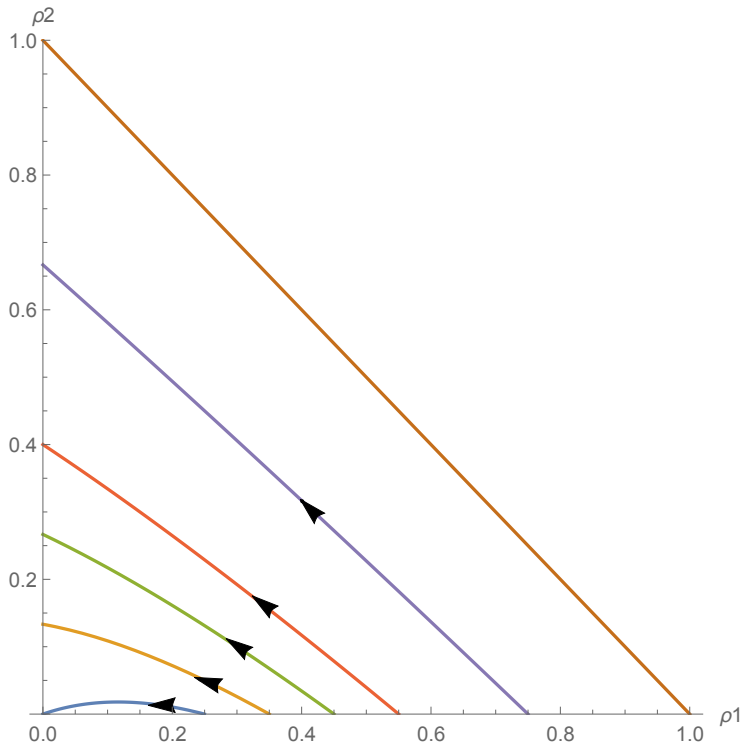

Figure 3.3: A sample of $\mathcal{H}^2$-curves for $\rho_1^0 > \rho_1^u$ and $\rho_2^0 = 0$ with $V_1 = 1$ and $V_2 = 0.75$.

always a solution to the RP (3.11) or not. From the first line in (3.12) we get the equations

$$\begin{cases} \sigma(\rho_1^L - \rho_1) = f_1(\rho_1^L, \rho_2^L) - f_1(\rho_1, \rho_2) \\ \sigma(\rho_2^L - \rho_2) = f_2(\rho_1^L, \rho_2^L) - f_2(\rho_1, \rho_2) \end{cases}$$
$$\Leftrightarrow \begin{cases} \sigma(\rho_1^L - \rho_1) = V_1(\rho_1^L - \rho_1)(1 - \rho_1^L - \rho_1) + V_1\rho_1\rho_2 \\ \sigma\rho_2 = \rho_2 V_2(1 - \rho_1 - \rho_2) \end{cases}$$

where a first solution is given by $\boldsymbol{\rho} = (\rho_1^R, 0)$ with the shock speed $\sigma = V_1(1 - \rho_1^R - \rho_1^L)$. The second line of (3.12) yields

$$\begin{cases} \gamma(\rho_1 - \rho_1^R) = f_1(\rho_1, \rho_2) - f_1(\rho_1^R, \rho_2^R) \\ \gamma(\rho_2 - \rho_2^R) = f_2(\rho_2, \rho_2) - f_2(\rho_1^R, \rho_2^R) \end{cases}$$
$$\Leftrightarrow \begin{cases} \gamma(\rho_1^R - \rho_1) = V_1(\rho_1^R - \rho_1)(1 - \rho_1^R - \rho_1) + V_1\rho_1\rho_2 \\ \gamma\rho_2 = \rho_2 V_2(1 - \rho_1 - \rho_2) \end{cases}$$

A first solution is $\boldsymbol{\rho} = (\rho_1^L, 0)$ with $\gamma = V_1(1 - \rho_1^R - \rho_1^L)$. One obtains that $\sigma = \gamma$. Thus, the solution of only one shock connecting $\boldsymbol{\rho}^L$ and $\boldsymbol{\rho}^R$ may be possible.
From now on $\rho_2^m \neq 0$. Hence, the solution to the Riemann Problem could also consist of two shock curves. The 1-shock curve from $\boldsymbol{\rho}^L$ going to an intermediate state $\boldsymbol{\rho}^m = (\rho_1^m, \rho_2^m) \in \mathcal{S}$

and the 2-shock curve connecting $\boldsymbol{\rho}^m$ with $\boldsymbol{\rho}^R$. It is necessary that $\boldsymbol{\rho}^m$ is an element of $\mathcal{S}$. If it lies outside of $\mathcal{S}$, the solution cannot be constructed by two shock curves. Both shocks have to fulfill the RH condition

$$\begin{aligned} &\begin{cases} \sigma(\rho_1^L - \rho_1^m) = f_1(\rho_1^L, \rho_2^L) - f_1(\rho_1^m, \rho_2^m) \\ \sigma(\rho_2^L - \rho_2^m) = f_2(\rho_1^L, \rho_2^L) - f_2(\rho_1^m, \rho_2^m) \end{cases} \\ \Leftrightarrow &\begin{cases} \sigma = V_1(1 - \rho_1^L - \rho_1^m) + V_1 \dfrac{\rho_1^m \rho_2^m}{\rho_1^L - \rho_1^m} \\ \sigma = V_2(1 - \rho_1^m - \rho_2^m) \end{cases} \end{aligned}$$

where $\rho_1^L \neq \rho_1^m$ and

$$\begin{aligned} &\begin{cases} \gamma(\rho_1^m - \rho_1^R) = f_1(\rho_1^m, \rho_2^m) - f_1(\rho_1^R, \rho_2^R) \\ \gamma(\rho_2^m - \rho_2^R) = f_2(\rho_1^m, \rho_2^m) - f_2(\rho_1^R, \rho_2^R) \end{cases} \\ \Leftrightarrow &\begin{cases} \gamma = V_1(1 - \rho_1^R - \rho_1^m) + V_1 \dfrac{\rho_1^m \rho_2^m}{\rho_1^R - \rho_1^m} \\ \gamma = V_2(1 - \rho_1^m - \rho_2^m) \end{cases} \end{aligned}$$

where $\rho_1^R \neq \rho_1^m$. Again, $\sigma = \gamma$ and solving for $\boldsymbol{\rho}^m = (\rho_1^m, \rho_2^m)$ yields the intermediate state

$$\begin{aligned} \rho_1^m &= \frac{V_2 \rho_1^L \rho_1^R}{(V_1 - V_2)(1 - \rho_1^L - \rho_1^R)}, \\ \rho_2^m &= -\left[\frac{V_1 - V_2}{V_2}(1 - \rho_1^L - \rho_1^R) - \rho_1^L - \rho_1^R + \frac{V_2 \rho_1^L \rho_1^R}{(V_1 - V_2)(1 - \rho_1^L - \rho_1^R)}\right] \end{aligned} \tag{3.14}$$

with

$$\begin{aligned} \sigma &= V_2(1 - \rho_1^m - \rho_2^m) \\ &= V_1(1 - \rho_1^L - \rho_1^R) \end{aligned} \tag{3.15}$$

and $V_1 \neq V_2$, $\rho_1^L + \rho_1^R \neq 1$. The solution is given by two shock curves only if the middle state lies inside of $\mathcal{S}$. We have to check the condition under which this holds.

Corollary 3.2.9. *For $\rho_1^L < \rho_1^u < \rho_1^R$ the intermediate state $\boldsymbol{\rho}^m$ with coordinates (3.14) lies in the interior of the simplex $\mathcal{S}$ and hence, the solution to the RP with data $(\rho_1^L, 0)$ and $(\rho_1^R, 0)$ consists of two intersecting shock curves, if*

$$\begin{aligned} \frac{V_1}{V_1 - V_2}\rho_1^L + \rho_1^R &\leq 1, \\ \rho_1^L + \frac{V_1}{V_1 - V_2}\rho_1^R &\geq 1. \end{aligned} \tag{3.16}$$

for $V_1 \neq V_2$.

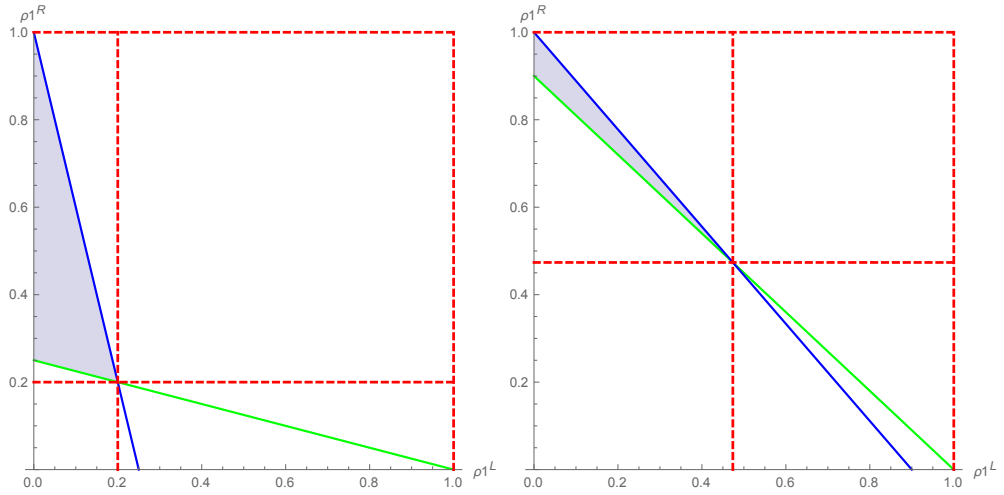

(a) $V_1 = 1$ and $V_2 = 0.75$

(b) $V_1 = 1$ and $V_2 = 0.1$

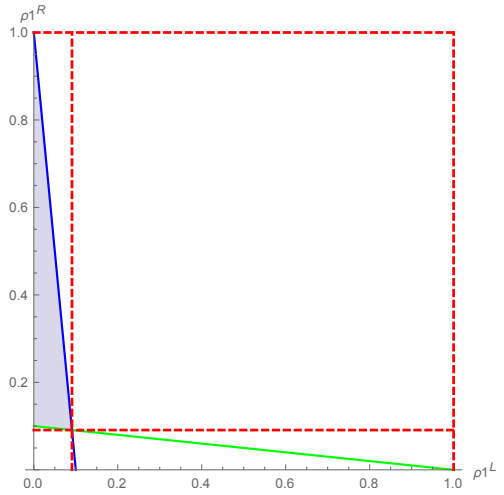

(c) $V_1 = 1$ and $V_2 = 0.9$

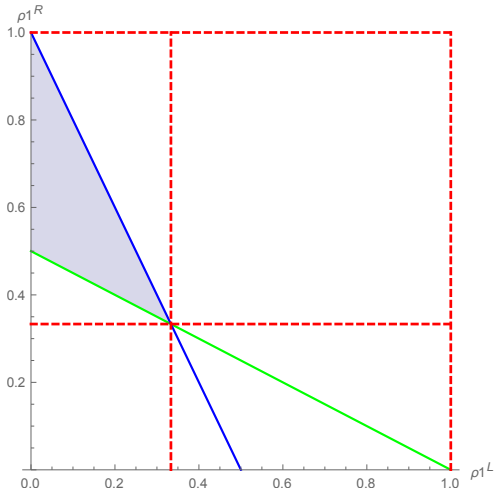

(d) $V_1 = 1$ and $V_2 = 0.5$

Figure 3.4: Values of initial data ρ_1^L and ρ_1^R ($\rho_2^L = \rho_2^R = 0$) for which condition (3.16) holds with different maximal velocities. The red lines denote the umbilic point and hence restrict the possible values of the initial data. The blue and green line are the values where equality holds in (3.16). Altogether, corollary 3.2.9 is fulfilled in the blue shaded region. Note that, differenet from the other plots, we are in the ρ_1^L-ρ_1^L-plane.

Proof. It is clear that $\boldsymbol{\rho}^m$ lies inside $\mathcal{S}$ if $\rho_1^m + \rho_2^m \leq 1$ and if $\rho_1^m, \rho_2^m > 0$. Hence, one must check these conditions. First, by adding up ρ_1^m and ρ_2^m from (3.14), we get

$$\rho_1^m + \rho_2^m = -\frac{V_1}{V_2}(1 - \rho_1^L - \rho_1^R) + 1.$$

Then,

$$\rho_1^m + \rho_2^m \leq 1 \Longleftrightarrow \rho_1^L + \rho_1^R \leq 1.$$

Second, $\rho_1^m > 0$ is equivalent to $\rho_1^L + \rho_1^R \leq 1$, too. But on the other hand, $\rho_2^m > 0$ if and only if

$$\frac{V_1}{V_1 - V_2}\rho_1^L + \rho_1^R \leq 1$$

and

$$\rho_1^L + \frac{V_1}{V_1 - V_2}\rho_1^R \geq 1.$$

For the maximal velocities we know that $V_1 > V_2 > 0$. Since $V_1 > V_1 - V_2$, we get

$$\frac{V_1}{V_1 - V_2} > 1$$

and hence condition (3.16) is stronger than $\rho_1^L + \rho_1^R \leq 1$. □

The second condition is needed because for $\rho_1^R < \frac{V_1 - V_2}{V_1}$ the curves of the second family exit the simplex $\mathcal{S}$ on the ρ_1-axis and not the ρ_2-axis and hence may intersect with the curves of the first family on the axis, i.e. on the boundary and not in the interior of $\mathcal{S}$. Then, the middle state (3.14) does not lie in the interior, either.

The set of values where (3.16) holds can be seen in figure 3.4 for different maximal velocities. The blue and green lines denote the vlaues of ρ_1^L and ρ_1^L where equality holds in (3.16). The shaded region is the set of values where the inequalities are fulfilled. Altogether, we can state the following.

Proposition 3.2.10. *For a RP with $\rho_1^L < \rho_1^u < \rho_1^R$ and $\rho_2^L = \rho_2^R = 0$ the Rankine Hugoniot condition (3.12) yields two solutions. The first consists of one shock with speed $\sigma = V_1(1 - \rho_1^L - \rho_1^R)$ connecting $\boldsymbol{\rho}^L$ to $\boldsymbol{\rho}^R$. The second solution contains one shock going from $\boldsymbol{\rho}^L$ to an intermediate state $\boldsymbol{\rho}^m$ and one from $\boldsymbol{\rho}^m$ to $\boldsymbol{\rho}^R$ with the same speed σ. The coordinates of the middle state are*

$$\begin{aligned} \rho_1^m &= \frac{V_2 \rho_1^L \rho_1^R}{(V_1 - V_2)(1 - \rho_1^L - \rho_1^R)} \\ \rho_2^m &= -\frac{V_1 - V_2}{V_2}(1 - \rho_1^L - \rho_1^R) + (\rho_1^L + \rho_1^R) - \frac{V_2 \rho_1^L \rho_1^R}{(V_1 - V_2)(1 - \rho_1^L - \rho_1^R)}. \end{aligned} \tag{3.17}$$

The second solution is restricted to initial data where $\boldsymbol{\rho}^m$ fulfills (3.16).

Depending on the position of ρ_1^L on the ρ_1-axis, the Hugoniot curves yield

1. $\rho_1^L < \rho_1^u$: then $S_2(\rho_1^L, 0) = \{\rho_2 = 0\}$ and $S_1(\rho_1^L, 0)$ is monotone in ρ_1
2. $\rho_1^L > \rho_1^u$: then $S_1(\rho_1^L, 0) = \{\rho_2 = 0\}$ and $S_2(\rho_1^L, 0)$ is monotone in ρ_1

Since $\boldsymbol{\rho}^R = (\rho_1^R, 0)$, it follows that for

1. $\rho_1^L < \rho_1^R < \rho_1^u$ the solution consists only of $S_2 = \{\rho_2 = 0\}$, for
2. $\rho_1^u < \rho_1^L < \rho_1^R$ the solution consists of $S_1 = \{\rho_2 = 0\}$ and for
3. $\rho_1^L < \rho_1^u < \rho_1^R$ the solution consists either only of S_1 or of S_1 and S_2, intersecting at (3.17) .

Note, that due to the behavior of the Hugoniot curves the solution consists either of one or two intersecting shock curves, depending on the initial data. If both values of the RP lie left or right of the umbilic point, we immediately get the same result as for the one species model. Here, the consistency with the LWR model for one species is given.

As a next step, it is interesting to see how the intermediate state computed from the RH behaves depending on the initial data. For this, we consider some special cases of RP. We start with values close to the umbilic point and examine $\boldsymbol{\rho}^m$.

Corollary 3.2.11. *If the initial data is given by $\rho_1^L = \rho_1^u - \epsilon$ and $\rho_1^R = \rho_1^u + \epsilon$ with $\epsilon > 0$, the intermediate state has the coordinates*

$$\begin{aligned} \rho_1^m &= \rho_1^u - \frac{\epsilon^2}{\rho_1^u} \\ \rho_2^m &= \frac{\epsilon^2}{\rho_1^u}. \end{aligned} \tag{3.18}$$

Then, one immediately sees that $\epsilon \to 0$ yields $\boldsymbol{\rho}^m = \boldsymbol{\rho}^u$. This is convenient since then both initial data equal $\boldsymbol{\rho}^u$. Now, if ϵ becomes bigger, the initial data lies more apart of the umbilical point and $\boldsymbol{\rho}^m$ wanders to smaller ρ_1 and bigger ρ_2. This goes on until $\epsilon = \rho_1^u$ and thus $\rho_1^L = 0$. At this point, we have

$$\begin{aligned} \rho_1^L &= 0 \\ \rho_1^R &= 2\rho_1^u \end{aligned} \tag{3.19}$$

and $\boldsymbol{\rho}^m = (0, \rho_1^u)$. Here, the shock speed does not depend on ρ_1^L and ρ_1^R

$$\sigma = V_1(1 - 2\rho_1^u) = V_2(1 - \rho_1^u) \tag{3.20}$$

and is always positive since $\rho_1^u < 1/2$. Moreover, here the intermediate state lies in the interior of the simplex $\mathcal{S}$ which is consistent with proposition 3.2.9 because the initial data fulfills (3.16). The described behavior can be seen in figure 3.5 where we also consider RP with initial data changing in a different relation to each other.

In figure (b) we see the intersecting Hugoniot curves for initial data with $\rho_1^L = \rho_1^u - \epsilon$ and $\rho_1^R = \rho_1^u + 2\epsilon$. This means that the distance between the umbilic point and the right initial datum ρ_1^R grows two times faster than the one between ρ_1^u and ρ_1^L.

In the other two plots (c) and (d) we see the same with 3ϵ and 4ϵ. In (d) we only see one curve because here the equality of condition (3.16) holds. This implies that for these

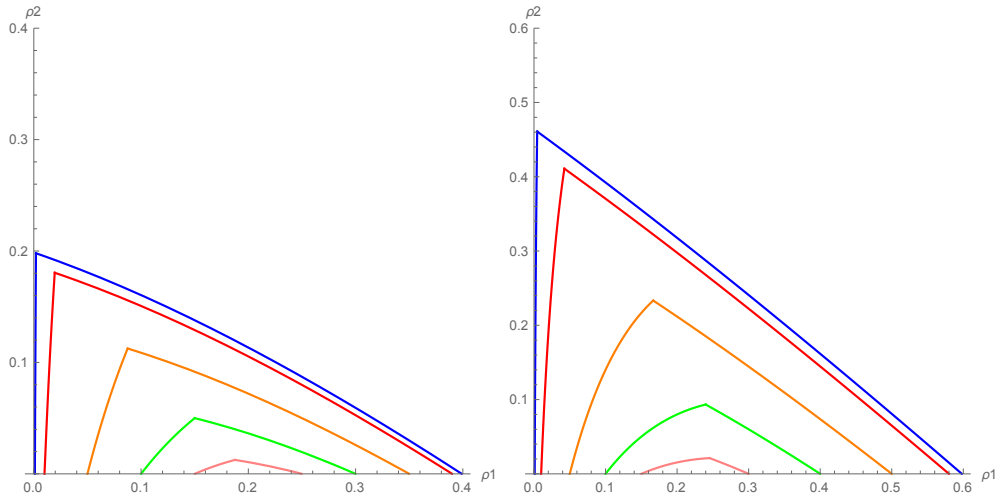

(a) $\rho_1^L = \rho_1^u - \epsilon$ and $\rho_1^R = \rho_1^u + \epsilon$.

(b) $\rho_1^L = \rho_1^u - \epsilon$ and $\rho_1^R = \rho_1^u + 2\epsilon$.

(c) $\rho_1^L = \rho_1^u - \epsilon$ and $\rho_1^R = \rho_1^u + 3\epsilon$.

(d) $\rho_1^L = \rho_1^u - \epsilon$ and $\rho_1^R = \rho_1^u + 4\epsilon$.

Figure 3.5: Sample of intersecting Hugoniot curves for $V_1 = 1$ and $V_2 = 0.75$ and different initial data on the ρ_1-axis. In the first three pictures, the solution consists of two shock waves intersecting in the interior of $\mathcal{S}$ while in the last one, the solution is given by one curve connecting $\boldsymbol{\rho}^L$ to $\boldsymbol{\rho}^R$.

data there is one shock curve connecting ρ_1^L to ρ_1^R. For data which does not fulfill (3.16) we have already seen that the solution consists of only one shock curve. We conclude the continuous dependence of the intermediate state from the initial data. Another special case is to start with initial data with nearly maximal distance in $\mathcal{S}$. This means that ρ_1^L is nearly 0 or ρ_1^R is nearly 1.

Corollary 3.2.12. *Consider the RP with* $\rho_1^L = 0$ *and* $\rho_1^R = 1 - \epsilon$ *with* $\epsilon > 0$. *The*

coordinates of the middle state are

$$\begin{aligned} \rho_1^m &= 0 \\ \rho_2^m &= 1 - \epsilon \left(1 - \frac{V_1 - V_2}{V_2}\right). \end{aligned} \tag{3.21}$$

Hence, $\boldsymbol{\rho}^m$ lies on the ρ_2-axis and moves downward for bigger ϵ. The shock speed is given by

$$\sigma = \epsilon V_1. \tag{3.22}$$

We observe that for $\epsilon \to 0$ the middle state equals $\boldsymbol{\rho}^m = (0, 1)$.
Altogether, we have described the intermediate state for all values of ρ_1^L and ρ_1^R, respectively. There is continuity between propositions 3.2.11 and 3.2.12. Mention, that the solution consists of two shocks with speed $\sigma = V_1(1 - \rho_1^L - \rho_1^R)$ for both shocks. Hence, the solution does not attain the value $\boldsymbol{\rho}^m$. For all initial data with $\rho_2^L = \rho_2^R = 0$ the solution of the two species LWR model is given by $\boldsymbol{\rho}(x,t) = (\rho_1(x,t), 0)$ with

$$\rho_1(x,0) = \begin{cases} \rho_1^L & \text{for} \quad x < \sigma t \\ \rho_1^R & \text{for} \quad x > \sigma t \end{cases}. \tag{3.23}$$

But before, one must check which of the solutions of proposition 3.2.10 is admissible and to which family the Hugoniot curves belong. For this purpose, the Lax condition must be checked.

Lemma 3.2.13. *A shock of the i-th family, connecting ρ^L to ρ^R with speed σ, is admissible in the sense of Lax [1957], if*

$$\lambda_i(\rho^R) \leq \sigma \leq \lambda_i(\rho^L) \tag{3.24}$$

holds.

If both initial data lie either left or right of the umbilical point, the solution will consist of only one shock. Checking the Lax inequality provides

1. for $\rho_1^L < \rho_1^R < \rho_1^u$ the condition $\lambda_2(\rho_1^R, 0) < \sigma < \lambda_2(\rho_1^L, 0)$ holds
2. for $\rho_1^u < \rho_1^L < \rho_1^R$ the condition $\lambda_1(\rho_1^R, 0) < \sigma < \lambda_1(\rho_1^L, 0)$ holds.

For $\rho_1^L < \rho_1^u < \rho_1^R$ we have the same shock speed for both shocks and thus the Lax inequality (3.24) is checked for only one shock from $\boldsymbol{\rho}^L$ to $\boldsymbol{\rho}^R$. The Lax admissibility conditions are

$$\begin{aligned} \lambda_1(\rho_1^R, 0) < \sigma < \lambda_1(\rho_1^L, 0), \\ \lambda_2(\rho_1^R, 0) < \sigma < \lambda_2(\rho_1^L, 0). \end{aligned} \tag{3.25}$$

with shock speed σ. The eigenvalues yield

$$\begin{aligned} \lambda_1(\rho_1^L, 0) &= V_2(1 - \rho_1^L), \\ \lambda_1(\rho_1^R, 0) &= V_1(1 - 2\rho_1^R), \\ \lambda_2(\rho_1^L, 0) &= V_1(1 - 2\rho_1^L), \\ \lambda_2(\rho_1^R, 0) &= V_2(1 - \rho_1^R). \end{aligned} \tag{3.26}$$

Hence, we get the next proposition.

Proposition 3.2.14. *The Lax admissibility demands that for $\rho_1^L < \rho_1^u < \rho_1^R$ the shock connecting ρ^L to ρ^R with speed σ is*

- *a 1-shock if $\rho_1^R > \phi(\rho_1^L)$ and $\phi(\rho_1^R) < \rho_1^L$*
- *a 2-shock if $\rho_1^R < \phi(\rho_1^L)$ and $\phi(\rho_1^R) > \rho_1^L$*
- *an over compressive shock if $\rho_1^R < \phi(\rho_1^L)$ and $\phi(\rho_1^R) < \rho_1^L$*

with the $\mathcal{C}^1$-function

$$\phi(\rho_1) = \frac{(1-\rho_1)V_1 - V_2}{V_1 - V_2}. \tag{3.27}$$

with $V_1 \neq V_2$.

Proof. From the expressions (3.26) one sees that

$$\begin{aligned} \lambda_1(\rho_1^R, 0) &< \sigma \\ \lambda_2(\rho_1^L, 0) &> \sigma. \end{aligned} \tag{3.28}$$

The other inequalities are obtained by computation

$$\begin{aligned} \sigma < \lambda_1(\rho_1^L) &\Leftrightarrow \phi(\rho_1^R) < \rho_1^L \\ \sigma > \lambda_2(\rho_1^R) &\Leftrightarrow \phi(\rho_1^L) > \rho_1^R. \end{aligned} \tag{3.29}$$

□

We observe that the existence of the umbilic point leads to overcompressive shocks. This is also discussed in Benzoni-Gavage and Colombo [2003]. Since we closed the case $\rho_1^L < \rho_1^R$ we now propose that $\rho_1^L > \rho_1^R$. By Dafermos [2010], the solution to a single PDE consists of a rarefaction wave. Since we are in the case of the second species absent, we can use this. The question is, whether the existence of the umbilic point affects the solution similarly to the previous discussed shock waves or not. The rarefaction waves are obtained by integration along the eigenvectors.

A sample of eigenvectors can be seen in figure 3.6, oriented so that $d\lambda_i \cdot \mathbf{v}_i > 0$ for $i = 1, 2$. Note that from theorem 3.2.3 both characteristic fields are genuinely nonlinear for data on the ρ_1-axis. One has already stated in lemma 3.2.2 that the eigenvectors coalesce in the umbilic point, too. We observe this in figure 3.6. On the ρ_1-axis the first eigenvector is parallel to the axis for $\rho_1 > \rho_1^u$ while the second one is parallel for $\rho_1 < \rho_1^u$. In the umbilic point (for the plots $\rho_1^u = 0.2$) they coincide. Moreover, the eigenvectors change continuously with the densities as can be seen in the zoom in figure (c) and (d). We do not integrate the curves explicitly here, because of the complexity of the algebraic terms of the eigenvectors. But we are able to compute the eigenvectors on the ρ_1-axis from equation

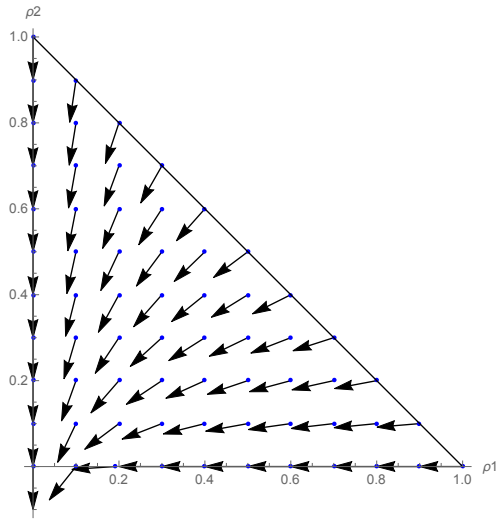

(a) Sample of eigenvectors of first family

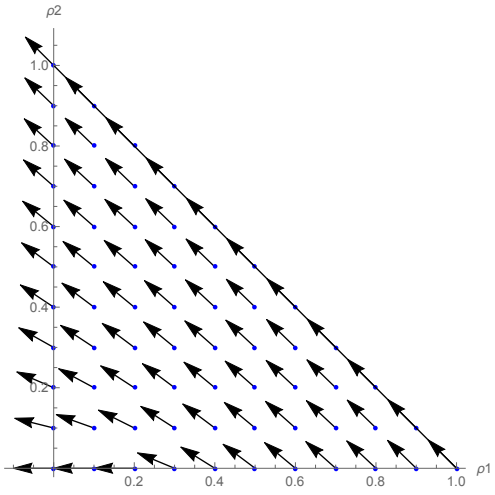

(b) Sample of eigenvectors of second family

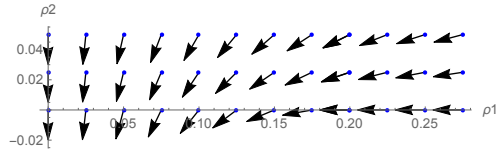

(c) Zoom of eigenvectors of first family around the umbilic point $\boldsymbol{\rho}^u = (0.2, 0)$.

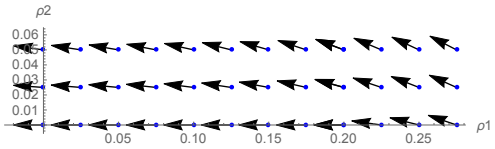

(d) Zoom of eigenvectors of second family around the umbilic point $\boldsymbol{\rho}^u = (0.2, 0)$.

Figure 3.6: Sample of eigenvectors with $V_1 = 1$ and $V_2 = 0.75$, oriented so that $d\lambda_i \cdot \mathbf{v}_i > 0$.

(3.9) by using $\rho_2 = 0$. Due to the behavior of the eigenvalues in (3.8) we also have to make a distinction for the eigenvectors.

$$\mathbf{v}_1(\rho_1, 0) = \begin{cases} \begin{pmatrix} -V_1\rho_1 \\ V_2(1-\rho_1) - V_1(1-2\rho_1) \end{pmatrix} & \text{for} \quad \rho_1 < \rho_1^u \\ \begin{pmatrix} V_1(1-3\rho_1) - V_2(1-\rho_1) \\ 0 \end{pmatrix} & \text{for} \quad \rho_1 > \rho_1^u \end{cases} \tag{3.30}$$

$$\mathbf{v}_2(\rho_1, 0) = \begin{cases} \begin{pmatrix} -V_1(1-2\rho_1) + V_2(1-\rho_1) \\ 0 \end{pmatrix} & \text{for} \quad \rho_1 < \rho_1^u \\ \begin{pmatrix} -V_1\rho_1 \\ -V_1(1-2\rho_1) + V_2(1-\rho_1) \end{pmatrix} & \text{for} \quad \rho_1 > \rho_1^u \end{cases} \tag{3.31}$$

We have already seen that in the umbilic point the eigenvectors coalesce.

$$\mathbf{v}_1(\rho_1^u, 0) = \mathbf{v}_2(\rho_1^u, 0) = \begin{pmatrix} -V_1\rho_1^u \\ 0 \end{pmatrix} \tag{3.32}$$

For $\rho_1^u < \rho_1^L$ the rarefaction wave of the first family, going through ρ_1^L, is given by

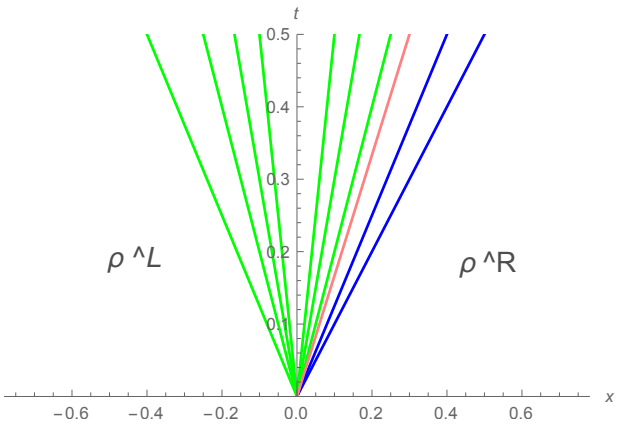

Figure 3.7: Example of a rarefaction wave. The green (blue) fan shows the rarefaction wave of the first (second) family. The red line separates the two waves although the solution consists of only one rarefaction wave. Here, $V_1 = 1,\ V_2 = 0.75,\ \rho_1^L = 0.9,\ \rho_1^R = 0.01$ and $\rho_2^L = \rho_2^R = 0$.

$\mathcal{R}_1(\rho_1^L, 0) = \{\rho_2 = 0\}$. If $\rho_1^R < \rho_1^u$ the 2-rarefaction wave is also described by $\mathcal{R}_2(\rho_1^R, 0) = \{\rho_2 = 0\}$. Hence, for $\rho_1^R < \rho_1^u < \rho_1^L$ and $\rho_2^R = \rho_2^L = 0$ the solution consists of two rarefaction waves with intermediate state $\boldsymbol{\rho}^m = (\rho_1^u, 0)$. Thereby, $\mathcal{R}_1(\rho_1^L, 0)$ goes from $\boldsymbol{\rho}^L$ to $\boldsymbol{\rho}^m$ and $\mathcal{R}_2(\rho_1^u, 0)$ connects the middle state with $\boldsymbol{\rho}^R$. The solution consists of only one rarefaction curve in the case that both initial data lie left (second family) or right (first family) of the umbilic point. This is consistent with figure 3.6 and is the only admissible solution in the sense of Lax [1957]. The two rarefaction curves are equal to each other and so the solution of the RP for the fast species ($\rho_2^L = \rho_2^R = 0$) for the LWR model of two species can again be constructed with the help of the standard LWR model. In the same way as for the shock curves we get $\boldsymbol{\rho}(x,t) = (\rho_1(x,t), 0)$, with

$$\rho_1(x,t) = \begin{cases} \rho_1^L & \text{for} \quad \dfrac{x}{t} < V_1(1 - 2\rho_1^L) \\ \dfrac{1}{2}(1 - \dfrac{x}{Vt}) & \text{for} \quad V_1(1 - 2\rho_1^L) < \dfrac{x}{t} < V(1 - 2\rho_1^R). \\ \rho_1^R & \text{for} \quad \dfrac{x}{t} > V_1(1 - 2\rho_1^R) \end{cases} \tag{3.33}$$

Again, we do not see the middle state because the solution does not attain this value. The existence of the umbilic point does not affect the solution of the RP for rarefaction waves, either. An example of two rarefaction waves is shown in figure 3.7. Left of the rarefaction wave the solution consists of $\boldsymbol{\rho}^L$. The green fan belongs to the rarefaction wave of the first family and the blue one to the second family. They are separated by the red line on which the intermediate state $\boldsymbol{\rho}^m$ lies. Right of the fan the solution equals $\boldsymbol{\rho}^R$. This is a continuous solution.

Closing this subsection, one has to mention that the existence of the solution to the RP (3.11) has not been proven completely algebraically due to the fact that the expressions

are hard to handle. We made use of Mathematica plots to understand the solution's construction and then used the fact that all shocks have the same speed and that the rarefaction waves are equal. Thus, we get the solution to the standard LWR model again.

In the next two parts, we consider a small perturbation of the studied special RP and also introduce the general RP. After that, we see that by a variation of the flux function for (3.5) we can find more than one umbilic point.

3.2.2 Perturbation of the Riemann problem

Since the RP on the ρ_1-axis has been studied in the last section, we now want to see whether the solution depends continuously on the initial data or not. Therefore, one can look at a small perturbation $\epsilon > 0$ of the Riemann Problem (3.11) which is (3.5) together with

$$\boldsymbol{\rho}(x,0) = \begin{cases} \boldsymbol{\rho}^L = (\rho_1^L, \epsilon) & \text{for} \quad x < 0 \\ \boldsymbol{\rho}^R = (\rho_1^R, \epsilon) & \text{for} \quad x > 0 \end{cases}. \tag{3.34}$$

We assume that there is a small number of vehicles of the slower species on the road, too. Now we want to examine how this small perturbation of the initial data affects the solution. We again examine the discontinuities and rarefaction waves. Two shocks with speeds σ and γ, connecting $\boldsymbol{\rho}^L$ to $\boldsymbol{\rho}^m$ and $\boldsymbol{\rho}^m$ to $\boldsymbol{\rho}^R$, have to fulfill the RH condition

$$\begin{aligned} &\begin{cases} \sigma(\rho_1^L - \rho_1^m) = f_1(\rho_1^L, \rho_2^L) - f_1(\rho_1^m, \rho_2^m) \\ \sigma(\rho_2^L - \rho_2^m) = f_2(\rho_1^L, \rho_2^L) - f_2(\rho_1^m, \rho_2^m) \end{cases} \\ \Leftrightarrow &\begin{cases} \sigma = V_1(1 - \rho_1^L - \rho_1^m) + V_1 \dfrac{\rho_1^m \rho_2^m - \epsilon \rho_1^L}{\rho_1^L - \rho_1^m} \\ \sigma = V_2(1 - \epsilon - \rho_2^m) + V_2 \dfrac{\rho_1^m \rho_2^m - \epsilon \rho_1^L}{\epsilon - \rho_2^m} \end{cases} \end{aligned} \tag{3.35}$$

$$\begin{aligned} &\begin{cases} \gamma(\rho_1^m - \rho_1^R) = f_1(\rho_1^m, \rho_2^m) - f_1(\rho_1^R, \rho_2^R) \\ \gamma(\rho_2^m - \rho_2^R) = f_2(\rho_1^m, \rho_2^m) - f_2(\rho_1^R, \rho_2^R) \end{cases} \\ \Leftrightarrow &\begin{cases} \gamma = V_1(1 - \rho_1^R - \rho_1^m) + V_1 \dfrac{\rho_1^m \rho_2^m - \epsilon \rho_1^R}{\rho_1^R - \rho_1^m} \\ \gamma = V_2(1 - \epsilon - \rho_2^m) + V_2 \dfrac{\rho_1^m \rho_2^m - \epsilon \rho_1^R}{\epsilon - \rho_2^m} \end{cases} \end{aligned} \tag{3.36}$$

Then, the two shock speeds are not equal. They differ by

$$\gamma - \sigma = V_2 \epsilon \frac{\rho_1^R - \rho_1^L}{\rho_2^m - \epsilon}. \tag{3.37}$$

One observes that the speed of the 2-shock is always greater than the speed of the 1-shock. For $\epsilon \to 0$ the speeds are the same again and equal to the shock speed of the unperturbed system. Here, different from the RP ρ_1-axis, the middle state appears in the

solution. This is convenient because the second species is present in this case. Now, the intermediate state $\boldsymbol{\rho}^m$ cannot be computed algebraically from (3.35) and (3.36) and thus the exact shock speeds cannot be found either. We can only solve equation (3.35) and (3.36) by inserting data for the RP. Moreover, the solution could consist of both, shocks and rarefactions because we are not in a one species case anymore.

By plotting the Hugoniot curves in figure 3.8, one sees that the Hugoniot curves depend continuously on the initial data. For data close to the ρ_1-axis the behavior of the curves changes only slightly. The rarefaction curves are again obtained by integrating along the eigenvectors (3.6). We get solutions different from the previous case, too, because the eigenvectors are not parallel to the $\{\rho_2 = 0\}$-axis for data lying in the interior of $\mathcal{S}$.

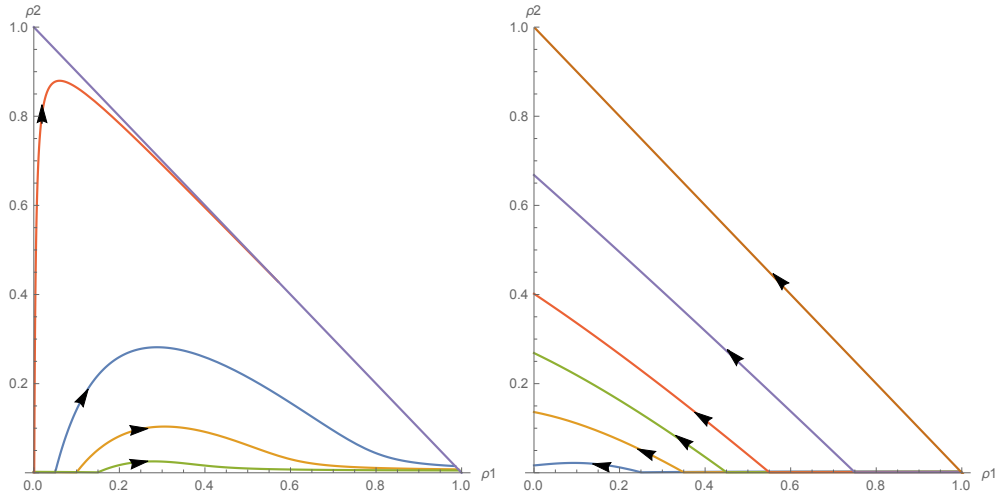

(a) Sample of $\mathcal{H}^1$-curves exiting a point near the ρ_1-axis, left of the umbilic point

(b) Sample of $\mathcal{H}^2$-curves exiting a point near the ρ_1-axis, left of the umbilic point

Figure 3.8: Sample of Hugoniot curves exiting a point near the ρ_1-axis with the umbilic point ($\boldsymbol{\rho}^u = (0.2, 0)$) where $V_1 = 1$ and $V_2 = 0.75$.

3.2.3 General Riemann problem

Until now, we have found a solution to the RP for data on the $\{\rho_2 = 0\}-$axis. We have also seen that the solution depends continuously on the initial data, because if we perturb the RP on the fast axis by $\epsilon > 0$, small, we will observe a small variation in the Lax curves. The general RP for the LWR model for two species is of the form

$$\begin{aligned} &\partial_t \rho_1 + \partial_x(\rho_1 V_1(1-\rho_1-\rho_2)) = 0 \\ &\partial_t \rho_2 + \partial_x(\rho_2 V_2(1-\rho_1-\rho_2)) = 0 \\ &\boldsymbol{\rho}(x,0) = \begin{cases} \boldsymbol{\rho}^L = (\rho_1^L, \rho_2^L) & \text{for} \quad x < 0 \\ \boldsymbol{\rho}^R = (\rho_1^R, \rho_2^R) & \text{for} \quad x > 0 \end{cases}. \end{aligned} \tag{3.38}$$

From 3.2.1 we know the expressions of the eigenvalues as

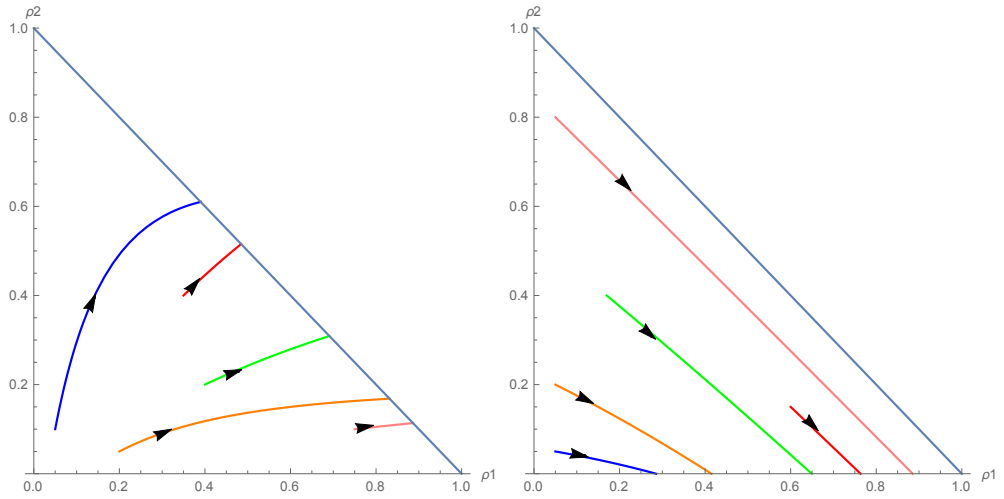

(a) Hugoniot curves for the first family. (b) Hugoniot curves for the second family.

Figure 3.9: Sample of Hugoniot curves with $V_1 = 1$ and $V_2 = 0.75$ for initial data lying in the interior of $\mathcal{S}$.

$$\begin{aligned}\lambda_1 =& \frac{1}{2}\Big[V_1(1-2\rho_1-\rho_2)+V_2(1-\rho_1-2\rho_2)\\ &-\sqrt{(V_1(1-2\rho_1-\rho_2)-V_2(1-\rho_1-2\rho_2))^2+4V_1V_2\rho_1\rho_2}\Big]\\ \lambda_2 =& \frac{1}{2}\Big[V_1(1-2\rho_1-\rho_2)+V_2(1-\rho_1-2\rho_2)\\ &+\sqrt{(V_1(1-2\rho_1-\rho_2)-V_2(1-\rho_1-2\rho_2))^2+4V_1V_2\rho_1\rho_2}\Big]\end{aligned}$$

The eigenvalues are hence functions of the density $\boldsymbol{\rho}$. The complexity of the expressions hinders us from further general algebraic research of system (3.38). We know that for initial data with small variation different from the umbilic point, the RP is well-posed. But for a general RP with data lying far apart, it is difficult to prove well-posedness due to the complexity of the expressions. The idea is to find a middle state $\boldsymbol{\rho}^m$ as the intersection of the two Lax curves $\mathcal{L}^1(\boldsymbol{\rho}^L)$ and $\mathcal{L}^2(\boldsymbol{\rho}^R)$. Mention that now the solution can also contain both shocks and rarefaction waves and on the $\{\rho_1+\rho_2\}$-axis contact discontinuities.

In figure 3.9 one sees samples of the first and second family shock curves. The rarefaction waves are obtained by integrating along the eigenvectors, which have already been plotted in figure 3.6. These plots give no reason why the RP (3.38) should be ill-posed as has already been stated by Benzoni-Gavage and Colombo [2003]. For data different from the umbilic point, the system is indeed strictly hyperbolic and around $\boldsymbol{\rho}^u$ we solved the RP. Moreover, the simplex $\mathcal{S}$ is convex and because of (3.10) we assume its invariance. But since we have no proof of well-posedness for all initial data we cannot be sure that the

lack of global strict hyperbolicity does not lead to ill-posedness. Then, we are not able to considerate the more general Cauchy problem because the method of wave front tracking is not possible since it claims the well-posedness of the general RP. We go on with a variation of the here discussed model. The idea is to change the velocity function and see how this affects the properties of the original model.

3.2.4 Variation of the velocity function

In the above discussion, we saw that the two species LWR model lacks strict hyperbolicity in one umbilic point on the boundary. This is reason why well-posedness is hard to prove for this model. We wish to overcome the existence of the umbilic point. For this purpose we modify system (3.5) by specifying the different classes of vehicles not only through different constants but also through their behavior to each other. For example, consider one species of cars and one of trucks. Then, one can assume that the slower moving trucks do not take the cars on the road into account, but only their own species. We thus change the flux function into

$$\mathbf{f}(\rho_1, \rho_2) = (\rho_1 V_1(1 - \rho_1 - \rho_2), \rho_2 V_2(1 - \rho_2))^\intercal.$$

Hence, the first entry is the same as for the original system (3.5). The second flux function only depends on ρ_2 and we obtain the system of PDEs

$$\begin{aligned} \partial_t \rho_1 + \partial_x(\rho_1 V_1(1 - \rho_1 - \rho_2)) &= 0 \\ \partial_t \rho_2 + \partial_x(\rho_2 V_2(1 - \rho_2)) &= 0 \end{aligned} \tag{3.39}$$

with maximal speeds $V_1 > V_2 > 0$ and $\rho_1, \rho_2 \in \mathcal{S}$, where

$$\mathcal{S} = \{(\rho_1, \rho_2) | \rho_1, \rho_2 \geq 0; \rho_1 + \rho_2 \leq 1\}.$$

By this variation we get a triangular system. Hence, we can solve the second equation of (3.39) for ρ_2 and insert the solution into the first. But from the Jacobian of the system we obtain that the lack of regularity hinders us from using this method to solve an initial value problem. The initial datum for the Riemann problem is equivalent to the original RP

$$\boldsymbol{\rho}(x, 0) = \begin{cases} \boldsymbol{\rho}^L = (\rho_1^L, \rho_2^L) & \text{for} \quad x < 0 \\ \boldsymbol{\rho}^R = (\rho_1^R, \rho_2^R) & \text{for} \quad x > 0 \end{cases}.$$

Using the results from the last subsection, the Jacobian matrix of the system is given by

$$J(\rho_1, \rho_2) = \begin{pmatrix} V_1(1 - 2\rho_1 - \rho_2) & -V_1\rho_1 \\ 0 & V_2(1 - 2\rho_2) \end{pmatrix}.$$

For this triangular matrix the eigenvalues are

$$\begin{aligned} \lambda_{one} &= V_1(1 - 2\rho_1 - \rho_2), \\ \lambda_{two} &= V_2(1 - 2\rho_2). \end{aligned}$$

The eigenvalues of (3.39) should again be ordered so that $\lambda_1 \leq \lambda_2$. Due to that, we look for umbilic points where the eigenvalues coalesce. In this case, we get an umbilic line instead of one point for the original model. In phase space, the line of joining eigenvalues is given by

$$\rho_u(\rho_1) = \rho_2(\rho_1) = \frac{V_1(1-2\rho_1) - V_2}{V_1 - 2V_2}.$$

Indeed, by plotting the points where the eigenvalues merge for some special values of V_1 and V_2 we observe an umbilic line. Then, the eigenvalues of (3.39) are given by

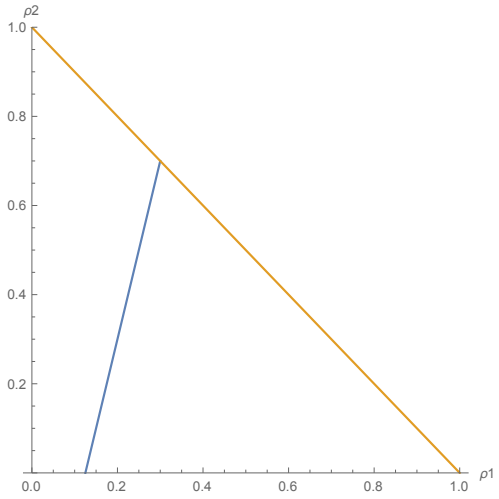

Figure 3.10: Values of ρ_1, ρ_2 where the eigenvalues coalesce for $V_1 = 1$ and $V_2 = 0.75$ together with the simplex $\mathcal{S}$.

$$\lambda_1 = \begin{cases} V_2(1-2\rho_2) & \text{for} \quad \boldsymbol{\rho} \in \mathcal{L} \\ V_1(1-2\rho_1-\rho_2) & \text{for} \quad \boldsymbol{\rho} \in \mathcal{R} \end{cases}$$
$$\lambda_2 = \begin{cases} V_1(1-2\rho_1-\rho_2) & \text{for} \quad \boldsymbol{\rho} \in \mathcal{L} \\ V_2(1-2\rho_2) & \text{for} \quad \boldsymbol{\rho} \in \mathcal{R} \end{cases}$$

with $\mathcal{L} = \{(\rho_1, \rho_2) \in \mathcal{S} \mid \rho_2 > \rho_u(\rho_1)\}$ and $\mathcal{R} = \{(\rho_1, \rho_2) \in \mathcal{S} \mid \rho_2 < \rho_u(\rho_1)\}$. The eigenvalues change role in the umbilic line. The eigenvectors of J can be computed as

$$\mathbf{v}_{one} = \begin{pmatrix} 1 \\ 0 \end{pmatrix}, \quad \mathbf{v}_{two} = \begin{pmatrix} -V_1\rho_1 \\ V_1(1-2\rho_1-\rho_2) - V_2(1-2\rho_2) \end{pmatrix}$$

and they change role in the umbilic line, too. So we obtain

$$v_1 = \begin{cases} \begin{pmatrix} -V_1\rho_1 \\ V_1(1-2\rho_1-\rho_2) - V_2(1-2\rho_2) \end{pmatrix} & \text{for} \quad \boldsymbol{\rho} \in \mathcal{L} \\ \begin{pmatrix} 1 \\ 0 \end{pmatrix} & \text{for} \quad \boldsymbol{\rho} \in \mathcal{R} \end{cases}$$

$$v_2 = \begin{cases} \begin{pmatrix} 1 \\ 0 \end{pmatrix} & \text{for} \quad \boldsymbol{\rho} \in \mathcal{L} \\ \begin{pmatrix} -V_1\rho_1 \\ V_1(1-2\rho_1-\rho_2) - V_2(1-\rho_2) \end{pmatrix} & \text{for} \quad \boldsymbol{\rho} \in \mathcal{R} \end{cases}$$

what can be seen in figure (3.11). Altogether the variation of the LWR model for two

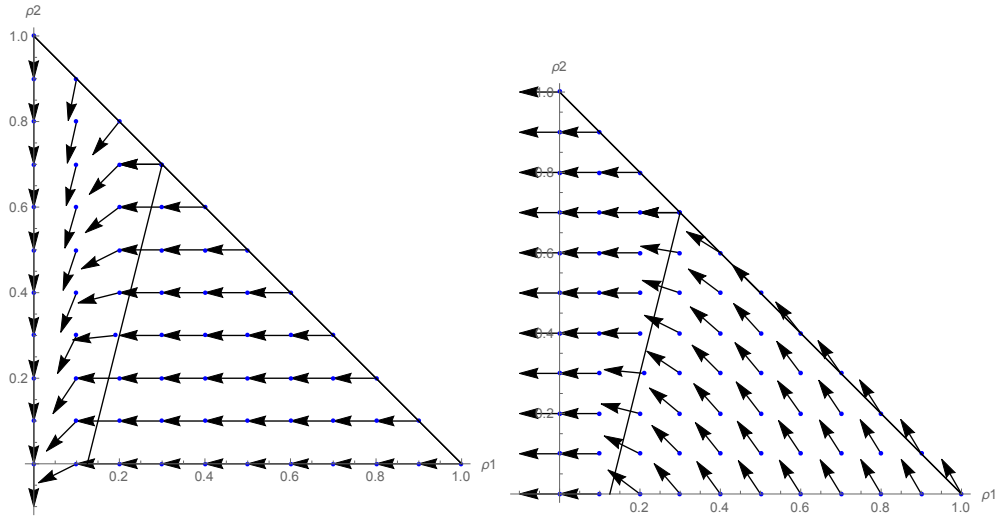

(a) Eigenvectors of first family (b) Eigenvectors of second family

Figure 3.11: Sample of eigenvectors for the varied LWR two species model with $V_1 = 1$ and $V_2 = 0.75$.

species does not eliminate the umbilic point. Instead it yields a whole line of umbilic points. Then, again it is not clear if a RP is well-posed for (3.39) and we cannot use theorems for strictly hyperbolic systems. Hence, we are again not in the position to use standard techniques for the proof of existence and uniqueness. Therefore, one must again examine different RP around the umbilic line.

For values of $\boldsymbol{\rho}^L$ and $\boldsymbol{\rho}^R$ that both lie on the left or right side of the umbilic line the RP is well-posed for small variation and all times. But the question is what happens if one lies on the left side and the other one lies on the right. Then, we have no theory proving existence and uniqueness of a solution. The purpose of modifying the velocity function was to get a strictly hyperbolic system of PDEs. Since this did not work due to the existence of an umbilic line we do not go on with further analysis of this model. But it is of course

interesting to study the well-podeness of the model and see if it provides the same or other difficulties as the original model.

Remark 3.2.15. *The variation of system (3.5) into the triangular system (3.39), by assuming one independent species, yields more points of intersecting eigenvalues. Hence, the hyperbolicity of (3.39) lacks on a whole line inside of $\mathcal{S}$. Due to that, theorems about well-posedness are missing. The question is, whether a RP can be found for this variation of the model that proves ill-posedness or if it can be proved to be well-posed instead. With the discussion and results from the original model in mind, we expect the varied model to be well-posed, too.*

With this remark we close the discussion of the LWR model for two species and continue the extension to a LWR model describing three different kinds of vehicles on the road.

4 LWR Model for three species

Until now, we have seen that the extension of the LWR model to a two species model provides difficulties, as there exist umbilic points where the system is not strictly hyperbolic. We transform this extension to a model suitable for three different types of vehicles and examine its hyperbolicity afterward.

4.1 Derivation of the model

Starting point is (3.39) with the flux function (3.4) where we add the third species 3 with density $\rho_3 > 0$ and maximal velocity $V_3 > 0$. Therewith, we get the three-dimensional flux

$$\mathbf{f}(\rho_1, \rho_2, \rho_3) = \begin{pmatrix} V_1\rho_1(1-\rho_1-\rho_2-\rho_3) \\ V_2\rho_2(1-\rho_1-\rho_2-\rho_3) \\ V_3\rho_3(1-\rho_1-\rho_2-\rho_3) \end{pmatrix}. \tag{4.1}$$

We assume that the first species is again the fastest and the third is the slowest. Of course, we define the densities ρ_1, ρ_2, ρ_3 on a set similar to the previous chapter. Altogether, we define the LWR model for three species.

Definition 4.1.1. *The LWR model for three different types of traffic participants is described by the following three PDEs*

$$\begin{aligned} &\partial_t\rho_1 + \partial_x(\rho_1 V_1(1-\rho_1-\rho_2-\rho_3)) = 0, \\ &\partial_t\rho_2 + \partial_x(\rho_2 V_2(1-\rho_1-\rho_2-\rho_3)) = 0, \\ &\partial_t\rho_3 + \partial_x(\rho_3 V_3(1-\rho_1-\rho_2-\rho_3)) = 0, \end{aligned} \tag{4.2}$$

with maximal speeds $V_1 > V_2 > V_3 > 0$. The system is defined on the three-dimensional simplex

$$\mathcal{S} = \{(\rho_1, \rho_2, \rho_3) | \rho_1, \rho_2, \rho_3 \geq 0; \rho_1 + \rho_2 + \rho_3 \leq 1\}.$$

With $\boldsymbol{\rho} = (\rho_1, \rho_2, \rho_3)^\intercal$ system (4.2) writes

$$\partial_t\boldsymbol{\rho} + J(\boldsymbol{\rho})\partial_x\boldsymbol{\rho} = 0$$

where $J(\boldsymbol{\rho})$ is the Jacobian

$$J(\boldsymbol{\rho}) = \begin{pmatrix} V_1(\psi+\rho_1\psi') & \rho_1 V_1\psi' & \rho_1 V_1\psi' \\ \rho_2 V_2\psi' & V_2(\psi+\rho_2\psi') & \rho_2 V_2\psi' \\ \rho_3 V_3\psi' & \rho_3 V_3\psi' & V_3(\psi+\rho_3\psi') \end{pmatrix},$$

with $\psi = 1 - \rho_1 - \rho_2 - \rho_3$ and $\psi' = -1$. The system is hyperbolic (Benzoni-Gavage and Colombo [2003]) but not strictly hyperbolic. It may produce umbilic points, lines or surfaces where one or more eigenvalues coincide. We want to discover these values of $\boldsymbol{\rho}$. Since now the characteristical polynomial is given by a third order polynomial it is already hard to find the eigenvalues due to the complexity of the expressions. The characteristical polynomial

$$\begin{aligned}\pi_3(\rho_1,\rho_2,\rho_3) = \lambda^3 &- \lambda^2\left[V_1(1-2\rho_1-\rho_2-\rho_3)+V_2(1-\rho_1-2\rho_2-\rho_3)+V_3(1-\rho_1-\rho_2-2\rho_3)\right]\\ &+\lambda[(1-\rho_1-\rho_2-\rho_3)^2(V_1V_2+V_2V_3+V_1V_3)\\ &-(1-\rho_1-\rho_2-\rho_3)(V_1V_2(\rho_1+\rho_2)+V_2V_3(\rho_2+\rho_3)+V_1V_3(\rho_1+\rho_3))]\\ &-V_1V_2V_3(1-\rho_1-\rho_2-\rho_3)^2(1-2\rho_1-2\rho_2-2\rho_3).\end{aligned} \tag{4.3}$$

yields algebraic expressions for the eigenvalues, only if we reduce the system to cases where one species is absent. But this cases are of interest, too, since the three species model should be consistent with the two species one. One would expect to get the same umbilic point as for the two species model. So the first step is to examine the hyperbolicity for one species absent. We demand that the eigenvalues are ordered as follows

$$\lambda_1 \le \lambda_2 \le \lambda_3. \tag{4.4}$$

This means that with λ_1 we always declare the smallest eigenvalue and we do not mix up the definitions through the following computations and plots.

Corollary 4.1.2. *For one density equal to zero the three species model reduces to a two species model and hence provides the same umbilic point as has been found there. Hence, we get three umbilic points $\rho_1^{u12}, \rho_1^{u23}$ and ρ_1^{u13}. Moreover, there exist three umbilic lines in the projections to the $\rho_i - \rho_j-$plane depending on the ordering of the maximal velocities. For $V_1 > V_2 > V_3$ the two umbilic lines are described by*

$$\begin{aligned}\rho_2(\rho_1) &= -\frac{\rho_1^{u23}}{\rho_1^{u13}}\rho_1 + \rho_1^{u23}\\ \rho_3(\rho_1) &= -\frac{V_2-V_3}{V_2-2V_3}\frac{2V_1-V_2}{V_1-V_2}\rho_1 + \frac{V_2-V_3}{V_2-2V_3}\\ &= -\frac{V_2-V_3}{V_2-2V_3}\frac{1}{\rho_1^{u12}}\rho_1 + \frac{V_2-V_3}{V_2-2V_3}\\ \rho_3(\rho_2) &= -\frac{V_1-V_3}{V_1-2V_3}\frac{V_1-2V_2}{V_1-V_2}\rho_2 + \frac{V_1-V_3}{V_1-2V_3}\end{aligned} \tag{4.5}$$

with $V_1 \neq 2V_2$, $V_2 \neq 2V_3$ and $V_1 \neq 2V_3$.

Proof. For $\rho_3 = 0$ the characteristical polynomial is

$$\begin{aligned}\pi_3(\rho_1,\rho_2,0) = \lambda^3 &- \lambda^2\left[V_1(1-2\rho_1-\rho_2)+V_2(1-\rho_1-2\rho_2)+V_3(1-\rho_1-\rho_2)\right]\\ &+\lambda[(1-\rho_1-\rho_2)^2(V_1V_2+V_2V_3+V_1V_3)\\ &-(1-\rho_1-\rho_2)(V_1V_2(\rho_1+\rho_2)+V_2V_3\rho_2+V_1V_3\rho_1)]\\ &-V_1V_2V_3(1-\rho_1-\rho_2)^2(1-2\rho_1-2\rho_2).\end{aligned}$$

The first eigenvalue can be found as

$$\lambda_1 = V_3(1 - \rho_1 - \rho_2).$$

Dividing π_3 by $(\lambda_1 - V_3(1 - \rho_1 - \rho_2))$ yields the characteristical polynomial of the two species LWR model with V_1 and V_2

$$\begin{aligned}\pi_R(\rho_1, \rho_2, 0) &= \lambda^2 - \lambda[V_1(1 - 2\rho_1 - \rho_2) + V_2(1 - \rho_1 - 2\rho_2)] + V_1V_2(1 - \rho_1 - \rho_2)(1 - 2\rho_1 - 2\rho_2) \\ &= (\beta_1 - \lambda)(\beta_2 - \lambda) - \alpha_1\alpha_2\end{aligned}$$

with the abbreviations (3.7) of the last chapter. Thus, we have the three eigenvalues

$$\begin{aligned}\lambda_1(\boldsymbol{\rho}) &= V_3(1 - \rho_1 - \rho_2) \\ \lambda_2(\boldsymbol{\rho}) &= \frac{1}{2}(\beta_1 + \beta_2 - \sqrt{\delta}) \\ \lambda_3(\boldsymbol{\rho}) &= \frac{1}{2}(\beta_1 + \beta_2 + \sqrt{\delta})\end{aligned}$$

where we already know that $\lambda_2(\boldsymbol{\rho}) = \lambda_3(\boldsymbol{\rho})$ for $\boldsymbol{\rho} = \boldsymbol{\rho}^u$. Then, we set $\lambda_1(\boldsymbol{\rho})$ equal to $\lambda_2(\boldsymbol{\rho})$ and $\lambda_3(\boldsymbol{\rho})$ and get the equations describing the values of coinciding eigenvalues in the ρ_1-ρ_2-plane

$$\begin{aligned}\rho_2(\rho_1) &= -\frac{V_2 - V_3}{2V_2 - V_3}\frac{2V_1 - V_2}{V_1 - V_2}\rho_1 + \frac{V_2 - V_3}{2V_2 - V_3} \\ &= -\frac{\rho_1^{u23}}{\rho_1^{u13}}\rho_1 + \rho_1^{u23} \\ \rho_2(\rho_1) &= 1 - \rho_1\end{aligned}$$

We examine the second equation in the next corollary. The first equation describes a linear dependency from ρ_2 of ρ_1. Its behavior varies with the maximal velocities V_1, V_2, and V_3 as do the umbilic points of the corresponding two species models.

Because of the freedom of choosing the indices $i = 1, 2, 3$ the above computation works for one arbitrary species absent and we obtain the other twoumbilic lines of (4.5). We have found the three umbilic points of the fitting two species models for $\rho_1 = 0$, $\rho_2 = 0$ or $\rho_3 = 0$ and umbilic lines described by (4.5) which depend on the maximal velocities. □

Thus, for $\rho_i = 0$, $i = 1, 2, 3$ the three species LWR model reduces to the two species one discussed in the last chapter but with three eigenvalues. From this point, the extension to three species is meaningful. We find more umbilic points algebraically for values of maximal density. Note that not all three umbilic lines must be important for the model since they may lie outside of the simplex $\mathcal{S}$ and we are only interested in umbilic points inside the model's set of definition.

Corollary 4.1.3. *A surface of coalescing eigenvalues is given for values of* $\boldsymbol{\rho}$ *with* $\rho_1 + \rho_2 + \rho_3 = 1$. *The existence and shape of this plane does not depend on the maximal velocities of the three different species.*

Proof. The relation $\rho_1+\rho_2+\rho_3 = 1$ implies that $\psi = 0$ and the characteristical polynomial (4.3) simplifies to

$$\pi_3(\rho_1, \rho_2, \rho_3) = -\lambda^2(\lambda + \rho_1 V_1 + \rho_2 V_2 + \rho_3 V_3).$$

Hence, the first eigenvalue is equal to $-(\rho_1 V_1 + \rho_2 V_2 + \rho_3 V_3)$ while the other two are equal to zero. So, the $\{\rho_1 + \rho_2 + \rho_3\}-$plane is an umbilic surface of the model. □

We provide an example visualizing the proceeding corollaries. For consistency, We choose values equal to the ones for the two species LWR model.

Example 4.1.4. *Consider the three species LWR model (4.2). To connect this example to the previous discussed we choose $V_1 = 1$, $V_2 = 0.75$ and $V_3 = 0.5$. The umbilic points $\boldsymbol{\rho}^{u12}, \boldsymbol{\rho}^{u23}$ and $\boldsymbol{\rho}^{u13}$ of the corresponding two species models are then given by*

$$\begin{aligned}\boldsymbol{\rho}^{u12} &= (0.2, 0, 0)\\ \boldsymbol{\rho}^{u23} &= (0, 0.25, 0)\\ \boldsymbol{\rho}^{u13} &= (0.33, 0, 0).\end{aligned}$$

There are only two umbilic lines because we have $V_1 = 2V_3$ and hence we get no line in the $\rho_2 - \rho_3-$plane from corollary 4.1.2. The umbilic lines in the $\rho_1 - \rho_2-$ and $\rho_1 - \rho_3-$plane are

$$\begin{aligned}\rho_2(\rho_1) &= -0.75\rho_1 + 0.25\\ \rho_3(\rho_1) &= 5\rho_1 - 1.\end{aligned}$$

Moreover, in these planes we see the projection of the umbilic surface where $\rho_1+\rho_2+\rho_3 = 1$ which does not depend on the maximal velocities. These projections are given by $\rho_2(\rho_1) = 1 - \rho_1$ and $\rho_3(\rho_1) = 1 - \rho_1$. All lines ca be seen in figure 4.1. We observe that the umbilic lines intersect the axes in the umbilic points. Altogether, these are all umbilic points, lines and surfaces we find on the boundaries of $\mathcal{S}$. Later on, we see three-dimensional plots of the eigenvalues for the values of the maximal velocity we use in this example.

The following theorem summarizes what we proofed for the existence of umbilic points.

Theorem 4.1.5. *The LWR model for three species given by (4.2) is hyperbolic on the set $\mathcal{S}$. It presents values of $\boldsymbol{\rho}$ where its eigenvalues coincide and hence lacks strict hyperbolicity. On the boundaries of $\mathcal{S}$ the umbilic points are in general described by 4.1.2 and 4.1.3.*

The existence of umbilic points prevents us from using standard theory, like compensated compactness, vanishing viscosity or wave front tracking, to proof well-posedness of the model. Moreover, we are not able to use the theory of Keyfitz and Kranzer [1979/80] since we have umbilic points on the boundaries here.

4.2 Numerical and graphical evaluation

Until now, we have algebraically found umbilic lines and one surface on the boundaries of $\mathcal{S}$. But to see if there are more umbilic points in the interior of $\mathcal{S}$, we need to study the

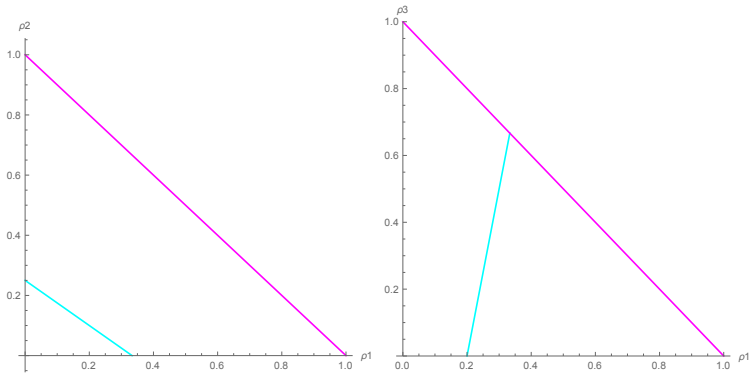

(a) Umbilic lines for $\rho_3 = 0$. (b) Umbilic lines for $\rho_2 = 0$.

Figure 4.1: Umbilic lines for the three species model with one density equal to zero. Here $V_1 = 1, V_2 = 0.75$ and $V_3 = 0.5$.

general terms of eigenvalues. The eigenvalues are computed by Mathematica. Again, we get huge expressions that we cannot handle algebraically. In (4.2.1) we see the result of Mathematica for the first eigenvalue of $J(\boldsymbol{\rho})$.

Remark 4.2.1. *The computation of the general eigenvalues of $J(\boldsymbol{\rho})$ with Mathematica yields very long and complex expressions. Below, we see an abbreviated formula for the first eigenvalue λ_1. Note that $Root[f, k]$ represents the exact k^{th} root of the polynomial equation $f(x_1) = 0$. The computation of Root yields an output of several pages. The other two eigenvalues are of the same shape as this one.*

$$\begin{aligned}\lambda_1(\rho_1,\rho_2,\rho_3) =& Root_{x_1}[-V_1V_2V_3 + 4V_1V_2V_3\rho_1 - 5V_1V_2V_3\rho_1^2 + 2V_1V_2V_3\rho_1^3 + \\ & 4V_1V_2V_3\rho_2 - 10V_1V_2V_3\rho_1\rho_2 + 6V_1V_2V_3\rho_1^2\rho_2 - \\ & 5V_1V_2V_3\rho_2^2 + 6V_1V_2V_3\rho_1\rho_2^2 + 2V_1V_2V_3\rho_2^3 + 4V_1V_2V_3\rho_3 - \\ & 10V_1V_2V_3\rho_1\rho_3 + 6V_1V_2V_3\rho_1^2\rho_3 - 10V_1V_2V_3\rho_2\rho_3 + \\ & 12V_1V_2V_3\rho_1\rho_2\rho_3 + 6V_1V_2V_3\rho_2^2\rho_3 - 5V_1V_2V_3\rho_3^2 + \\ & 6V_1V_2V_3\rho_1\rho_3^2 + 6V_1V_2V_3\rho_2\rho_3^2 + \\ & 2V_1V_2V_3\rho_3^3 + (V_1V_2 + V_1V_3 + V_2V_3 - 3V_1V_2\rho_1 - 3V_1V_3\rho_1 - \\ & 2V_2V_3\rho_1 + 2V_1V_2\rho_1^2 + 2V_1V_3\rho_1^2 + V_2V_3\rho_1^2 - \\ & 3V_1V_2\rho_2 - 2V_1V_3\rho_2 - 3V_2V_3\rho_2 + 4V_1V_2\rho_1\rho_2 + \\ & 3V_1V_3\rho_1\rho_2 + 3V_2V_3\rho_1\rho_2 + 2V_1V_2\rho_2^2 + V_1V_3\rho_2^2 + \\ & 2V_2V_3\rho_2^2 - 2V_1V_2\rho_3 - 3V_1V_3\rho_3 - 3V_2V_3\rho_3 + \\ & 3V_1V_2\rho_1\rho_3 + 4V_1V_3\rho_1\rho_3 + 3V_2V_3\rho_1\rho_3 + 3V_1V_2\rho_2\rho_3 + \\ & 3V_1V_3\rho_2\rho_3 + 4V_2V_3\rho_2\rho_3 + V_1V_2\rho_3^2 + 2V_1V_3\rho_3^2 + \\ & 2V_2V_3\rho_3^2)x_1 + (-V_1 - V_2 - V_3 + 2V_1\rho_1 + V_2\rho_1 + V_3\rho_1 + \\ & V_1\rho_2 + 2V_2\rho_2 + V_3\rho_2 + V_1\rho_3 + V_2\rho_3 + 2V_3\rho_3)x_1^2 + x_1^3, 1].\end{aligned}$$

Due to the complexity of the terms, it is not possible to look for umbilic points inside the simplex, algebraically. However, we can use plots in the three-dimensional phase space $\mathcal{S}$ to understand where the eigenvalues may coalesce. For that purpose, we have to use special values of V_1, V_2 and V_3. This implies that we discuss the existence of umbilic points in the interior of the simplex only for special cases and we cannot in general proof the results we get. We use the maximal velocities of example 4.1.4. Then, Mathematica finds no other umbilic surfaces aside from the congestion axis 4.2 that we have already computed.

In a three- dimensional plot it is not possible to image two-dimensional lines and so we try to get a feeling for the eigenvalues by plotting their level sets and see if they intersect. The level set of the eigenvalue λ_i to the value $c \in \mathbb{R}$ is given by

$$L_c(\lambda_i) = \{(\rho_1, \rho_2, \rho_3) \mid \lambda_i(\rho_1, \rho_2, \rho_3) = c\}.$$

We have already computed the values of the coalescing eigenvalues for one density equal two zero. From this we know that there are umbilic points on the boundaries. We use this as starting point and plot the corresponding level sets for special values for the maximal velocities. One can observe the points in figure 4.2.

(a) shows the level set of the eigenvalues for $\lambda_i = 0.6$, $i = 2, 3$. We only see two surfaces as the first eigenvalue does not attain the value 0.6. Because of the ordering (4.4) it is the smallest eigenvalue and hence not faster than the slowest maximal velocity $V_3 = 0.5$. The blue and red surface touch in the point $\boldsymbol{\rho} = (0.2, 0, 0)$ which we recognize as the umbilic point from 3.10 of the two species LWR model in the last chapter.

Figure (b) and (c) show the level sets for $\lambda_i = 0.33$ and $\lambda_i = 0.375$ with $i = 1, 2, 3$. We recognize the two other umbilic points for the corresponding two species models. In (d) the level sets for $\lambda_i = 0$, $i = 1, 2, 3$ are plotted and we indeed observe that the second and third eigenvalue coalesce on the whole $\{\rho_1 + \rho_2 + \rho_3\}-$surface.

We plot four more level sets $L_c(\lambda_i)$ to see if there may be other umbilic points in the triangle $\mathcal{S}$. For that purpose, we define the interesting values where $L_c \in \mathcal{S}$ for at least two eigenvalues. From 4.2 it follows that the values of interest are $c \in [0, 0.75]$.

From the plots 4.3 we see that the level sets of the eigenvalues interfere with each other only by touching not by crossing. This means that there are no surfaces of umbilic points but the $\{\rho_1 + \rho_2 + \rho_3 = 1\}-$plane that we found algebraically. One also recognizes that 4.1 shows the lines where the eigenvalues coalesce in the projection of the simplex in the $\rho_1 - \rho_2$- and $\rho_1 - \rho_3$-plane. In 4.3 the surfaces only touch in one point because they are level sets of the eigenvalues and hence they coalesce for one value of $\boldsymbol{\rho}$, respectively.

For smaller λ_i the surfaces flatten out until they are flat for $\lambda_i = 0$ with $i = 1, 2, 3$. Hence, the surfaces are not expected to intersect there.

Remember that the ordering of the eigenvalues is fix for the plots. The green (blue, red) surfaces is always the first (second, third) eigenvalue. This confirms the assumption that the eigenvalues coalesce only on the boundaries of $\mathcal{S}$ and that the surfaces do just touch and not cross.

Remark 4.2.2. *The discussion of umbilic points of the three species LWR model is complicated due to the expressions of its eigenvalues. On the boundaries of the simplex $\mathcal{S}$ we*

have a complete description of the values where eigenvalues coalesce. But we considered special values to plot level sets of the λ_i, $i = 1, 2, 3$ to see if there are more umbilic points in the interior. The result is that we do not expect any other umbilic points than the ones on the boundary. But we are not able to proof this assumption due to the complexity that this model delivers.

The lack of strict hyperbolicity yields the necessity to study the well-posedness without the use of standard theorems near the umbilic points. Nevertheless, there is no reason to expect the model to be ill-posed. Aside from that, in the interior of $\mathcal{S}$ we get well-posedness for values with small variation. Altogether, the extension of the LWR model to a two and three species model seems reasonable even though it provides difficulties to prove its well-posedness.

One can proceed this extension to models allowing n different kind of cars. By Benzoni-Gavage and Colombo [2003] these models are hyperbolic but expected to yield umbilic points, too. We are not able to proof well-posedness for a general Riemann problem in the two species case because the expressions are complicated there, too. This implies that the existence and uniqueness for solutions to a Riemann problem or Cauchy problem can not be proved for a LWR model with arbitrary number of vehicle types.

We close the study of the LWR model for different numbers of car species and introduce another traffic model in the next chapter.

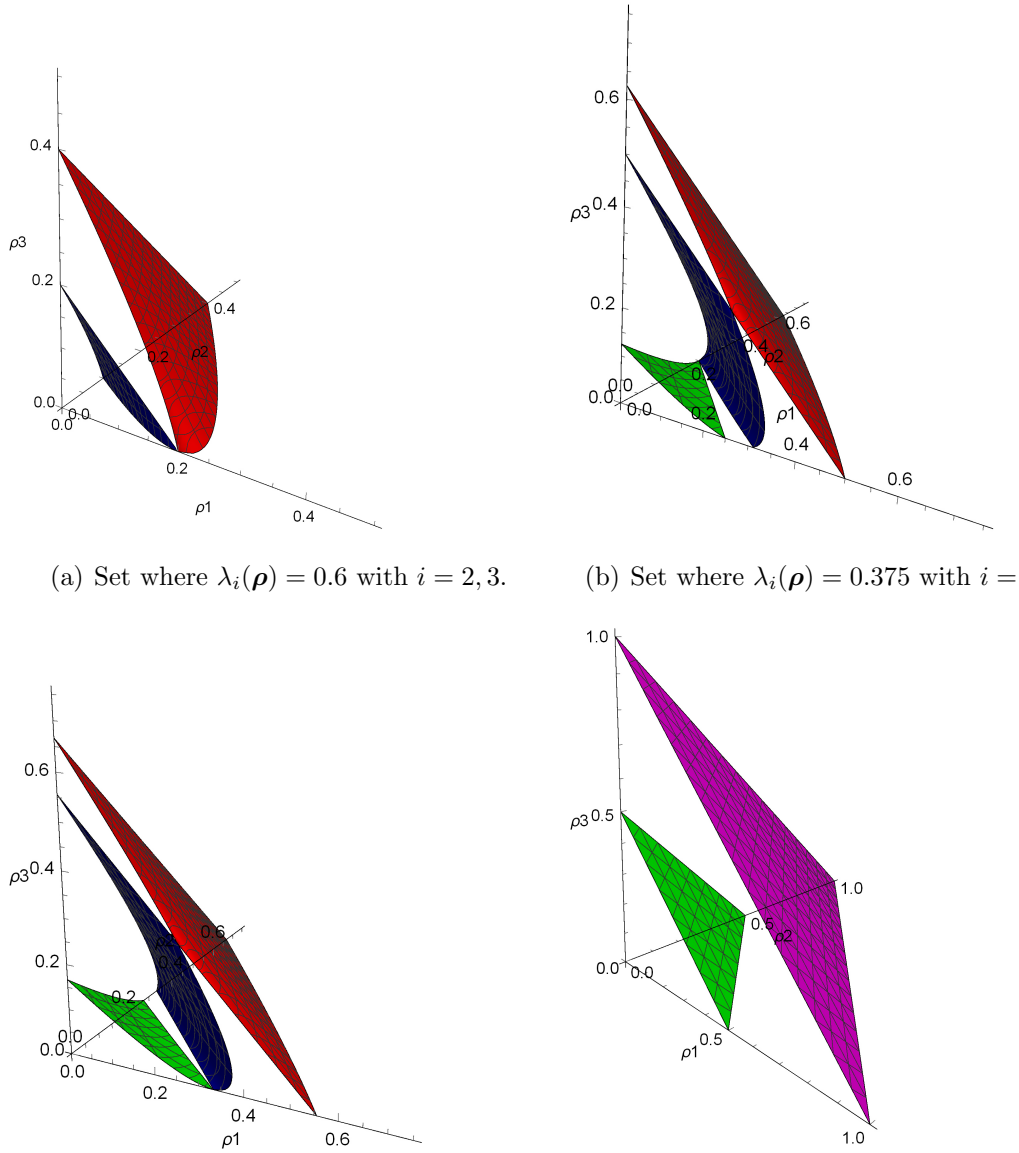

(a) Set where $\lambda_i(\boldsymbol{\rho}) = 0.6$ with $i = 2, 3$.

(b) Set where $\lambda_i(\boldsymbol{\rho}) = 0.375$ with $i = 1, 2, 3$.

(c) Set where $\lambda_i(\boldsymbol{\rho}) = 0.33$ with $i = 1, 2, 3$.

(d) Set where $\lambda_i(\boldsymbol{\rho}) = 0$ with $i = 1, 2, 3$.

Figure 4.2: Values of $\boldsymbol{\rho}$ where eigenvalues coalesce in phase space. The green (blue, red) surface shows the first (second, third) eigenvalue. The points where the surfaces touch are the umbilic points of the corresponding two species models with the third species absent. In (a) the first eigenvalue has no level, (d) shows the $\{\rho_1 + \rho_2 + \rho_3 = 1\}$-surface (magenta), where two eigenvalues coincide.

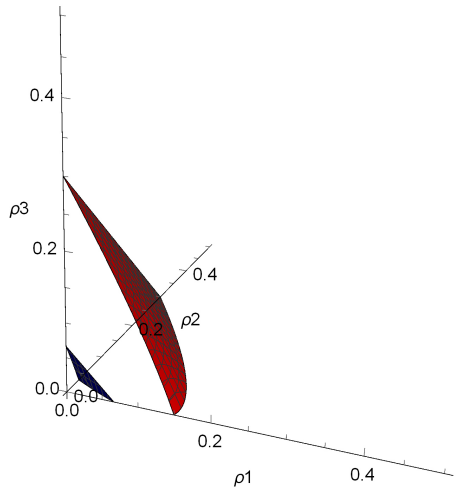

(a) Set where $\lambda_i(\boldsymbol{\rho}) = 0.7$ with $i = 2, 3$.

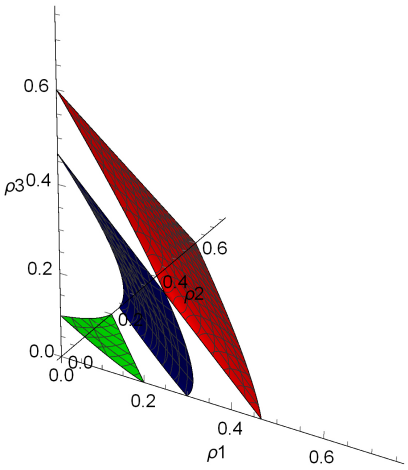

(b) Set where $\lambda_i(\boldsymbol{\rho}) = 0.4$ with $i = 1, 2, 3$.

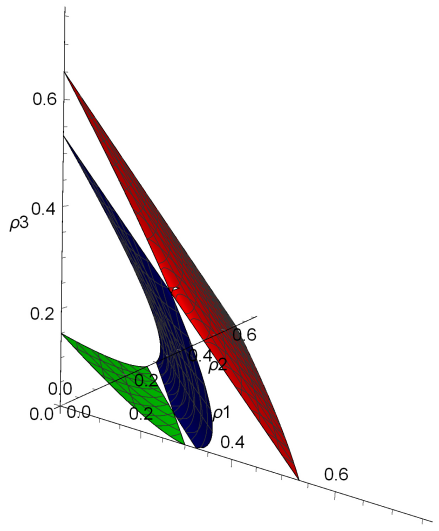

(c) Set where $\lambda_i(\boldsymbol{\rho}) = 0.35$ with $i = 1, 2, 3$.

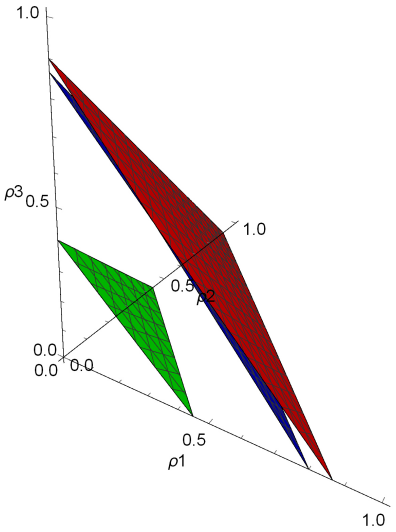

(d) Set where $\lambda_i(\boldsymbol{\rho}) = 0.1$ with $i = 1, 2, 3$.

Figure 4.3: Values of $\boldsymbol{\rho}$ where eigenvalues coalesce in phase space. The green (blue, red) surface shows the first (second, third) eigenvalue. The points where the surfaces touch are the umbilic points of the corresponding two species models with the third species absent.

5 Aw-Rascle-Zhang (ARZ) Model

After the study of the LWR model for one, two and three species, we now introduce the Aw-Rascle-Zhang (ARZ) model with a relaxation term. First, we define the model which consists of two equations. After stating basic theorems about the well-posedness of the system, we compute the Chapman Enskog expansion to see its relaxation behavior and its connection to the LWR model.

5.1 Introduction of the Model

The here introduced traffic model was first mentioned by Aw and Rascle [2000] and Zhang [2002]. As starting point we use the conservation law of the LWR model for one species with density $\rho(x,t)$ and velocity $u(x,t)$. Like for the LWR model, the space $x \in \mathbb{R}$ and time $t \in \mathbb{R}^+$ variables are one-dimensional. We omit writing the variables x and t for clarity

$$\partial_t \rho + \partial_x(\rho u) = 0.$$

Then, the LWR model assumes that the velocity is a function of density, only. We do not use this assumption here but a separate PDE that models the velocity. It is related to the momentum equation of gas dynamics. But there exist substantial differences between gas dynamics and traffic as is stated in Daganzo [1995]. For example a gas molecule responds to events happening in front and behind it while cars only see incidents in front of them. Therefore, the function $h(\rho(x,t))$ is defined

$$h(\rho) = c\rho^\gamma \tag{5.1}$$

with constants $c, \gamma > 0$. Aw and Rascle [2000] call $h(\rho)$ a pressure law related to gas dynamics. Another interpretation from Fan et al. [2014] is to call $h(\rho)$ the hesitation function because we have $h(0) = 0$ and $h'(\rho) > 0$ and thus $h(\rho)$ acts repressive on the velocity. It hesitates the traffic with growing density. The second equation is defined as

$$\partial_t(u + h(\rho)) + u\ \partial_x(u + h(\rho)) = 0.$$

Since the right hand side of the equation equals zero, it is called homogeneous. Note, that this is not a conservation law because it has not been derived from a conserved variable like the LWR model was. Here, we also define the inhomogeneous equation as it is done by Fan et al. [2014]

$$\partial_t(u + h(\rho)) + u\ \partial_x(u + h(\rho)) = \frac{U_{eq}(\rho) - u}{\tau}$$

where $U_{eq}(\rho)$ describes the equilibrium velocity function depending only on the density and $\tau > 0$ is the relaxation time scale. We already know the function $U_{eq}(\rho)$ from the LWR model for one species. There, we derive it from the assumption that the velocity depends on the density uniquely. We define the maximal velocity $V > 0$ by setting $U_{eq}(\rho) = V\psi(\rho)$ with the $\mathcal{C}^1$- function ψ. The Greenshields velocity function we deduced in (2.4) is obtained for $\psi(\rho) = 1 - \rho$. Putting all this together leads to the Aw-Rascle and Zang (ARZ) model.

Definition 5.1.1. *The ARZ model is a second order traffic model. It contains one equation modeling the car density $\rho(x,t)$ and one describing the velocity $u(x,t)$. The homogeneous system of PDE is given by*

$$\begin{aligned} \partial_t \rho + \partial_x(\rho u) &= 0 \\ \partial_t(u + h(\rho)) + u\ \partial_x(u + h(\rho)) &= 0 \end{aligned} \tag{5.2}$$

with the hesitation function $h(\rho) = c\rho^\gamma$, where $c, \gamma > 0$. The inhomogeneous model contains a relaxation term with the equilibrium velocity function $U_{eq}(\rho)$ and the relaxation time scale $\tau > 0$

$$\begin{aligned} \partial_t \rho + \partial_x(\rho u) &= 0, \\ \partial_t(u + h(\rho)) + u\ \partial_x(u + h(\rho)) &= \frac{U_{eq}(\rho) - u}{\tau}. \end{aligned} \tag{5.3}$$

The Riemann problem for this model describes the value of density and velocity at time $t = 0$

$$\begin{aligned} \rho(x,0) &= \begin{cases} \rho^L & for \quad x < 0 \\ \rho^R & for \quad x > 0 \end{cases} \\ u(x,0) &= \begin{cases} u^L & for \quad x < 0 \\ u^R & for \quad x > 0 \end{cases} \end{aligned}. \tag{5.4}$$

Multiplying the first equation with $h'(\rho)$ and adding this to the second one yields

$$\begin{aligned} \partial_t \rho + \partial_x(\rho u) &= 0 \\ \partial_t u + (u - \rho h(\rho))\partial_x u &= 0. \end{aligned}$$

Then, we can write the homogeneous model in one equation

$$\partial_t \mathbf{U} + J(\mathbf{U})\partial_x \mathbf{U} = 0$$

with $\mathbf{U} = (\rho, u)^\intercal$ and the Jacobian

$$J(\mathbf{U}) = \begin{pmatrix} u & \rho \\ 0 & u - \rho h'(\rho) \end{pmatrix}.$$

The eigenvalues of $J(\boldsymbol{\rho})$ are computed as

$$\begin{aligned} \lambda_1 &= u - \rho h'(\rho) \\ \lambda_2 &= u \end{aligned}$$

and yield that (5.2) is strictly hyperbolic except for $\rho = 0$. Moreover, this model fulfills the expectation that the characteristic speeds are smaller than the car velocities since the cars should not be influenced by occasions behind them.

Further discussion of the analysis of this model is done by Aw and Rascle [2000] and Zhang [2002]. We state the results here.

Proposition 5.1.2. *Consider the above system (5.2). Then, the following statements hold:*

1. *The system is strictly hyperbolic, except at the origin.*
2. *For any function h which satisfies (5.1), and for any Riemann data $\rho(x,0)$ and $u(x,0)$ in the region $\mathcal{R} := \{(\rho,u) \in \mathbb{R}^2 | 0 \leq u \leq V - h(\rho), \rho \geq 0, 0 \leq u \leq V\}$, there exists a unique solution to the Riemann problem associated with (5.2) and the data (5.4). This solution satisfies the subsequent principles.*
3. *For all times, the solution remains with values in the invariant region $\mathcal{R}$. In particular, the velocity and the density are non negative and bounded from above.*
4. *The propagation speed of any wave involving a state U is at most equal to its velocity u, i.e. no information travels faster than the velocity of cars.*
5. *The qualitative properties of the solution are as expected. Braking corresponds to a shock, accelerating to a rarefaction.*
6. *When one of the Riemann data is near the vacuum, the solution presents instabilities.*

The last point of this proposition deals with what happens in the case $\rho = 0$. We know that there, the system (5.2) lacks hyperbolicity. Here, the existence of an umbilic point leads to instabilities. This means that the solution to the RP depends continuously on the initial data everywhere except near the vacuum.

But we can consider the ARZ model excluding the origin and still have an invariant set as it is defined in 3.2.4. Hence, the lack of strict hyperbolicity is not dramatic for the ARZ model. Nevertheless, we face problems with the case $\rho = 0$ in the later discussion of the inhomogeneous model (5.3). For a detailed study see Godvik and Hanche-Olsen [2008]. A discussion of global entropic solutions for this model is done in Aw [2014].

The focus of this thesis lies in the connection between the LWR and the ARZ model. In the next section, we make a Chapman Enskog expansion of this model to get a viscous right hand side of the conservation law and study the mentioned connection.

5.2 Chapman Enskog Expansion

We expand the inhomogeneous ARZ model via Chapman Enskog. The Chapman Enskog expansion (CEE) is a tool often used in gas dynamics as in Chapman and Cowling [1970] or Liu [1987]. Since it is a formal expansion and since the ARZ model is related to gas dynamics despite of some basic differences we apply the CEE for this model. The CEE

does not expand solutions but the equations of a PDE although it can be used to examine the behavior of solutions Bedjaoui et al. [2004]. In our case well-posedness is not necessary because we focus on the parabolicity of the viscous term and the connection to LWR.

The expansion of u in τ supplies us with a viscous right hand side of the conservation law. It describes the relaxation of the waves of the system with time. First consider (5.3)

$$\begin{aligned} \partial_t \rho + \partial_x(\rho u) &= 0 \\ \partial_t(u + h(\rho)) + u\ \partial_x(u + h(\rho)) &= \frac{U_{eq}(\rho) - u}{\tau}. \end{aligned}$$

Rewriting the second equation yields

$$\tau\left[\partial_t(u + h(\rho)) + u\ \partial_x(u + h(\rho))\right] = U_{eq}(\rho) - u.$$

Then, if we allow $\tau = 0$ we obtain that $u = U_{eq}(\rho)$ and hence get the scalar conservation law which equals the LWR model

$$\partial_t \rho + \partial_x(\rho U_{eq}(\rho)) = 0.$$

But we want to understand the relaxation as $\tau \to 0$ and hence the scalar conservation law does not describe this process properly. Instead, we ask for a conservation law with a viscous right hand side like

$$\partial_t \rho + \partial_x(\rho U_{eq}(\rho)) = \partial_x(\beta(\rho)\partial_x \rho)$$

with $\beta(\rho) > 0$. To compute β we use the inhomogeneous acceleration equation from (5.3)

$$\partial_t(u + h(\rho)) + u\ \partial_x(u + h(\rho)) = \frac{U_{eq}(\rho) - u}{\tau} \tag{5.5}$$

and expand u.

Corollary 5.2.1. *The expansion of the velocity function $u(x,t)$ in the relaxation time rate τ is given by*

$$u = U_{eq}(\rho) + \tau u^1 + \mathcal{O}(\tau^2).$$

with the second order term

$$u^1 = \rho(U'_{eq}(\rho) + h'(\rho))U_{eq}(\rho)\partial_x \rho + \mathcal{O}(\tau)$$

for $\tau > 0$.

Proof. We have to assume that there are no other terms with order τ arising by differentiation. Otherwise, the following computation would make no sense. The velocity u is expanded in the time rate τ to order two

$$u = U_{eq}(\rho) + \tau u^1 + \mathcal{O}(\tau^2). \tag{5.6}$$

The first order term u^1 is computed from (5.5). Therefore, we solve (5.6) for u_1 and insert the PDE

$$\begin{aligned} u_1 =& \frac{u - U_{eq}(\rho)}{\tau} + \mathcal{O}(\tau) \\ =& - \left[\partial_t(u + h(\rho)) + u\partial_x(u + h(\rho)) + \mathcal{O}(\tau)\right]. \end{aligned}$$

Then, the derivatives are computed and the first equation of (5.3) provides

$$\begin{aligned} u^1 =& - \left[\partial_t u + h'(\rho)\partial_t\rho + u\partial_x u + uh'(\rho)\partial_x\rho + \mathcal{O}(\tau)\right] \\ =& - \left[(U'_{eq}(\rho) + h'(\rho))\partial_t\rho + U_{eq}(\rho)(U'_{eq}(\rho) + h'(\rho))\partial_x\rho + \mathcal{O}(\tau)\right] \\ =& - \left[-(U'_{eq}(\rho) + h'(\rho))\partial_x(\rho u) + U_{eq}(\rho)(U'_{eq}(\rho) + h'(\rho))\partial_x\rho + \mathcal{O}(\tau)\right]. \end{aligned}$$

Finally, we obtain

$$\begin{aligned} u^1 =& - \left[-U_{eq}(\rho)(U'_{eq}(\rho) + h'(\rho))\partial_x\rho - \rho(U'_{eq}(\rho) + h'(\rho))\partial_x u + U_{eq}(\rho)(U'_{eq}(\rho) + h'(\rho))\partial_x\rho + \mathcal{O}(\tau)\right] \\ =& \rho(U'_{eq}(\rho) + h'(\rho))U'_{eq}(\rho)\partial_x\rho + \mathcal{O}(\tau). \end{aligned}$$

□

As a next step, the expansion of $u(x,t)$ can be used to compute the relaxation term.

Corollary 5.2.2. *The Chapman Enskog expansion provides us with a scalar conservation law with a right hand side*

$$\partial_t\rho + \partial_x(\rho U_{eq}(\rho)) = \tau\partial_x(\beta(\rho)\partial_x\rho) + \mathcal{O}(\tau^2) \tag{5.7}$$

where $\tau > 0$ *and*

$$\beta(\rho) = -\rho^2 U'_{eq}(\rho)(U'_{eq}(\rho) + h'(\rho)).$$

For $\tau = 0$ *we get the scalar conservation law again.*

Proof. Inserting the expansion of u into the first equation of (5.3)

$$\partial_t\rho + \partial_x(\rho u) = 0$$

yields

$$\partial_t\rho + \partial_x(\rho(U_{eq}(\rho) + \tau u_1 + \mathcal{O}(\tau^2)) = 0$$

which is equivalent to

$$\partial_t\rho + \partial_x(\rho U_{eq}(\rho)) = -\tau\partial_x(\rho u^1) + \mathcal{O}(\tau^2).$$

On the left hand side one recognizes the conservation law while on the rightnhand side we insert u^1 and finally get the viscous term

$$\begin{aligned} \partial_t\rho + \partial_x(\rho U_{eq}(\rho)) =& - \tau\partial_x(\rho^2 U'_{eq}(\rho)(U'_{eq}(\rho) + h'(\rho))\rho_x) + \mathcal{O}(\tau^2) \\ =& \tau\partial_x(\beta(\rho)\partial_x\rho) + \mathcal{O}(\tau^2) \end{aligned}$$

with

$$\beta(\rho) = -\rho^2 U'_{eq}(\rho)(U'_{eq}(\rho) + h'(\rho)).$$

□

As we have already called the term on the right hand side viscous, we ask $\beta(\rho)$ to be positive. Then, (5.7) is a parabolic PDE which is well studied and understood. We now check the term $\beta(\rho)$ for positiveness with the definition of the traffic variables and functions in mind.

Since ρ is the traffic density it is for sure greater or equal to zero. If $\rho = 0$, also $\beta = 0$ and hence we have no parabolic equation. But as the ARZ model leaks stability around the origin (Godvik and Hanche-Olsen [2008]), it is not surprising that we conclude problems for this value also for the Chapman Enskog expansion. If we consider the ARZ model on the interval $\rho \in [\epsilon, 1]$, we still have an invariant set and we would not loose the well-posedness of the system. We conclude $\rho > 0$ for our discussion.

Moreover, $U'_{eq}(\rho)$ is negative because the equilibrium velocity $U_{eq}(\rho) = V\psi(\rho)$ is expected to be a decreasing function. If we, for example, use the Greenshields function of the LWR model, $U'_{eq}(\rho) = -V$.

The hesitation function $h(\rho)$ is defined to be increasing, so $h'(\rho) > 0$. Now, $U'_{eq}(\rho)+h'(\rho)$ must be positive. For h we choose $h = c\rho^\gamma$ with $\gamma > 0$. Then, for $\rho = 0$, the expression $U'_{eq}(\rho) + h'(\rho)$ would be negative. But we have already excluded the case $\rho = 0$. Hence, we get a condition for the constants V and c. Altogether, β is positive under the following conditions and so the system converges and equation (5.7) is parabolic.

1. $\rho > 0$
2. $h'(\rho) > 0$
3. $U'_{eq}(\rho) < 0$
4. $U'_{eq}(\rho) + h'(\rho) > 0$.

If we use the expression (5.1) and the Greenshields velocity function for U_{eq}, the last property of the enumeration leads to a condition for the constants c and V depending on ρ. We get

$$U'_{eq}(\rho) + h'(\rho) = -V + c\gamma\rho^{\gamma-1} > 0.$$

The above discussion leads to the following theorem.

Theorem 5.2.3. *The Chapman Enskog expansion yields a parabolic PDE*

$$\partial_t\rho + \partial_x(\rho U_{eq}(\rho)) = \tau\partial_x(\beta(\rho)\partial_x\rho) + \mathcal{O}(\tau^2)$$

with

$$\beta(\rho) = -\rho^2 U'_{eq}(\rho)(U'_{eq}(\rho) + h'(\rho))$$

under the condition that $\rho > 0$, $U'_{eq}(\rho) < 0$, $h'(\rho) > 0$ and $U'_{eq}(\rho) + h'(\rho) > 0$. In the case $\rho = 0$ the viscous right hand side vanishes.

A parabolic PDE is well studied and understood, as in Dafermos [2010] and Serre [1999]. Hence, the CEE gives us a tool to understand the LWR with a viscous term. Moreover, we get a connection between the ARZ and the LWR model. One can interpret the LWR

model as the equilibrium limit of the ARZ model. The other way around, one can say that the ARZ model is an extension to a second order traffic model of the LWR first order model.

It is important that exclude the possibility $\rho = 0$. In the next two chapters, we expand the ARZ model to two and three species as we did for the LWR. We meet some difficulties there that we can overcome by a variation of the hesitation and equilibrium function similar to the LWR model.

6 ARZ Model for two species

The ARZ model and its connection to the LWR model for one species are the topic of the previous chapter. The LWR model is the limit of the inhomogeneous ARZ model for $\tau = 0$ and the CEE provides us with a parabolic conservation law. We now introduce an expansion of the ARZ model to a two species model as we did for the LWR model. The expansion is motivated by the same reasons as for the LWR model. Therefore, we consider different types of vehicles on the road. Moreover, it is of interest whether the same connection exists between the two species ARZ and LWR models as for the one species or not. First, we introduce the model and second we apply the CEE, again.

6.1 Introduction of the Model

For the two species LWR model we have the following variables describing species 1 and 2. The first species has density ρ_1 and maximal velocity V_1, while species 2 is modeled via ρ_2 with maximal velocity V_2. We assumed that $V_1 > V_2 > 0$ and $\rho_1 + \rho_2 \leq 1$. With that we introduced the LWR model for two species in 3.1.

Now, the ARZ model for one species consists of two PDE. Species 1 is then described by its density ρ_1 and its velocity u_1. For the second species we set ρ_2 and u_2. The inhomogeneous ARZ model (5.3) also contains the equilibrium velocity function $U_{eq}(\rho)$. We extend it in the same way as we did for the LWR model. Thus, we get $\mathbf{U}_{eq} = (U_{1,eq}, U_{2,eq})^\intercal$ with

$$\begin{aligned} U_{1,eq} &= V_1\psi(\rho_1 + \rho_2) \\ U_{2,eq} &= V_2\psi(\rho_1 + \rho_2) \end{aligned} \tag{6.1}$$

with the monotone decreasing $\mathcal{C}^1-$function $\psi(\rho_1+\rho_2)$ fulfilling $\psi' < 0$ and $\psi(0) = 1, \psi(1) = 0$. For example, the Greenshields velocity function yields $\mathbf{U}_{eq} = (V_1(1 - \rho_1 - \rho_2), V_2(1 - \rho_1 - \rho_2))^\intercal$. In addition, for the hesitation function h we use the extension $\mathbf{h} = (h_1, h_2)^\intercal$. Similar to the one species ARZ we get

$$\begin{aligned} h_1 &= c_1(\rho_1 + \rho_2)^\gamma \\ h_2 &= c_2(\rho_1 + \rho_2)^\gamma \end{aligned} \tag{6.2}$$

with $c_1, c_2 > 0$ and $\gamma > 0$. We see that h_1 and h_2 depend on the sum of the densities, only. Hence, one can define $h(\rho_1 + \rho_2) = (\rho_1 + \rho_2)^\gamma$. Different from the LWR model the equations are coupled through the hesitation and the equilibrium velocity function.

Definition 6.1.1. *The ARZ model describing two different kinds of traffic participants is given by the four partial differential equations*

$$\begin{aligned}\partial_t\rho_1 + \partial_x(\rho_1 u_1) &= 0\\ \partial_t(u_1+h_1) + u_1\partial_x(u_1+h_1) &= 0\\ \partial_t\rho_2 + \partial_x(\rho_2 u_2) &= 0\\ \partial_t(u_2+h_2) + u_2\partial_x(u_2+h_2) &= 0\end{aligned}$$

where the hesitation functions h_1 and h_2 are given by (6.2) with $c_1, c_2 > 0$. With the relaxation time scale $\tau > 0$ we get the inhomogeneous model with relaxation term

$$\begin{aligned}\partial_t\rho_1 + \partial_x(\rho_1 u_1) &= 0\\ \partial_t(u_1+h_1) + u_1\partial_x(u_1+h_1) &= \frac{U_{1,eq}-u_1}{\tau}\\ \partial_t\rho_2 + \partial_x(\rho_2 u_2) &= 0\\ \partial_t(u_2+h_2) + u_2\partial_x(u_2+h_2) &= \frac{U_{2,eq}-u_2}{\tau}\end{aligned} \tag{6.3}$$

with (6.1) for the equilibrium velocity functions. We assume $V_1 > V_2 > 0$. The Riemann problem is of the form

$$\boldsymbol{\rho}(x,0) = \begin{cases}\boldsymbol{\rho}^L = (\rho_1^L, \rho_2^L) for x < 0\\ \boldsymbol{\rho}^R = (\rho_1^R, \rho_2^R) for x > 0\end{cases}$$
$$\mathbf{u}(x,0) = \begin{cases}\mathbf{u}^L = (u_1^L, u_2^L) for x < 0\\ \mathbf{u}^R = (u_1^R, u_2^R) for x > 0\end{cases}.$$

The ARZ model has not been studied for more than one population, yet. In Weidmann et al. [2014] the ARZ model is investigated for a two-way one-lane extension. Thus, there are cars going in two different directions on a two-way road. But this extension is not the same as we adapt here since it is still one-dimensional. Because of that, we have no theorems about its well-posedness. Since we have a system of four PDEs it is hard to compute the eigenvalues of the corresponding Jacobian. We omit the discussion of well-posedness, here.

We are interested in the relaxation behavior and the connection to the LWR two species model. Well-posedness is not necessary for the CEE and hence we can do this without examining it for this model even though it is of interest, too.

6.2 Chapman Enskog Expansion

From above we know that the ARZ model for two populations has not been studied, yet. Since we found a parabolic equation out of the one species model by the CEE, we want to study the two populations model the same way. In the next chapter, we also introduce the

three species ARZ model and compute the CEE there. Therefore, we skip the proof of the stated corollaries here and refer to the three populations case. Consider (6.3)

$$\begin{aligned}\partial_t\rho_1 + \partial_x(\rho_1 u_1) &= 0\\ \partial_t(u_1+h_1) + u_1\partial_x(u_1+h_1) &= \frac{U_{1,eq}-u_1}{\tau}\\ \partial_t\rho_2 + \partial_x(\rho_2 u_2) &= 0\\ \partial_t(u_2+h_2) + u_2\partial_x(u_2+h_2) &= \frac{U_{2,eq}-u_2}{\tau}\end{aligned}$$

and multiply the second and fourth equation with τ. Similar to the one species one sets $\tau = 0$ and gets the LWR model for two populations

$$\begin{aligned}\partial_t\rho_1 + \partial_x(\rho_1 U_{1,eq}) &= 0\\ \partial_t\rho_2 + \partial_x(\rho_2 U_{2,eq}) &= 0\end{aligned}$$

with (6.1). In the next corollary, we expand u_1 and u_2 in τ.

Corollary 6.2.1. *For the two species ARZ model we have to make two expansions*

$$\begin{aligned}u_1 &= U_{1,eq} + \tau u_1^1 + \mathcal{O}(\tau^2)\\ u_2 &= U_{2,eq} + \tau u_2^1 + \mathcal{O}(\tau^2).\end{aligned}$$

with $\tau > 0$ and the second order terms u_1^1 and u_2^1 which are computed from the corresponding momentum equations of (6.3).

We omit writing the expressions of u_1^1 and u_2^1 because they are similar as for three species. We compute u_1^1 from the second equation of (6.3) and u_2^1 from the fourth. Then, we derive two equations with right hand sides

$$\begin{aligned}\partial_t\rho_1 + \partial_x(\rho_1 U_{1,eq}) &= \tau\partial_x(\beta_{11}\partial_x\rho_1 + \beta_{12}\partial_x\rho_2) + \mathcal{O}(\tau^2)\\ \partial_t\rho_2 + \partial_x(\rho_2 U_{2,eq}) &= \tau\partial_x(\beta_{21}\partial_x\rho_1 + \beta_{22}\partial_x\rho_2) + \mathcal{O}(\tau^2)\end{aligned}$$

and we state a second corollary.

Corollary 6.2.2. *From the CEE for two species we get two conservation laws with right hand side which we combine in one equation*

$$\partial_t\boldsymbol{\rho} + \partial_x(\boldsymbol{\rho} U_{eq}) = \tau\partial_x(\beta\partial_x\boldsymbol{\rho}) + \mathcal{O}(\tau^2) \tag{6.4}$$

with $\boldsymbol{\rho} = (\rho_1, \rho_2)^\intercal$ and the matrix $\beta(\boldsymbol{\rho})$

$$\begin{pmatrix}\beta_{11} & \beta_{12}\\ \beta_{21} & \beta_{22}\end{pmatrix}.$$

The entries of β are given by

$$\begin{aligned}\beta_{11} &= -(V_1\psi' + c_1h')\rho_1\psi'(\rho_1V_1 + \rho_2V_2)\\ \beta_{12} &= -(V_1\psi' + c_1h')\rho_1(\psi'(\rho_1V_1 + \rho_2V_2) + \psi(V_2 - V_1))\\ \beta_{22} &= -(V_2\psi' + c_2h')\rho_2\psi'(\rho_2V_2 + \rho_1V_1)\\ \beta_{21} &= -(V_2\psi' + c_2h')\rho_2(\psi'(\rho_2V_2 + \rho_1V_1) + \psi(V_1 - V_2)).\end{aligned}$$

Proof. For the computation of β we refer to the three species case. Here, we only explain the derivatives of the hesitation and equilibrium velocity function. In (6.2) we assumed that the hesitation function depends only on the sum of the densities

$$\begin{aligned} h_1 =& c_1 h(\rho_1 + \rho_2) \\ h_2 =& c_2 h(\rho_1 + \rho_2). \end{aligned}$$

Then, the derivatives are

$$\begin{aligned} \frac{\partial h(\rho_1 + \rho_2)}{\partial \rho_i} =& h'(\rho_1 + \rho_2) \\ \frac{\partial h_j(\rho_1, \rho_2)}{\partial \rho_i} =& c_j h'(\rho_1 + \rho_2) \end{aligned}$$

for $i, j = 1, 2$. The same holds for $\mathbf{U}_{eq}$

$$\begin{aligned} U_{1,eq} =& V_1 \psi(\rho_1 + \rho_2) \\ U_{2,eq} =& V_2 \psi(\rho_1 + \rho_2). \end{aligned}$$

Hence, for the derivatives we get

$$\begin{aligned} \frac{\partial \psi(\rho_1 + \rho_2)}{\partial \rho_i} =& \psi'(\rho_1 + \rho_2) \\ \frac{\partial \mathbf{U}_{j,eq}}{\partial \rho_i} =& V_j \psi'(\rho_1 + \rho_2) \end{aligned}$$

with $i, j = 1, 2$. □

In contrast to the previous chapter β is a matrix. Hence, (5.7) is a parabolic equation, if $\beta(\boldsymbol{\rho})$ is positive definite. Inserting the entries of β yields

$$\begin{pmatrix} (V_1\psi' + c_1 h')\rho_1 \psi' R & (V_1\psi' + c_1 h')\rho_1(\psi' R + \psi(V_2 - V_1)) \\ (V_2\psi' + c_2 h')\rho_2(\psi' R + \psi(V_1 - V_2)) & (V_2\psi' + c_2 h')\rho_2 \psi' R \end{pmatrix} \tag{6.5}$$

where $R = \rho_1 V_1 + \rho_2 V_2$. Now β is not symmetric and we have to consider its symmetric part for positive definiteness. Hence, we check if all the leading principal minors of $\beta_s = 1/2(\beta + \beta^\intercal)$ are positive, i.e. if $\beta_{s,11} > 0$ and if $\det(\beta_s) > 0$. We state the conditions under which β_s and thus β is positive definite.

Theorem 6.2.3. *The Chapman Enskog expansion for the two species ARZ model grants the two-dimensional conservation law with right hand side*

$$\partial_t \boldsymbol{\rho} + \partial_x(\boldsymbol{\rho} U_{eq}) = \tau \partial_x(\beta \partial_x \boldsymbol{\rho}) + \mathcal{O}(\tau^2)$$

with the matrix β from (6.5) and $\tau > 0$. The equation is parabolic, if β is positive definite. That holds under the following conditions

1. $\rho_1, \rho_2 > 0$

2. $V_1 > V_2$
3. $\psi' < 0$
4. $a_1 > 0$
5. $a_2 > 0$
6. $a_2 > a_1$
7. $2\,|p|\,b_1(a_2 + a_1) > (p^2 + b_1^2)(a_2 - a_1)$

with the functions defined in (7.7). For $\tau = 0$ one obtains the LWR model for two species, again.

We observe that the ARZ model for two populations is in the same way connected to the LWR two species model as the corresponding one population models are. We do not allow zero densities similar to the previous chapter. We have not studied the solution of the two species ARZ model. But we know that in the one species case we face instabilities near the vacuum and we have to exclude the origin for CEE there, too. Hence, it is not surprising that zero density does not work here either.

Remark 6.2.4. *We exclude the case that $V_1 = V_2$ and of course we assumed from the beginning that $V_1 > V_2 > 0$. Nevertheless, the case where both maximal velocities are equal is interesting even though the system is degenerate parabolic. By looking at the equations for $\tau = 0$ one observes why this is reasonable*

$$\begin{aligned}\partial_t \rho_1 + \partial_x(\rho_1 V_1 \psi) &= 0\\ \partial_t \rho_2 + \partial_x(\rho_2 V_2 \psi) &= 0.\end{aligned}$$

Adding up the two equations yields

$$\partial_t(\rho_1 + \rho_2) + \partial_x((V_1\rho_1 + V_2\rho_2)\psi) = 0.$$

For $V_1 = V_2 = V$ one gets the closed equation with $q = \rho_1 + \rho_2$

$$\partial_t q + V\partial_x(q\psi(q)) = 0$$

and it suffices to solve the PDE for q. The two equation model can therefore be dispensed in this special case.

It is clear that the two species model with $V_1 = V_2$ simplifies to a single PDE because it equals two times a one species model. Altogether, the expansion to a two species ARZ model is justified because it provides a parabolic expansion of the two species LWR. But clearly the lack of knowledge about the well-posedness of the system prevents the model from interpretation and use of the traffic point of view. Note that the properties of the two species CEE apply to the one species model.

We now consider a variation of the ARZ model for two species similar to the variation of the LWR two species model.

6.3 Variation of the ARZ Model for two species

We have already discussed a variation of the two species LWR model, hence we introduce a variation for the ARZ two populations model, too. For detailed computation we refer to the three species case. We again consider (6.3)

$$\begin{aligned}\partial_t\rho_1 + \partial_x(\rho_1 u_1) &= 0\\ \partial_t(u_1+h_1) + u_1\partial_x(u_1+h_1) &= \frac{U_{1,eq}-u_1}{\tau}\\ \partial_t\rho_2 + \partial_x(\rho_2 u_2) &= 0\\ \partial_t(u_2+h_2) + u_2\partial_x(u_2+h_2) &= \frac{U_{2,eq}-u_2}{\tau}.\end{aligned}$$

Now, one can make different assumptions on the functions h_1, h_2 and $U_{1,eq}, U_{2,eq}$ than we did before. We assume that the faster species are cars while the slower species are for example trucks. The faster moving cars have to observe the whole traffic situation and hence adapt their behavior depending on both densities, their own and that of the trucks. For the hesitation and equilibrium velocity functions this yields

$$\begin{aligned}h_1 &= c_1 h(\rho_1+\rho_2)\\ U_{1,eq} &= V_1\psi(\rho_1+\rho_2).\end{aligned}$$

The second species, the trucks, is slower than the first species. One can assume that the trucks only mind their own species and not the faster traveling cars. This can be observed in traffic situations, too. Therefore, the hesitation and equilibrium velocity depend on ρ_2, only.

$$\begin{aligned}h_2 &= c_2 h(\rho_2)\\ U_{2,eq} &= V_2\psi(\rho_2).\end{aligned}$$

This leads to the ARZ model for cars and trucks

Definition 6.3.1. *The variation of the assumptions on the hesitation and equilibrium velocity function lead to a model where the equations modeling species* 2 *are decoupled from the ones describing species* 1

$$\begin{aligned}\partial_t\rho_1 + \partial_x(\rho_1 u_1) &= 0\\ \partial_t(u_1 + c_1 h(\rho_1+\rho_2)) + u_1\partial_x(u_1 + c_1 h(\rho_1+\rho_2)) &= \frac{V_1\psi(\rho_1+\rho_2)-u_1}{\tau}\\ \partial_t\rho_2 + \partial_x(\rho_2 u_2) &= 0\\ \partial_t(u_2 + c_2 h(\rho_2)) + u_2\partial_x(u_2 + c_2 h(\rho_2)) &= \frac{V_2\psi(\rho_2)-u_2}{\tau}\end{aligned}$$

with $h(\boldsymbol{\rho}) = (\rho_1+\rho_2)^\gamma$ *and* $\gamma > 0$. *For the velocity function we set* $\psi(\boldsymbol{\rho}) = (1-\rho_1-\rho_2)$.

Then, one can again do a CEE and see if the variation leads to different conditions than the original model does. The terms slightly change due to the varied assumptions on the functions h_1, h_2 and $U_{1,eq}, U_{2,eq}$. But apart from that, the computation is analog and so we just give the results. A neat study is done for the three species model.

Proposition 6.3.2. *For a variation of the hesitation and equilibrium velocity functions the CEE yields two conservation laws with viscous right hand side*

$$\partial_t \boldsymbol{\rho} + \partial_x(\boldsymbol{\rho} U_{eq}) = \tau \partial_x(\beta \partial_x \boldsymbol{\rho}) + \mathcal{O}(\tau^2)$$

with the matrix β

$$\beta(\boldsymbol{\rho}) = \begin{pmatrix} (V_1\psi' + c_1 h')\rho_1^2 U_{1,eq}' & (V_1\psi' + c_1 h')\rho_1((\rho_1 V_1 + \rho_2 V_2)\psi' + (V_2 - V_1)\psi)) \\ 0 & (V_2\psi' + c_2 h')\rho_2^2 V_2 \psi' \end{pmatrix}$$

which is different from the original one (6.5). It is positive definite under the following conditions

1. $\rho_1, \rho_2 > 0$
2. $V_1, V_2 > 0$
3. $\psi' < 0$
4. $a_1 > 0$
5. $a_2 > 0$
6. $a_2 > a_1$
7. $2\,|p|\, b_1(a_2 + a_1) > (p^2 + b_1^2)(a_2 - a_1)$
8. $V_1 \neq V_2$

with the abbreviations (7.7). For $\tau = 0$ *we get the varied LWR model.*

Thus, the variation leads to conditions similar to the original ones. Note, that the modified model consists of a combination of the one and the two species ARZ model. The first two equations which model the faster species 1 are of two species type due to the assumption that the cars mind both densities. But the last two equations describing species 2 are of one species type because we considered the trucks to see only their own kind on the road. Hence, the equations for the second species can be solved without the equations for ρ_1 and u_1. This means that the variation yields a triangular system.

The knowledge about well-posedness of the one species model can be used to find the solution for ρ_2 and we can insert this in the first two equations and obtain two equations modeling ρ_1 and u_1. Then, we use proposition (5.1.2) a second time to obtain the solution for the first species.

In the next chapter, we develop the three species ARZ model similar to the two species one. There, we proof the CEE and hence get a proof for the two species case even though this case is more intricate.

7 ARZ Model for three species

Since we examined the LWR model also for three species, we consider the ARZ model for three species and see, if we get the same connection between the models as before. First, we introduce the model and its functions h_i and $U_{eq,i}$ with $i = 1, 2, 3$ by adding a third species to the two populations model. Again, this model has not been studied, yet.

The CEE is done with the complete computation. We conclude that proving parabolicity requires properties of the traffic functions that we are not able to motivate from a traffic point of view. Secondly, we consider a variation of the three species case allowing the study of different cases.

7.1 Introduction of the Model

We introduce the third species with the variables $\rho_3(x,t), u_3(x,t)$, the functions $h_3(\boldsymbol{\rho}), U_{eq,3}(\boldsymbol{\rho})$ and the constants $V_3, c_3 > 0$. Now, we have $\boldsymbol{\rho} = (\rho_1, \rho_2, \rho_3)^\intercal$. The third species is the slowest and hence $V_1 > V_2 > V_3 > 0$. This yields a system of six equations. It has to be noted here, that there are no theorems about the well-posedness of this system in literature. The hesitation and equilibrium velocity function have to be expanded to three species. Hence, we get

$$\begin{aligned} h_1(\boldsymbol{\rho}) &= c_1 h(\rho_1 + \rho_2 + \rho_3) \\ h_2(\boldsymbol{\rho}) &= c_2 h(\rho_1 + \rho_2 + \rho_3) \\ h_3(\boldsymbol{\rho}) &= c_3 h(\rho_1 + \rho_3 + \rho_3) \\ U_{1,eq}(\boldsymbol{\rho}) &= V_1 \psi(\rho_1 + \rho_2 + \rho_3) \\ U_{2,eq}(\boldsymbol{\rho}) &= V_2 \psi(\rho_1 + \rho_2 + \rho_3) \\ U_{3,eq}(\boldsymbol{\rho}) &= V_3 \psi(\rho_1 + \rho_2 + \rho_3). \end{aligned} \tag{7.1}$$

Definition 7.1.1. *The three species ARZ model is defined by the following partial differential equations*

$$\begin{aligned} \partial_t \rho_1 + \partial_x(\rho_1 u_1) &= 0 \\ \partial_t(u_1 + h_1) + u_1 \partial_x(u_1 + h_1) &= 0 \\ \partial_t \rho_2 + \partial_x(\rho_2 u_2) &= 0 \\ \partial_t(u_2 + h_2) + u_2 \partial_x(u_2 + h_2) &= 0 \\ \partial_t \rho_3 + \partial_x(\rho_3 u_3) &= 0 \\ \partial_t(u_3 + h_3) + u_3 \partial_x(u_3 + h_3) &= 0. \end{aligned}$$

The inhomogeneous model is given by

$$\begin{aligned}
\partial_t \rho_1 + \partial_x(\rho_1 u_1) &= 0 \\
\partial_t(u_1 + h_1) + u_1 \partial_x(u_1 + h_1) &= \frac{U_{1,eq} - u_1}{\tau} \\
\partial_t \rho_2 + \partial_x(\rho_2 u_2) &= 0 \\
\partial_t(u_2 + h_2) + u_2 \partial_x(u_2 + h_2) &= \frac{U_{2,eq} - u_2}{\tau} \\
\partial_t \rho_3 + \partial_x(\rho_3 u_3) &= 0 \\
\partial_t(u_3 + h_3) + u_3 \partial_x(u_3 + h_3) &= \frac{U_{3,eq} - u_3}{\tau}
\end{aligned} \tag{7.2}$$

with the assumptions (7.1) on the hesitation and equilibrium velocity functions and the constants $V_1 > V_2 > V_3 > 0$ *and* $c_1, c_2, c_3 > 0$. *For the Riemann problem we have*

$$\boldsymbol{\rho}(x,0) = \begin{cases} \boldsymbol{\rho}^L = (\rho_1^L, \rho_2^L, \rho_3^L) & \text{for } x < 0 \\ \boldsymbol{\rho}^R = (\rho_1^R, \rho_2^R, \rho_3^R) & \text{for } x > 0 \end{cases}$$
$$\mathbf{u}(x,0) = \begin{cases} \mathbf{u}^L = (u_1^L, u_2^L, u_3^L) & \text{for } x < 0 \\ \mathbf{u}^R = (u_1^R, u_2^R, u_3^R) & \text{for } x > 0 \end{cases}.$$

Similar to the two populations ARZ model we cannot state theorems about the well-posedness of the RP since it has not been studied, yet. In addition, the corresponding Jacobian is a six dimensional matrix and it is clear that even though the ARZ model for one species had simple eigenvalues we expect more complicated ones here. Again, we omit the discussion of well-posedness because we are more interested in the connection to the LWR model and the relaxation behavior. Nevertheless, the well-posedness is an interesting question and the assumption of existence is necessary for further consideration.

In the next section, we expand the inhomogeneous model in the Chapman Enskog way.

7.2 Chapman Enskog Expansion

The CEE for the three species ARZ model is related to the one and two species expansion. The statements and computations are analog to the discussions before and because the computation for three species is more complicated we do it more thoroughly, here. For

this, we use the inhomogeneous model (7.2)

$$\begin{aligned}
\partial_t \rho_1 + \partial_x(\rho_1 u_1) &= 0 \\
\partial_t(u_1 + h_1) + u_1 \partial_x(u_1 + h_1) &= \frac{U_{1,eq} - u_1}{\tau} \\
\partial_t \rho_2 + \partial_x(\rho_2 u_2) &= 0 \\
\partial_t(u_2 + h_2) + u_2 \partial_x(u_2 + h_2) &= \frac{U_{2,eq} - u_2}{\tau} \\
\partial_t \rho_3 + \partial_x(\rho_3 u_3) &= 0 \\
\partial_t(u_3 + h_3) + u_3 \partial_x(u_3 + h_3) &= \frac{U_{3,eq} - u_3}{\tau}.
\end{aligned}$$

If we allow $\tau = 0$, we have the three species LWR model

$$\begin{aligned}
\partial_t \rho_1 + \partial_x(\rho_1 U_{1,eq}) &= 0 \\
\partial_t \rho_2 + \partial_x(\rho_2 U_{2,eq}) &= 0 \\
\partial_t \rho_3 + \partial_x(\rho_3 U_{3,eq}) &= 0.
\end{aligned} \tag{7.3}$$

But since we are interested in a conservation law with viscous right hand side this is not sufficient. We expand u_1, u_2 and u_3 instead.

Corollary 7.2.1. *Expanding the functions u_i with $i = 1, 2, 3$ in τ in a Chapman Enskog way yields*

$$\begin{aligned}
u_1 &= U_{1,eq} + \tau u_1^1 + \mathcal{O}(\tau^2) \\
u_2 &= U_{2,eq} + \tau u_2^1 + \mathcal{O}(\tau^2) \\
u_3 &= U_{3,eq} + \tau u_3^1 + \mathcal{O}(\tau^2)
\end{aligned}$$

with the second order terms u_1^1, u_2^1, u_3^1 and $\tau > 0$. We can summarize the second order terms for $i = 1, 2, 3$

$$\begin{aligned}
u_i^1 =& (V_i\psi' + c_i h'(\rho))(\psi' R + (V_1 - V_i)\psi)\partial_x \rho_1 \\
&+ (V_i\psi' + c_i h'(\rho))(\psi' R + (V_2 - V_i)\psi)\partial_x \rho_2 \\
&+ (V_i\psi' + c_i h'(\rho))(\psi' R + (V_3 - V_i)\psi)\partial_x \rho_3.
\end{aligned}$$

Proof. We compute the terms u_i^1 from the inhomogeneous momentum equations of (7.2). One can abbreviate the computation by doing it for the general case i with $i = 1, 2, 3$. Therefore, we combine the three momentum equations with the index i

$$\partial_t(u_i + h_i) + u_i \, \partial_x(u_i + h_i) = \frac{U_{i,eq} - u_i}{\tau}.$$

We do the same for the expansion

$$u_i = U_{i,eq} + \tau u_i^1 + \mathcal{O}(\tau^2)$$

and then compute u_i^1 from the momentum equation like we did in the one species case. Since here the functions h_i and $U_{i,eq}$ depend on $\boldsymbol{\rho}$ we obtain derivatives of ρ_i for $i = 1, 2, 3$. Again, we assume that no other terms of order τ arise during the differentiation of the functions and variables

$$\begin{aligned} u_i^1 =& \frac{u_i - U_{i,eq}}{\tau} + \mathcal{O}(\tau) \\ =& - \left[\partial_t(u_i + h_i) + u_i\ \partial_x(u_i + h_i) + \mathcal{O}(\tau)\right]. \end{aligned}$$

The derivatives can be computed and the first equation of (7.2) gives

$$\begin{aligned} u_i^1 =& - \left[\partial_t(u_i + h_i) + u_i\partial_x(u_i + h_i) + \mathcal{O}(\tau)\right] \\ =& - \left[(V_i\psi' + c_ih'(\rho))(\partial_t\rho_1 + \partial_t\rho_2 + \partial_t\rho_3) + u_i(V_i\psi' + c_ih'(\rho))(\partial_x\rho_1 + \partial_x\rho_2 + \partial_x\rho_3) + \mathcal{O}(\tau)\right] \\ =& - (V_i\psi' + c_ih'(\rho))[(-\partial_x(\rho_1u_1) - \partial_x(\rho_2u_2) - \partial_x(\rho_3u_3)) + u_i(\partial_x\rho_1 + \partial_x\rho_2 + \partial_x\rho_3) + \mathcal{O}(\tau)] \\ =& - (V_i\psi' + c_ih'(\rho))[-(\rho_1\partial_xu_1 + \rho_2\partial_xu_2 + \rho_3\partial_xu_3) + (V_1 - V_i)\psi\partial_x\rho_1 + (V_2 - V_i)\psi\partial_x\rho_2 \\ & + (V_3 - V_i)\psi\partial_x\rho_3 + \mathcal{O}(\tau)] \end{aligned}$$

where we used $\partial_x u_i = \partial_x U_{i,eq} + \mathcal{O}(\tau)$ and the assumptions (7.1). Finally, we obtain

$$\begin{aligned} u_i^1 =& (V_i\psi' + c_ih'(\rho))[\psi'(\rho_1V_1 + \rho_2V_2 + \rho_3V_3)(\partial_x\rho_1 + \partial_x\rho_2 + \partial_x\rho_3) + (V_1 - V_i)\psi\partial_x\rho_1 \\ & + (V_2 - V_i)\psi\partial_x\rho_2 + (V_3 - V_i)\psi\partial_x\rho_3 + \mathcal{O}(\tau)] \\ =& \ (V_i\psi' + c_ih'(\rho))(\psi'R + (V_1 - V_i)\psi)\partial_x\rho_1 \\ & + (V_i\psi' + c_ih'(\rho))(\psi'R + (V_2 - V_i)\psi)\partial_x\rho_2 \\ & + (V_i\psi' + c_ih'(\rho))(\psi'R + (V_3 - V_i)\psi)\partial_x\rho_3. \end{aligned}$$

□

Since we know u_i^1 we insert it in the conservation laws of (7.2) for $i = 1, 2, 3$

$$\begin{aligned} \partial_t\rho_1 + \partial_x(\rho_1U_{1,eq}) =& - \tau\partial_x(\rho_1u_1^1) + \mathcal{O}(\tau^2) \\ =& \tau\partial_x(\beta_{11}\partial_x\rho_1 + \beta_{12}\partial_x\rho_2 + \beta_{13}\partial_x\rho_3) + \mathcal{O}(\tau^2) \\ \partial_t\rho_2 + \partial_x(\rho_2U_{2,eq}) =& - \tau\partial(\rho_2u_2^1) + \mathcal{O}(\tau^2) \\ =& \tau\partial_x(\beta_{21}\partial_x\rho_1 + \beta_{22}\partial_x\rho_2 + \beta_{23}\partial_x\rho_3) + \mathcal{O}(\tau^2) \\ \partial_t\rho_3 + \partial_x(\rho_3U_{3,eq}) =& - \tau\partial_x(\rho_3u_3^1) + \mathcal{O}(\tau^2) \\ =& \tau\partial_x(\beta_{31}\partial_x\rho_1 + \beta_{32}\partial_x\rho_2 + \beta_{33}\partial_x\rho_3. \end{aligned} \tag{7.4}$$

The vector $\boldsymbol{\rho} = (\rho_1, \rho_2, \rho_3)^\intercal$ implies a three dimensional system with matrix $\beta(\boldsymbol{\rho})$

$$\begin{pmatrix} \beta_{11} & \beta_{12} & \beta_{13} \\ \beta_{21} & \beta_{22} & \beta_{23} \\ \beta_{31} & \beta_{32} & \beta_{33} \end{pmatrix}$$

which we describe in the next corollary.

Corollary 7.2.2. *For the three species ARZ model one obtains a three-dimensional system of viscous conservation laws from the Chapman Enskog expansion*

$$\partial_t \boldsymbol{\rho} + \partial_x(\boldsymbol{\rho} U_{eq}) = \tau \partial_x(\beta \partial_x \boldsymbol{\rho}) + \mathcal{O}(\tau^2) \tag{7.5}$$

with $\tau > 0$ and the matrix $\beta(\boldsymbol{\rho})$

$$\beta_{ij}(\boldsymbol{\rho}) = \left(-(V_i\psi' + c_i h'(\rho))\rho_i(\psi' R + (V_j - V_i)\psi)\right)_{ij}. \tag{7.6}$$

Here R stands for the weighted sum $R = \rho_1 V_1 + \rho_2 V_2 + \rho_3 V_3$.

Proof. One obtains (7.5) by writing the three single viscous conservation laws in one vector-valued equation. Then, we have to compute the entries of β with the help of the term u_i^1 for $i = 1, 2, 3$. For the first equation of (7.4) β_{11} equals the factor of $\partial_x \rho_1$ times $(-\rho_1)$ of u_1^1 while β_{12} equals the factor of $\partial_x \rho_2$ times $(-\rho_1)$ and so on. This yields

$$\begin{aligned}
\beta_{11} &= -(V_1\psi' + c_1 h'(\rho))\rho_1\psi' R \\
\beta_{12} &= -(V_1\psi' + c_1 h'(\rho))\rho_1(\psi' R + (V_2 - V_1)\psi) \\
\beta_{13} &= -(V_1\psi' + c_1 h'(\rho))\rho_1(\psi' R + (V_3 - V_1)\psi) \\
\beta_{21} &= -(V_2\psi' + c_2 h'(\rho))\rho_2(\psi' R + (V_1 - V_2)\psi) \\
\beta_{22} &= -(V_2\psi' + c_2 h'(\rho))\rho_2\psi' R \\
\beta_{23} &= -(V_2\psi' + c_2 h'(\rho))\rho_2(\psi' R + (V_3 - V_2)\psi) \\
\beta_{31} &= -(V_3\psi' + c_3 h'(\rho))\rho_3(\psi' R + (V_1 - V_3)\psi) \\
\beta_{32} &= -(V_3\psi' + c_3 h'(\rho))\rho_3(\psi' R + (V_2 - V_3)\psi) \\
\beta_{33} &= -(V_3\psi' + c_3 h'(\rho))\rho_3\psi' R
\end{aligned}$$

and summarizing leads to (7.6). □

The same computation can be done with general functions h_i and $U_{i,eq}$ but this makes it more complicated and less clear and so we omit it. As we are interested in the connection to the LWR model, where we used the Greenshields velocity function, it is sufficient to investigate the CEE only for special functions.

Next, we check whether (7.5) is indeed parabolic. Therefore, the matrix $\beta(\boldsymbol{\rho})$ is examined for positive definiteness. It is not symmetric, hence we consider its symmetric part β_s which is defined by

$$\beta_s = \frac{1}{2}(\beta + \beta^\intercal).$$

With the abbreviations

$$\begin{aligned}
a_i &= (V_i\psi' + c_i h'(\rho))\rho_i \\
b_1 &= (V_1 - V_2)\psi \\
b_2 &= (V_1 - V_3)\psi \\
b_3 &= (V_2 - V_3)\psi \\
p_i &= \rho_i V_i \psi' \\
p &= \sum_{i=1}^{3} p_i = R\psi'
\end{aligned} \tag{7.7}$$

we can rewrite the matrix β

$$\beta = -\begin{pmatrix} a_1 p & a_1(p-b_1) & a_1(p-b_2) \\ a_2(p+b_1) & a_2 p & a_2(p-b_3) \\ a_3(p+b_2) & a_3(p+b_3) & a_3 p \end{pmatrix}$$

and for β_s we obtain

$$\beta_s = -\frac{1}{2}\begin{pmatrix} 2a_1 p & p(a_1+a_2)-b_1(a_1-a_2) & p(a_1+a_3)-b_2(a_1-a_3) \\ p(a_1+a_2)-b_1(a_1-a_2) & 2a_2 p & p(a_2+a_3)-b_3(a_2-a_3) \\ p(a_1+a_3)-b_2(a_1-a_3) & p(a_2+a_3)-b_3(a_2-a_3) & 2a_3 p \end{pmatrix}.$$

This matrix is three-dimensional and thus its three principal minors have to be checked for positiveness. Under the following three conditions β_s is positive definite what implies the positive definiteness of β

$$\begin{aligned} \beta_{s,11} &> 0 \\ \det\begin{pmatrix} \beta_{s,11} & \beta_{s,12} \\ \beta_{s,21} & \beta_{s,22} \end{pmatrix} &> 0 \\ \det(\beta_s) &> 0. \end{aligned} \tag{7.8}$$

For consistency with the two species model we discuss the first two minors first, because they imply the correctness of the stated properties there.

Theorem 7.2.3. *The matrix $\beta_s(\boldsymbol{\rho})$ fulfills the first two conditions of (7.8), if the following statements hold for the variables ρ_1, ρ_2, the functions h_i, ψ and the constants V_1, V_2*

1. $\rho_1, \rho_2 > 0$
2. $V_1, V_2 > 0$
3. $\psi' < 0$
4. $a_1 > 0$
5. $a_2 > 0$
6. $2\,|p|\, b_1(a_2+a_1) > (p^2+b_1^2)(a_2-a_1)$
7. $V_1 \neq V_2$.

and the abbreviations (7.7).

Proof. The first condition

$$\beta_{s,11} = -(V_1\psi' + c_1 h'(\rho))\rho_1\psi' R > 0$$

is fulfilled, if $\rho_1 > 0$ and $V_1, c_1 > 0$ and if $\psi' < 0$ and $V_1\psi' + c_1 h'(\rho) > 0$. For the second condition one gets

$$\begin{aligned}\det\begin{pmatrix}\beta_{s,11} & \beta_{s,12}\\ \beta_{s,21} & \beta_{s,22}\end{pmatrix} &= \left(-\frac{1}{2}\right)^2 \det\begin{pmatrix}2a_1p & p(a_1+a_2)-b_1(a_1-a_2)\\ p(a_1+a_2)-b_1(a_1-a_2) & 2a_2p\end{pmatrix}\\ &= \frac{1}{4}\left[4a_1a_2p^2 - [p(a_1+a_2)-b_1(a_1-a_2)]^2\right]\\ &= \frac{1}{4}[-(p^2+b_1^2)(a_1-a_2)^2 + 2pb_1(a_1-a_2)(a_1+a_2)].\end{aligned}$$

From above we know that $p = R\psi' < 0$ and $b_1 = (V_1 - V_2)\psi > 0$ holds if $V_1 \neq V_2$. Then, $a_1 > 0$ implies $a_2 > 0$ and we obtain that $a_2 > a_1$. This is reasonable because $a_i = (V_i\psi' + c_i h'(\rho))\rho_i$ and we know that $\psi' = -1$ and $V_1 > V_2$. Moreover, we need $\rho_2 > 0$ and $V_2, c_2 > 0$. Hence, we demand that

$$2\,|p|\,b_1(a_2-a_1)(a_2+a_1) > (p^2+b_1^2)(a_2-a_1)^2$$

and for $a_2 > a_1$ this equals

$$2\,|p|\,b_1(a_2+a_1) > (p^2+b_1^2)(a_2-a_1).$$

Altogether one sees that the first and second minor are indeed positive for the claimed properties if this inequality holds. □

Mention that from the first two conditions we only get properties for the first and second species and not for the third. This is why it was not necessary to prove the parabolicity for the two species model. Moreover, we see that for $\rho_3 = 0$ we get the two species viscous conservation laws with exact the same properties of the corresponding variables, functions and constants.

In the next theorem we examine the third minor.

Theorem 7.2.4. *The third minor of the symmetric part of β is positive if*

$$[|p|\,(a_1+a_2) - b_1(a_2-a_1)][|p|\,(a_1+a_3) - b_2(a_3-a_1)][|p|\,(a_2+a_3) - b_3(a_3-a_2)] > 8a_1a_2a_3\,|p|^3$$

and if

$$\begin{aligned}[|p| &> b_1\\ [|p| &> b_2\\ [|p| &> b_3.\end{aligned}$$

Under this conditions and with the properties of 7.2.3 the matrix β_s and hence β itself is positive definite.

Proof. The third condition wants $\det(\beta_s)$ to be positive. One gets

$$\begin{aligned}
&\det(\beta_s)\\
&= \left(-\frac{1}{2}\right)^3 \det \begin{pmatrix} 2a_1p & p(a_1+a_2)-b_1(a_1-a_2) & p(a_1+a_3)-b_2(a_1-a_3) \\ p(a_1+a_2)-b_1(a_1-a_2) & 2a_2p & p(a_2+a_3)-b_3(a_2-a_3) \\ p(a_1+a_3)-b_2(a_1-a_3) & p(a_2+a_3)-b_3(a_2-a_3) & 2a_3p \end{pmatrix}
\end{aligned}$$

$$\begin{aligned}
=&\frac{1}{8}\left[-8a_1a_2a_3p^3 - 2[p(a_1+a_2)-b_1(a_1-a_2)][p(a_1+a_3)-b_2(a_1-a_3)][p(a_2+a_3)-b_3(a_2-a_3)]\right.\\
&+2a_1p[p(a_2+a_3)-b_3(a_2-a_3)]^2 + 2a_2p[p(a_1+a_3)-b_2(a_1-a_3)]^2\\
&\left.+2a_3p[p(a_1+a_2)-b_1(a_1-a_2)]^2\right].
\end{aligned} \tag{7.9}$$

From the positiveness of the first and second minor we already know that

$$4a_1a_2p^2 - (p(a_1+a_2)-b_1(a_1-a_2))^2 > 0$$

and so we obtain

$$-[p(a_1+a_2)-b_1(a_1-a_2)]^2 > -4a_1a_2p^2.$$

The multiplication with $2a_3|p|$ leads to

$$-2a_3|p|[p(a_1+a_2)-b_1(a_1-a_2)]^2 > -8a_1a_2a_3|p|^3.$$

Since this estimation can be done for each of the three last terms of (7.9) this leads to

$$\begin{aligned}
\det(\beta_s) >&\frac{1}{8}\left[-16a_1a_2a_3|p|^3\right.\\
&\left.+2[|p|(a_1+a_2)-b_1(a_2-a_1)][|p|(a_1+a_3)-b_2(a_3-a_1)][|p|(a_2+a_3)-b_3(a_3-a_2)]\right.
\end{aligned}$$

together with $a_2 > a_1$, $a_3 > a_2$ and $a_3 > a_1$ and the conditions of 7.2.3. This implies that $\det(\beta_s) > 0$ if

$$[|p|(a_1+a_2)-b_1(a_2-a_1)][|p|(a_1+a_3)-b_2(a_3-a_1)][|p|(a_2+a_3)-b_3(a_3-a_2)] > 8a_1a_2a_3|p|^3$$

and if

$$\begin{aligned}
|p|(a_1+a_2)-b_1(a_2-a_1) &> 0\\
|p|(a_1+a_3)-b_2(a_3-a_1) &> 0\\
|p|(a_2+a_3)-b_3(a_3-a_2) &> 0.
\end{aligned}$$

This is equivalent to

$$\begin{aligned}
|p| &> b_1\\
|p| &> b_2\\
|p| &> b_3
\end{aligned}$$

what yields the stated inequalities. □

The conditions that imply positiveness of the second and third minor of β_s are not satisfying because they are not self explaining from a traffic point of view. The reason for this lies in the intricate expressions resulting from the CEE for the symmetric part of β. In the course of this thesis it was not possible to break down the inequalities to properties of the associated traffic functions and constants. Only the first minor leads to properties which are reasonable from the perspective of the LWR model and also from the characteristical traffic features. The assumptions we made about the velocity and hesitation functions are reasonable.

Since the different populations mix on a road the two functions are expected to depend on the sum of all vehicle densities. Moreover, the hesitation and the velocity function describe factors that act on the traffic from the outside, i.e. their meaning is not developed from the traffic participants directly but from their behavior to occasions from the outside like the conditions of the road and driving laws. Therefore, it is also convenient that we choose the same functions h and ψ for all populations and differ only by different constants.

Finally, the ARZ model for three species is consistent with the one and two populations model. In fact, we proved the two species case via the three species model. We conclude that the model we introduced as three species ARZ model is reasonable although the properties for parabolicity are not self explaining and the relation between the inequalities resulting from CEE and the corresponding constants is not examined in this thesis.

Note, that there exist other ways of examining the relaxation behavior and also the connection to the LWR model than it is done here. One possibility is to use a higher order of τ, i.e. to expand the velocity not for power 1 of τ but to a higher power. Additionally, we have already discussed that there are basic differences between gas molecules and traffic participants. Hence, one may suggest to use a different expansion for the ARZ model instead of the CEE.

The section below, regards a variation of the three species model by changing the assumptions on the hesitation and equilibrium velocity function in the same way as we did for the two species model.

7.3 Variation of the ARZ Model for three species

In the previous chapter, we concluded that the ARZ model for three populations is parabolic under special conditions. We now consider a variation of this model. Similar to the two species model one could classify the different participants of traffic not only by the constants V_i and c_i, but also by their behavior towards the other vehicles. For example, the trucks normally are not influenced by the other cars on the road like we considered for two

populations. We use the ARZ model for three species again

$$\begin{aligned}
\partial_t \rho_1 + \partial_x(\rho_1 u_1) &= 0 \\
\partial_t(u_1 + h_1) + u_1 \partial_x(u_1 + h_1) &= \frac{U_{1,eq} - u_1}{\tau} \\
\partial_t \rho_2 + \partial_x(\rho_2 u_2) &= 0 \\
\partial_t(u_2 + h_2) + u_2 \partial_x(u_2 + h_2) &= \frac{U_{2,eq} - u_2}{\tau} \\
\partial_t \rho_3 + \partial_x(\rho_3 u_3) &= 0 \\
\partial_t(u_3 + h_3) + u_3 \partial_x(u_3 + h_3) &= \frac{U_{3,eq} - u_3}{\tau}.
\end{aligned} \tag{7.10}$$

In order to consider different cases, the matrix M is introduced to define the hesitation and equilibrium functions h_i and $U_{eq,i}$.

$$\begin{aligned}
U_{eq,i} &= V_i \psi \left(\sum_{j=1}^{3} m_{ij} \rho_j \right) \\
h_i &= c_i h \left(\sum_{j=1}^{3} m_{ij} \rho_j \right)
\end{aligned} \tag{7.11}$$

with $m_{ij}\{0,1\}$ where $m_{ij} = 0; 1$ depending on the case we are considering. To get the ARZ model for three species without variation we would use 1 for all entries. Since $m_{ij} = \{0,1\}$ for the derivatives are computed as

$$\begin{aligned}
\frac{\partial h_i}{\partial \rho_k} &= c_i m_{ik} h'(\sum_{j=1}^{3} m_{ij} \rho_j) \\
\frac{\partial U_{i,eq}}{\partial \rho_k} &= V_i m_{ik} \psi'(\sum_{j=1}^{3} m_{ij} \rho_j).
\end{aligned} \tag{7.12}$$

Hence, the functions h and ψ depend on the sum of the densities as they did in the original model. With this formulation we are able to compute the CEE once and consider different models afterward.

Corollary 7.3.1. *The expansion of u_i is similar to the original case*

$$u_i^1 = U_{i,eq} + \tau u_i^1 + \mathcal{O}(\tau^2)$$

with the modified term for u_i^1

$$\begin{aligned}
u_i^1 =& (V_i \psi' + c_i h')[\psi' \sum_{k=1}^{3} V_k \rho_k (m_{k1} m_{i1} \partial_x \rho_1 + m_{k2} m_{i2} \partial_x \rho_2 + m_{k3} m_{i3} \partial_x \rho_3) \\
&+ \psi m_{i1}((V_1 - V_i)\partial_x \rho_1 + m_{i2}(V_2 - V_i)\partial_x \rho_2 + m_{i3}(V_3 - V_i)\partial_x \rho_3) + \mathcal{O}(\tau)]
\end{aligned}$$

where $m_{ij} = \{0,1\}$.

Proof. We make the same computation as in (7.2) but with the new assumptions (7.11). Hence, we have to differ the functions h_i and $U_{i,eq}$ for the various species, first.

$$\begin{aligned}
-u_i^1 =&\partial_t(u_i+h_i)+u_i\partial_x(u_i+h_i)+\mathcal{O}(\tau)\\
=&\frac{\partial(u_i+h_i)}{\partial\rho_1}\partial_t\rho_1+\frac{\partial(u_i+h_i)}{\partial\rho_2}\partial_t\rho_2+\frac{\partial(u_i+h_i)}{\partial\rho_3}\partial_t\rho_3\\
&+u_i\frac{\partial(u_i+h_i)}{\partial\rho_1}\partial_x\rho_1+u_i\frac{\partial(u_i+h_i)}{\partial\rho_2}\partial_x\rho_2+u_i\frac{\partial(u_i+h_i)}{\partial\rho_3}\partial_x\rho_3+\mathcal{O}(\tau)\\
=&-\frac{\partial(u_i+h_i)}{\partial\rho_1}\partial_x(\rho_1u_1)-\frac{\partial(u_i+h_i)}{\partial\rho_2}\partial_x(\rho_2u_2)-\frac{\partial(u_i+h_i)}{\partial\rho_3}\partial_x(\rho_3u_3)\\
&+u_i\frac{\partial(u_i+h_i)}{\partial\rho_1}\partial_x\rho_1+u_i\frac{\partial(u_i+h_i)}{\partial\rho_2}\partial_x\rho_2+u_i\frac{\partial(u_i+h_i)}{\partial\rho_3}\partial_x\rho_3+\mathcal{O}(\tau)\\
=&-\frac{\partial(u_i+h_i)}{\partial\rho_1}\rho_1\partial_xu_1-\frac{\partial(u_i+h_i)}{\partial\rho_2}\rho_2\partial_xu_2-\frac{\partial(u_i+h_i)}{\partial\rho_3}\rho_3\partial_xu_3\\
&+(u_i-u_1)\frac{\partial(u_i+h_i)}{\partial\rho_1}\partial_x\rho_1+(u_i-u_2)\frac{\partial(u_i+h_i)}{\partial\rho_2}\partial_x\rho_2+(u_i-u_3)\frac{\partial(u_i+h_i)}{\partial\rho_3}\partial_x\rho_3+\mathcal{O}(\tau).
\end{aligned}$$

Hereupon, we compute $\partial_x u_i$ with the help of the expansion of u_i and obtain

$$\begin{aligned}
u_i^1 =&\frac{\partial(U_{eq,i}+h_i)}{\partial\rho_1}\rho_1\sum_{k=1}^{3}\frac{\partial U_{eq,1}}{\partial\rho_k}\partial\rho_k+\frac{\partial(U_{eq,i}+h_i)}{\partial\rho_2}\rho_2\sum_{k=1}^{3}\frac{\partial U_{eq,2}}{\partial\rho_k}\partial\rho_k+\frac{\partial(U_{eq,i}+h_i)}{\partial\rho_3}\rho_3\sum_{k=1}^{3}\frac{\partial U_{eq,3}}{\partial\rho_k}\partial\rho_k\\
&+(U_{eq,1}-U_{eq,i})\frac{\partial(U_{eq,i}+h_i)}{\partial\rho_1}\partial_x\rho_1+(U_{eq,2}-U_{eq,i})\frac{\partial(U_{eq,i}+h_i)}{\partial\rho_2}\partial_x\rho_2\\
&+(U_{eq,3}-U_{eq,i})\frac{\partial(U_{eq,i}+h_i)}{\partial\rho_3}\partial_x\rho_3+\mathcal{O}(\tau)
\end{aligned}$$

what leads to claimed formula for u_i^1, if we insert the derivatives (7.12). One can also order

the terms by the derivative of ρ_i and obtains

$$\begin{aligned}
u_i^1 =&[\frac{\partial(U_{eq,i}+h_i)}{\partial\rho_1}\rho_1\frac{\partial U_{eq,1}}{\partial\rho_1}+\frac{\partial(U_{eq,i}+h_i)}{\partial\rho_2}\rho_2\frac{\partial U_{eq,2}}{\partial\rho_1}+\frac{\partial(U_{eq,i}+h_i)}{\partial\rho_3}\rho_3\frac{\partial U_{eq,3}}{\partial\rho_3}\\
&+(U_{eq,1}-U_{eq,i})\frac{\partial(U_{eq,i}+h_i)}{\partial\rho_1}]\partial_x\rho_1\\
&+[\frac{\partial(U_{eq,i}+h_i)}{\partial\rho_1}\rho_1\frac{\partial U_{eq,1}}{\partial\rho_1}+\frac{\partial(U_{eq,i}+h_i)}{\partial\rho_2}\rho_2\frac{\partial U_{eq,2}}{\partial\rho_1}+\frac{\partial(U_{eq,i}+h_i)}{\partial\rho_3}\rho_3\frac{\partial U_{eq,3}}{\partial\rho_3}\\
&+(U_{eq,2}-U_{eq,i})\frac{\partial(U_{eq,i}+h_i)}{\partial\rho_1}]\partial_x\rho_2\\
&+[\frac{\partial(U_{eq,i}+h_i)}{\partial\rho_1}\rho_1\frac{\partial U_{eq,1}}{\partial\rho_1}+\frac{\partial(U_{eq,i}+h_i)}{\partial\rho_2}\rho_2\frac{\partial U_{eq,2}}{\partial\rho_1}+\frac{\partial(U_{eq,i}+h_i)}{\partial\rho_3}\rho_3\frac{\partial U_{eq,3}}{\partial\rho_3}\\
&+(U_{eq,3}-U_{eq,i})\frac{\partial(U_{eq,i}+h_i)}{\partial\rho_1}]\partial_x\rho_3+\mathcal{O}(\tau)
\end{aligned}$$

what we need to compute $\beta(\boldsymbol{\rho})$ afterward. □

We computed the terms u_i^1 and from this we obtain the entries of the matrix $\beta(\boldsymbol{\rho})$ of the right hand side of the conservation laws as we see in the next corollary.

Corollary 7.3.2. *The variation of the ARZ model for three populations of vehicles with the matrix M yields the conservation law with right hand side*

$$\partial_t\rho+\partial_x(\rho U_{eq})=\tau\partial_x(\beta\partial_x\rho)+\mathcal{O}(\tau^2) \tag{7.13}$$

with the varied entries of the matrix β

$$\beta_{ij}=\left(-(V_i\psi'+c_ih'(\rho))\rho_i(\psi' r+(V_j-V_i)\psi)\right)_{ij}. \tag{7.14}$$

$$\begin{aligned}
\beta_{11}=&-(V_1\psi'+c_1h')\rho_1\psi'(m_{11}\rho_1V_1+m_{12}\rho_2V_2+m_{13}\rho_3V_3)\\
\beta_{12}=&-(V_1\psi'+c_1h')\rho_1(\psi'(m_{11}\rho_1V_1+m_{12}\rho_2V_2+m_{13}\rho_3V_3)+m_{12}(V_2-V_1)\psi)\\
\beta_{13}=&-(V_1\psi'+c_1h')\rho_1(\psi'(m_{11}\rho_1V_1+m_{12}\rho_2V_2+m_{13}\rho_3V_3)+m_{13}(V_3-V_1)\psi)\\
\beta_{21}=&-(V_2\psi'+c_2h')\rho_2(\psi'(m_{11}\rho_1V_1+m_{12}\rho_2V_2+m_{13}\rho_3V_3)+m_{21}(V_1-V_2)\psi)\\
\beta_{22}=&-(V_2\psi'+c_2h')\rho_2\psi'(m_{11}\rho_1V_1+m_{12}\rho_2V_2+m_{13}\rho_3V_3)\\
\beta_{23}=&-(V_2\psi'+c_2h')\rho_2(\psi'(m_{11}\rho_1V_1+m_{12}\rho_2V_2+m_{13}\rho_3V_3)+m_{23}(V_3-V_2)\psi)\\
\beta_{31}=&-(V_3\psi'+c_3h')\rho_3(\psi'(m_{11}\rho_1V_1+m_{12}\rho_2V_2+m_{13}\rho_3V_3)+m_{31}(V_1-V_3)\psi)\\
\beta_{32}=&-(V_3\psi'+c_3h')\rho_3(\psi'(m_{11}\rho_1V_1+m_{12}\rho_2V_2+m_{13}\rho_3V_3)+m_{32}(V_2-V_3)\psi)\\
\beta_{33}=&-(V_3\psi'+c_3h')\rho_3\psi'(m_{11}\rho_1V_1+m_{12}\rho_2V_2+m_{13}\rho_3V_3)
\end{aligned} \tag{7.15}$$

Proof. As we have already mentioned in the proof of the last corollary, we can use the term of u_i^1 to compute $\beta(\boldsymbol{\rho})$. Therefore, we multiply u_1^1 with ρ_1 and obtain the first line of β. Applying the same method for the second and third line leads to (7.15). □

We study three different examples by using special matrices M, now. By this we obtain special traffic occasions where not all species see each other. According to the two species model we consider a traffic situation with two different species of cars and one of trucks. Then, we regard one species of cars and two of trucks and finally we discuss a triangular system with bicycles, cars and trucks.

Example 7.3.3. *Two species of cars and one species of trucks*
Consider a traffic situation where species 1 *and* 2 *describe cars and species* 3 *are trucks. Then, the first and second population observe the whole traffic and hence their functions* h_i *and* $U_{i,eq}$ *depend on all three densities. As for the two species model we assume that the third species, the trucks, only see their own kind on the road and hence do not mind the densities of the other two populations. For the hesitation and equilibrium velocity function this yields*

$$\begin{aligned} h_1 &= c_1 h(\rho_1+\rho_2+\rho_3)\\ h_2 &= c_2 h(\rho_1+\rho_2+\rho_3)\\ h_3 &= c_3 h(\rho_3)\\ U_{1,eq} &= V_1\psi(\rho_1+\rho_2+\rho_3)\\ U_{2,eq} &= V_2\psi(\rho_1+\rho_2+\rho_3)\\ U_{3,eq} &= V_3\psi(\rho_3). \end{aligned} \tag{7.16}$$

The matrix M *is of the form*

$$M = (m_{ij})_{i,j=1}^3 = \begin{pmatrix} 1 & 1 & 1\\ 1 & 1 & 1\\ 0 & 0 & 1 \end{pmatrix}$$

and from (7.15) we can directly compute the matrix β *of the CEE*

$$\begin{aligned} \beta_{11} &= -(V_1\psi' + c_1h')\rho_1\psi'(\rho_1V_1+\rho_2V_2)\\ \beta_{12} &= -(V_1\psi' + c_1h')\rho_1(\psi'(\rho_1V_1+\rho_2V_2) + (V_2-V_1)\psi\\ \beta_{13} &= -(V_1\psi' + c_1h')\rho_1(\psi'(\rho_1V_1+\rho_2V_2) + \rho_3V_3\psi' + (V_3-V_1)\psi\\ \beta_{21} &= -(V_2\psi' + c_2h')\rho_2(\psi'(\rho_1V_1+\rho_2V_2) + (V_1-V_2)\psi)\\ \beta_{22} &= -(V_2\psi' + c_2h')\rho_2\psi'(\rho_1V_1+\rho_2V_2)\\ \beta_{23} &= -(V_2\psi' + c_2h')\rho_2(\psi'(\rho_1V_1+\rho_2V_2) + \rho_3V_3\psi' + (V_3-V_2)\psi\\ \beta_{31} &= 0\\ \beta_{32} &= 0\\ \beta_{33} &= -(V_3\psi' + c_3h')\rho_3^2V_3\psi'. \end{aligned}$$

If we check β for positive definiteness, we again consider the symmetric part β_s and examine its principal minors. With the abbreviations (7.7), β can be written as

$$\beta = -\begin{pmatrix} a_1(p_1+p_2) & a_1(p_1+p_2-b_1) & a_1(p-b_2) \\ a_2(p_1+p_2+b_1) & a_2(p_1+p_2) & a_2(p-b_3) \\ 0 & 0 & a_3p_3 \end{pmatrix}$$

what yields β_s

$$\beta_s = -\frac{1}{2}\begin{pmatrix} 2a_1(p_1+p_2) & (p_1+p_2)(a_1+a_2)-b_1(a_1-a_2) & a_1(p-b_2) \\ (p_1+p_2)(a_1+a_2)-b_1(a_1-a_2) & 2a_2(p_1+p_2) & a_2(p-b_3) \\ a_1(p-b_2) & a_2(p-b_3) & 2a_3p_3 \end{pmatrix}.$$

Hence, the first condition

$$\beta_{s,11} = -(V_1\psi' + c_1h')\rho_1\psi'(\rho_1V_1+\rho_2V_2) > 0$$

is fulfilled, if $\rho_1 > 0$ and $V_1, c_1 > 0$ and if $\psi' < 0$ and $V_1\psi' + c_1h' > 0$. Moreover, for the weighted sum we know that $\rho_1V_1 + \rho_2V_2 > 0$. For the second condition one similarly to the two species case gets

$$\det\begin{pmatrix} \beta_{s,11} & \beta_{s,12} \\ \beta_{s,21} & \beta_{s,22} \end{pmatrix} = \frac{1}{4}\left[4a_1^2(p_1+p_2)^2 - [(p_1+p_2)(a_1+a_2)-b_1(a_1-a_2)]^2\right]$$

This is positive, if the properties of 7.2.3 hold. We see that the weighted sum of ρ_1 and ρ_2 is positive from these conditions. They equal the ones of the two species model. But in contrast to the original model the third minor changes slightly

$$\begin{aligned}\det(\beta_s) =& \frac{1}{8}\left[-8a_1a_2a_3(p_1+p_2)^2p_3 - 2[(p_1+p_2)(a_1+a_2)-b_1(a_1-a_2)][a_1(p-b_2)][a_2(p-b_3)]\right. \\ &+ 2a_1(p_1+p_2)[a_2(p-b_3)]^2 + 2a_2(p_1+p_2)[a_1(p-b_2)]^2 \\ &\left.+2a_3p_3[(p_1+p_2)(a_1+a_2)-b_1(a_1-a_2)]^2\right]\end{aligned}$$

but again it not easy to see the cases where it is positive. Note, that we have $p_1, p_2, p_3 < 0$ from the Greenshileds velocity function. Together with the conditions of the first two minors and the properties of 7.2.4 this is positive. Because all principal minors of $\beta_s(\boldsymbol{\rho})$ are positive for the above conditions, β_s and also β is positive definite and thus system (7.10) is parabolic under the assumptions (7.16) for the traffic functions.

From the first example we observe that the variation of the model leads to a parabolic result from the CEE but the associated conditions are hard to find, too. By assuming two species of cars and one of trucks we deduce the three species model to an extended two species one because the PDEs describing the third species, the trucks, are decoupled from the rest and we can solve these in the one species model way. But then, the PDEs

modeling the two car populations are of two species type, if we insert the solution of the third species. From this view it is not surprising that the CEE yields a parabolic equation again. This variation connects the previous discussed one and two species models.

The second example we regard is a triangular case, i.e. that the first species sees all three, the second sees two, itself and one other, and the third sees only one species, itself.

Example 7.3.4. *Triangular system*
One could also assume that one species minds all the other species on the road as for example fast drivers need to do. The second species describes slower moving cars that see themselves and the third species on the road which are trucks. This leads to the following assumptions on the functions h_1, h_2, h_3 *and* $U_{1,eq}, U_{2,eq}, U_{3,eq}$

$$\begin{aligned}
h_1 &= c_1 h(\rho_1 + \rho_2 + \rho_3)\\
h_2 &= c_2 h(\rho_2 + \rho_3)\\
h_3 &= c_3 h(\rho_3)\\
U_{1,eq} &= V_1 \psi(\rho_1 + \rho_2 + \rho_3)\\
U_{2,eq} &= V_2 \psi(\rho_2 + \rho_3)\\
U_{3,eq} &= V_3 \psi(\rho_3).
\end{aligned}$$

From M

$$M = (m_{ij})_{i,j=1}^{3} = \begin{pmatrix} 1 & 1 & 1 \\ 0 & 1 & 1 \\ 0 & 0 & 1 \end{pmatrix}$$

we see that this example leads to a triangular system. The CCE yields

$$\begin{aligned}
\beta_{11} &= -(V_1\psi' + c_1 h')\rho_1^2 V_1 \psi'\\
\beta_{12} &= -(V_1\psi' + c_1 h')\rho_1((\rho_1 V_1 + \rho_2 V_2)\psi' + (V_2 - V_1)\psi)\\
\beta_{13} &= -(V_1\psi' + c_1 h')\rho_1((\rho_1 V_1 + \rho_2 V_2 + \rho_3 V_3)\psi' + (V_3 - V_1)\psi)\\
\beta_{21} &= 0\\
\beta_{22} &= -(V_2\psi' + c_2 h')\rho_2^2 V_2 \psi'\\
\beta_{23} &= -(V_2\psi' + c_2 h')\rho_2((\rho_2 V_2 + \rho_3 V_3)\psi' + (V_3 - V_2)\psi)\\
\beta_{31} &= 0\\
\beta_{32} &= 0\\
\beta_{33} &= -(V_3\psi' + c_3 h')\rho_3^2 V_3 \psi'.
\end{aligned}$$

Then the positive definiteness can be examined similar to the first example. With the above abbreviations we obtain

$$\beta = -\begin{pmatrix} a_1 p_1 & a_1(p_1 + p_2 - b_1) & a_1(p - b_2) \\ 0 & a_2 p_2 & a_2(p_2 + p_3 - b_3) \\ 0 & 0 & a_3 p_3 \end{pmatrix}$$

what yields β_s

$$\beta_s = -\frac{1}{2}\begin{pmatrix} 2a_1p_1 & a_1(p_1+p_2-b_1) & a_1(p-b_2) \\ a_1(p_1+p_2-b_1) & 2a_2p_2 & a_2(p_2+p_3-b_3) \\ a_1(p-b_2) & a_2(p_2+p_3-b_3) & 2a_3p_3 \end{pmatrix}.$$

Once more we check the positive definiteness of β_s*. The first minor*

$$\beta_{s,11} = -a_1p_1 = -(V_1\psi' + c_1h'(\rho))\rho_1^2V_1\psi'$$

is positive for $(V_1\psi' + c_1h'(\rho)) > 0$ *since we know* $\psi' < 0$*,* $\rho_1 > 0$ *and* $V_1 > 0$*. Then, the second minor leads to*

$$\det\begin{pmatrix}\beta_{s,11} & \beta_{s,12}\\ \beta_{s,21} & \beta_{s,22}\end{pmatrix} = \frac{1}{4}\left[4a_1a_2p_1p_2 - a_1^2(p_1+p_2-b_1)^2\right].$$

From the conditions of the first minor we obtain for $a_1 > 0$

$$4a_2p_1p_2 > a_1(p_1+p_2-b_1)^2.$$

The third minor can be computed as

$$\begin{aligned}\det(\beta_s) = &-\frac{1}{8}[8a_1a_2a_3p_1p_2p_3 + 2a_1^2a_2(p_1+p_2-b_1)(p-b_2)(p_2+p_3-b_3)\\ &- 2a_1^2a_2p_2(p-b_2)^2 - 2a_1a_2^2p_1(p_2+p_3-b_3)^2 - 2a_1^2a_3p_3(p_1+p_2-b_1)^2]\end{aligned}$$

and we demand that

$$\begin{aligned}&4a_2a_3p_1p_2p_3 + 2a_1^2a_2(p_1+p_2-b_1)(p-b_2)(p_2+p_3-b_3)\\ &> a_1a_2p_2(p-b_2)^2 + a_2^2p_1(p_2+p_3-b_3)^2 + a_1a_3p_3(p_1+p_2-b_1)^2.\end{aligned}$$

Even though this special variation leads to a simpler triangular system, the conditions for positiveness are again intricate and not self explaining. One needs to check whether the above inequalities are fulfilled for the functions defined in (7.7) what was not possible in the course of this thesis.

Summing up, the variation of the ARZ model for three species leads to parabolic equations for functions fulfilling the stated inequalities. Nevertheless these conditions can not be deduced just from the characteristical traffic variables as was done for one species. With the matrix M one can consider more examples than the ones presented here, but all will lead to a parabolic viscous conservation law with inequalities as in the two presented examples.

Of course, it is possible to extend the ARZ model to a multi species model with more than three species but since we have not proved the well-posedness of the model for multi species and since we get complicated results from the CEE for two species already, there is no reason to go on with an extension to multi species in the same way.

8 Conclusion

The aim of this thesis is to advance multi species traffic models. We discussed two different macroscopic models and extended them to allowing three different populations of traffic participants. The Lighthill-Whitham and Richards (LWR) model is of first order because it is derived from conservation of cars. The Aw-Rascle Zhang (ARZ) model is of second order since it contains one equation for the density and one modeling the velocity.

The extension of the LWR model to a two population model provides difficulties since global hyperbolicity is not given. There exists one umbilic point on the boundary of the set where we define the system where the eigenvalues coalesce. Due to that, we have no similar model that has been discussed and we cannot use standard theory of partial differential equations to prove well-posedness. Moreover, the model, although it is of simple structure, yields intricate expressions for the corresponding eigenvalues and vectors. From there, it takes a great amount to discuss its well-posedness.

Here, we consider a Riemann problem where one species is absent, i.e. its density equals zero. We show that the solution to this Riemann problem fits to the solution of the one species LWR model and that this solution depends continuously on the initial data. The neat description of this special Riemann problem delivers a good understanding of the two species model's features.

For the general Riemann problem we conclude that due to the complexity of expressions it is not possible to solve it algebraically. We also consider a variation of this model through the velocity function with the aim to dispose the existence of an umbilic point but we observe that this variation leads to a whole line of umbilic points.

The consideration of a three species model provides even more difficulties because now the eigenvalues cannot be computed algebraically. With Mathematica we compute the eigenvalues and obtain a full description of the model's umbilic points for three species. There exist more values of coalescing eigenvalues than for two species and we observe that they lie on the boundaries again. We are able to describe the umbilic surface and the umbilic lines of the model algebraically. Since the points lie on the boundaries we know that inside of the definition set the Riemann problem is well-posed for data with small variation. On the boundaries we obtain a case similar to the two species model.

Altogether, the extension of the LWR model is an example of a system of partial differential equations that provides a lack of global hyperbolicity. The special characteristic that the umbilic points lie on the boundaries is different from models discussed before. Although the well-posedness is not proven for a general Riemann problem, the neat study of the Riemann problem for the two species model around its umbilic point provides a good understanding of the model.

The ARZ model provides an umbilic point, too. It is not of first order and hence different from the LWR model. Here, the umbilic point leads to instabilities around the vacuum. The extension of the ARZ model to multi species is proposed in this thesis and since it has not been done before, we lack theory about its well-posedness.

The main focus of this work lies on the relaxation behavior of the ARZ model and its connection to the LWR model. Due to that, we omit the discussion of well-posedness for the multi species extension. For the original ARZ model the the Chapman Enskog expansion (CEE) produces a conservation law with right hand side which is parabolic under some constraints we put on the corresponding variables, constants and functions. Through the CEE we can interpret the ARZ model as an extension of the LWR model providing a viscous right hand side for the LWR model.

In the two and three species case we are not able to give properties of the traffic functions ensuring parabolicity. The associated inequalities give conditions on the traffic functions and constants. This is not done in the course of this thesis due to the complexity of the expressions. The variation of the corresponding functions from a traffic point of view leads to a less intricate model but nevertheless the conditions for parabolicity are not self explanatory. The idea of this variation is to distinguish the different traffic participants not only by their constants but also by their behavior towards the other traffic members. We assume that there are vehicles on the road that do not see all the other species.

Summing up, the multi species traffic models with their corresponding problems, yield a large basis for further examination. On the one hand, the LWR for multi species represents an interesting model which provides umbilic points on the boundaries of the definition set. On the other hand, the CEE for the ARZ model leads to a viscous conservation law which is much easier to handle.

Bibliography

A. Aw. Existence of a global entropic weak solution for the Aw-Rascle model. *Int. J. Evol. Equ.*, 9(1):53–70, 2014. ISSN 1549-2907.

A. Aw and M. Rascle. Resurrection of "second order" models of traffic flow. *SIAM J. Appl. Math.*, 60(3):916–938 (electronic), 2000. ISSN 0036-1399. doi: 10.1137/S0036139997332099. URL http://dx.doi.org/10.1137/S0036139997332099.

N. Bedjaoui, C. Klingenberg, and P. G. LeFloch. On the validity of Chapman-Enskog expansions for shock waves with small strength. *Port. Math. (N.S.)*, 61(4):479–499, 2004. ISSN 0032-5155.

S. Benzoni-Gavage and R. M. Colombo. An n-populations model for traffic flow. *European J. Appl. Math.*, 14(5):587–612, 2003. ISSN 0956-7925. doi: 10.1017/S0956792503005266. URL http://dx.doi.org/10.1017/S0956792503005266.

A. Bressan. *Hyperbolic systems of conservation laws*, volume 20 of *Oxford Lecture Series in Mathematics and its Applications*. Oxford University Press, Oxford, 2000. ISBN 0-19-850700-3. The one-dimensional Cauchy problem.

S. Chapman and T. G. Cowling. *The mathematical theory of non-uniform gases. An account of the kinetic theory of viscosity, thermal conduction and diffusion in gases*. Third edition, prepared in co-operation with D. Burnett. Cambridge University Press, London, 1970.

R. M. Colombo and A. Marson. A Hölder continuous ODE related to traffic flow. *Proc. Roy. Soc. Edinburgh Sect. A*, 133(4):759–772, 2003. ISSN 0308-2105. doi: 10.1017/S0308210500002663. URL http://dx.doi.org/10.1017/S0308210500002663.

C. M. Dafermos. *Hyperbolic conservation laws in continuum physics*, volume 325 of *Grundlehren der Mathematischen Wissenschaften [Fundamental Principles of Mathematical Sciences]*. Springer-Verlag, Berlin, third edition, 2010. ISBN 978-3-642-04047-4. doi: 10.1007/978-3-642-04048-1. URL http://dx.doi.org/10.1007/978-3-642-04048-1.

C. F. Daganzo. Requiem for second-order fluid approximations of traffic flow. *Transportation Research Part B: Methodological*, 29(4):277–286, 1995.

S. Fan, M. Herty, and B. Seibold. Comparative model accuracy of a data-fitted generalized Aw-Rascle-Zhang model. *Netw. Heterog. Media*, 9(2):239–268, 2014. ISSN 1556-1801. doi: 10.3934/nhm.2014.9.239. URL http://dx.doi.org/10.3934/nhm.2014.9.239.

M. Godvik and H. Hanche-Olsen. Existence of solutions for the Aw-Rascle traffic flow model with vacuum. *J. Hyperbolic Differ. Equ.*, 5(1):45–63, 2008. ISSN 0219-8916. doi: 10.1142/S0219891608001428. URL http://dx.doi.org/10.1142/S0219891608001428.

B. Greenshields. A study of traffic capacity. *Highway Research Board*, 14:448–477, 1934.

R. Haberman. *Mathematical models: mechanical vibrations, population dynamics, and traffic flow*, volume 21. Siam, 1998.

D. Hoff. Invariant regions for systems of conservation laws. *Trans. Amer. Math. Soc.*, 289 (2):591–610, 1985. ISSN 0002-9947. doi: 10.2307/2000254. URL http://dx.doi.org/10.2307/2000254.

B. L. Keyfitz and H. C. Kranzer. A system of nonstrictly hyperbolic conservation laws arising in elasticity theory. *Arch. Rational Mech. Anal.*, 72(3):219–241, 1979/80. ISSN 0003-9527. doi: 10.1007/BF00281590. URL http://dx.doi.org/10.1007/BF00281590.

P. D. Lax. Hyperbolic systems of conservation laws. II. *Comm. Pure Appl. Math.*, 10: 537–566, 1957. ISSN 0010-3640.

M. J. Lighthill and G. B. Whitham. On kinematic waves. II. A theory of traffic flow on long crowded roads. *Proc. Roy. Soc. London. Ser. A.*, 229:317–345, 1955. ISSN 0962-8444.

S. Liu, F. Chen, and Z. Wang. Existence of global L^p solutions to a symmetric system of Keyfitz–Kranzer type. *Appl. Math. Lett.*, 52:96–101, 2016. ISSN 0893-9659. doi: 10.1016/j.aml.2015.08.011. URL http://dx.doi.org/10.1016/j.aml.2015.08.011.

T.-P. Liu. Hyperbolic conservation laws with relaxation. *Comm. Math. Phys.*, 108(1): 153–175, 1987. URL http://projecteuclid.org/euclid.cmp/1104116362.

P. I. Richards. Shock waves on the highway. *Operations Res.*, 4:42–51, 1956. ISSN 0030-364X.

M. D. Rosini. *Macroscopic models for vehicular flows and crowd dynamics: theory and applications*. Understanding Complex Systems. Springer, Heidelberg, 2013. ISBN 978-3-319-00154-8; 978-3-319-00155-5. doi: 10.1007/978-3-319-00155-5. URL http://dx.doi.org/10.1007/978-3-319-00155-5. Classical and non-classical advanced mathematics for real life applications, With a foreword by Marek Niezgódka.

D. Serre. *Systems of conservation laws. 1.* Cambridge University Press, Cambridge, 1999. ISBN 0-521-58233-4. doi: 10.1017/CBO9780511612374. URL http://dx.doi.org/10.1017/CBO9780511612374. Hyperbolicity, entropies, shock waves, Translated from the 1996 French original by I. N. Sneddon.

M. Shearer and R. Levy. *Partial differential equations*. Princeton University Press, Princeton, NJ, 2015. ISBN 978-0-691-16129-7; 0-691-16129-1. An introduction to theory and applications.

U. Weidmann, U. Kirsch, and M. Schreckenberg. *Pedestrian and Evacuation Dynamics 2012*. Springer Science & Business, 2014.

H. M. Zhang. A non-equilibrium traffic model devoid of gas-like behavior. *Transportation Research Part B: Methodological*, 36(3):275–290, 2002.

Acknowledgement

I acknowledge, with gratitude, my debt of thanks to Professor Christian Klingenberg for his advice and enouragement and to Professor Rinaldo Colombo for his guidance and inspiration on Skype and during my stay in Brescia.
Moreover, I want to thank my whole family and my friends

Erklärung

Hiermit erkläre ich, dass ich diese Arbeit selbstständig verfasst und keine anderen als die angegebenen Quellen und Hilfsmittel benutzt und die aus fremden Quellen direkt oder indirekt übernommenen Gedanken als solche kenntlich gemacht habe. Die Arbeit habe ich bisher keinem anderen Prüfungsamt in gleicher oder vergleichbarer Form vorgelegt. Sie wurde bisher nicht veröffentlicht.